

© 2016

Qin Zhao

ALL RIGHTS RESERVED

**DESIGN OF FUNCTIONAL BEVERAGE EMULSION SYSTEMS
FOR IMPROVED CITRAL STABILITY
AND COENZYME Q10 BIOAVAILABILITY**

By
QIN ZHAO

A Dissertation submitted to the
Graduate School-New Brunswick
Rutgers, The State University of New Jersey
In partial fulfillment of the requirements

For the degree of
Doctor of Philosophy
Graduate Program in Food Science

Written under the direction of
Dr. Qingrong Huang

And approved by

New Brunswick, New Jersey

October 2016

ABSTRACT OF THE DISSERTATION

Design of Functional Beverage Emulsion Systems for Improved Cital Stability and Coenzyme Q₁₀ Bioavailability

By **QIN ZHAO**

Dissertation Director:

Dr. Qingrong Huang

Functional beverages, usually fortified with nutraceuticals in addition to flavors, can provide specific health benefits beyond the refreshing tastes. The general scope of the current study was to develop a functional beverage prototype infused with citral and coenzyme Q₁₀ (CoQ₁₀). Citral, one of the most popular flavors with strong lemon aroma, has the problem of being easily degraded and oxidized in the acidic beverage applications. And CoQ₁₀, a lipophilic nutraceutical with health benefits for cardiovascular diseases and energy-boosting, has rather low bioavailability in common supplements. Therefore, our specific objectives were to improve both citral's stability and CoQ₁₀'s bioavailability in the developed functional beverages by using nanoemulsion-based delivery systems.

For citral stability studies, our results suggested that its chemical stability can be greatly improved with proper selection of antioxidants and emulsifiers in the nanoemulsion systems. The reduced form of CoQ₁₀, known as ubiquinol or Q₁₀H₂, proved to be effective as a potent antioxidant in protecting citral from degradation during storage when its concentration was optimized at 0.10 wt% (Q₁₀H₂/citral ratio of 1:1).

Moreover, the effects of different emulsifiers in stabilizing citral were further examined. In detail, two synthetic surfactants (polysorbate, sugar ester), and three natural emulsifiers (saponin, lecithin, and lyso-lecithin) were tested and compared. Results indicated saponin (i.e. Q-Naturale) and lyso-lecithin (i.e. LPC20) had significantly improved effects in protecting citral from degradation and inhibiting the generation of the major off-flavors (*p*-cresol, α ,*p*-dimethylstyrene, *p*-methylacetophenone).

To access CoQ₁₀ bioavailability, both *in vitro* and *in vivo* tests were performed with our optimized nanoemulsion formulation and an oil dispersion control. Based on the promising bioaccessibility results indicated by two *in vitro* digestion models (pH-stat lipolysis model & TNO gastrointestinal model - TIM-1), CoQ₁₀'s pharmacokinetics and tissue distributions after ingestion were further examined using animal models. Results of pharmacokinetics revealed a 2.65-folds increase for the area under curve (AUC) of CoQ₁₀ in our nanoemulsion group compared with the control, indicating the oral bioavailability of CoQ₁₀ was significantly improved. A characteristic “two-peak” pattern was observed in the concentration-time curves, suggesting CoQ₁₀'s relatively slow absorption kinetics and the possible effect of enterohepatic recycling. Moreover, CoQ₁₀'s tissue distribution data further proved its increased absorption and uptake levels in major organs tissues after dosing with the nanoemulsion.

In conclusion, our developed nanoemulsion formulation greatly improved citral stability and CoQ₁₀ bioavailability. The obtained results will be valuable references for the food industry to formulate and develop functional beverages fortified with lipophilic nutraceuticals and sensitive flavors.

ACKNOWLEDGEMENT

The Ph.D. training is really like one of the most amazing adventures in my life. With a lot of ups and downs during the journey, I am now excited to see myself just an inch away from the wonderland! Before landing, I want to take this opportunity to acknowledge all the ‘crew members’ that helped me during my 6-year-long journey.

First of all, I would like to express my gratitude towards the ‘captain’ - my dissertation advisor Dr. Qingrong Huang, for his tremendous guidance and support for my study, research and life at the Department of Food Science, Rutgers University. It was Dr. Huang’s excellence in academics and optimism in personality confirmed my decision to get on board. He is not only my mentor, but also my friend, who introduced me into the area of functional foods that aligns perfectly with my research interests and career goals. Dr. Huang is always supportive in guiding me with new directions in research, and is patient enough in training me to be confident in my research areas. Without his help and understanding, I will be far away from the destination.

Next, I want to acknowledge other three committee members, Dr. Chi-Tang Ho and Dr. Thomas G. Hartman from the Department of Food Science, Rutgers University, and Dr. Shiming Li, from Huanggang Normal University. I strongly appreciate their valuable suggestions and comments regarding my research proposal and dissertation. I also want to thank Dr. Jiuliang Zhang at Huazhong Agricultural University for offering me the resources and conditions for the *in vivo* animal experiments.

Then, to all my labmates and friends at Rutgers, I would say it’s a great pleasure to know and work with you. Thanks for all the good and bad memories that we

experienced together. Special thanks to Dr. Xiaoqing Yang for training me with emulsion techniques and Gas Chromatography skills, which laid a solid foundation for my current research. Thanks Yaqi Lan for working together with me for the *in vitro* TIM-1 model, and Jieyu Zhu for assisting me with part of the analytical measurements.

My Ph.D. study will not be possible without the financial support obtained from funding agents and collaborating companies. I would like to thank U.S. Department of Agriculture, American Lecithin Company and Advanced Orthomolecular Research Inc. for supporting my research projects. Additionally, I greatly appreciate Oceans Omega LLC, International Flavors & Fragrances Inc., LifeFlo Inc., and PIM Brands LLC for offering me R&D internships or part-time opportunities in the food and related industries. These valuable experiences not only broadened my vision in research, but also made me confident with my future career.

I want to extend my special appreciation to Rutgers Bible Study Group (RBSG) and Rutgers Community Christian Church (RCCC), where I found my spiritual home and had so many unforgettable moments together with fellow friends to learn GOD's word. Thanks GOD for renewing my strength every time when I got tired and weary!

Finally, I would like to sincerely thank my parents for their unconditional love and support for all the time, and my beloved wife Chunxin Xia for joining my life! It's never enough for me to say thank you and love you. This dissertation is dedicated to my dearest families.

TABLE OF CONTENTS

ABSTRACT OF THE DISSERTATION.....	ii
ACKNOWLEDGEMENT.....	iv
TABLE OF CONTENTS	vi
LIST OF TABLES	x
LIST OF FIGURES	xi
CHAPTER 1: BACKGROUND INTRODUCTION	1
1.1. Emulsion science and technology	1
1.1.1. Emulsion classification	1
1.1.2. Emulsion preparation methods.....	4
1.2. Beverage Emulsion	7
1.2.1. Classification.....	8
1.2.2. Recent development and trends	9
1.3. Functional beverage	13
1.4. Citral	14
1.4.1. Challenges with citral's application.....	15
1.4.2. Strategies to prevent citral from degradation	16
1.5. Coenzyme Q ₁₀	19
1.5.1. Problems associated with CoQ ₁₀ as dietary supplement	20
1.5.2. Strategies to improve CoQ ₁₀ 's bioavailability	21
1.6. Bioavailability.....	23
1.6.1. Bioaccessibility and common <i>in vitro</i> models	25
1.6.2. Transport coefficient.....	29
1.6.3. Systemic metabolism	30
1.6.4. <i>In vitro</i> and <i>in vivo</i> correlations	32
CHAPTER 2: HYPOTHESIS AND OBJECTIVES.....	35
2.1. Hypothesis	35

2.2. Objectives	36
CHAPTER 3: EFFECT OF COENZYME Q10 ON CITRAL STABILITY AND OFF-FLAVOR FORMATION IN NANOEMULSIONS	38
3.1. Introduction.....	38
3.2. Materials and methods	39
3.2.1. Materials	39
3.2.2. Emulsion preparation and storage.....	39
3.2.3. Particle size measurement.....	40
3.2.4. Measurement of citral	41
3.2.5. GC-Mass analysis of citral's degradation products	41
3.2.6. Statistical analysis.....	42
3.3. Results and discussion	42
3.3.1. Physical stability of citral-loaded emulsions with and without Q ₁₀ H ₂	42
3.3.2. Stability of citral in emulsions with and with Q ₁₀ H ₂	44
3.3.3. Comparison between ubiquinol-10 and ubiquinone-10	51
3.3.4. Evaluation of the major citral degradation compounds	54
3.3.5. Effect of ubiquinol-10 on lipid oxidation.....	57
3.4. Conclusions.....	58
CHAPTER 4: EFFECT OF EMULSIFIER TYPE ON THE FORMATION OF NANOEMULSION AND CITRAL STABILITY IN THESE SYSTEMS.....	59
4.1. Introduction.....	59
4.2. Materials and methods	61
4.2.1. Materials	61
4.2.2. Nanoemulsion preparation	62
4.2.3. Control group preparation.....	62
4.2.4. Storage tests	63
4.2.5. Particle size distribution and zeta potential measurements.....	63

4.2.6.	Measurement of citral	64
4.2.7.	GC-Mass analysis of degradation products.....	64
4.2.8.	Statistical analysis.....	65
4.3.	Results and discussion	65
4.3.1.	Physical stability of citral-loaded colloidal systems during storage	65
4.3.2.	Stability of citral in micelle and emulsion systems.....	70
4.3.3.	Evaluation of the major citral degradation compounds	75
4.3.4.	Evaluation of lipid degradation products	77
4.4.	Conclusions.....	79
CHAPTER 5: IN VITRO DETERMINATION OF COENZYME Q10 BIOACCESSIBILITY.....		82
5.1.	Introduction.....	82
5.2.	Materials and methods	83
5.2.1.	Materials	83
5.2.2.	Testing formulation preparation.....	84
5.2.3.	Titration based pH-stat lipolysis model	84
5.2.4.	Determination of the extent of lipolysis and bioaccessibility	85
5.2.5.	TIM-1 model.....	86
5.2.6.	Extraction and analysis of Q ₁₀	88
5.2.7.	Measurements of the bioaccessibility of Q ₁₀ versus Q ₁₀ H ₂	88
5.2.8.	Statistical analysis.....	89
5.3.	Results and discussion	89
5.3.1.	Nanoemulsion formulation optimization for Q ₁₀	89
5.3.2.	Using pH-stat model to determine the bioaccessibility of Q ₁₀ formulations	92
5.3.3.	Using TIM-1 model to determine the bioaccessibility of Q ₁₀ formulations.....	95
5.3.4.	Discussion of the results obtained from two in vitro systems.....	99
5.3.5.	Bioaccessibility of Q ₁₀ H ₂ versus Q ₁₀ determined by the pH-stat model	100

5.4. Conclusions.....	102
CHAPTER 6: IN VIVO DETERMINATION OF COENZYME Q10 BIOAVAILABILITY - PHARMACOKINETICS AND TISSUE DISTRIBUTION STUDIES.....	104
6.1. Introduction.....	104
6.2. Materials and methods	105
6.2.1. Materials	105
6.2.2. Testing formulation preparation.....	105
6.2.3. Pharmacokinetics study.....	106
6.2.4. Tissue distribution study	107
6.2.5. HPLC determination and analysis of Q ₁₀	108
6.2.6. Statistical analysis.....	109
6.3. Results and discussion	109
6.3.1. Pharmacokinetics study of Q ₁₀	109
6.3.2. Tissue uptake and distribution of Q ₁₀	112
6.4. Conclusions.....	117
CHAPTER 7: SUMMARY AND FUTURE WORK	119
7.1. Summary of the dissertation	119
7.2. Future work and directions	120
APPENDICES.....	123
A. Optimization and validation of the SPME-GC method for citral measurement	123
B. Reagents and secretion fluids preparation for the TIM-1 model.....	126
REFERENCES.....	127

LIST OF TABLES

Table 1. Classification of emulsion type based on diameter and thermodynamic stability.	2
Table 2. Claims and justifications that can be made on beverage products. (Reprinted from Ref. 31)	11
Table 3. Examples of the composition and calorie content of some commercial beverage products currently on the market. (Adapted from Ref. 31)	12
Table 4. Recent progress in protecting citral and similar monoterpene derivatives from degradation in model systems.	16
Table 5. Recent progress in probing or improving CoQ ₁₀ 's bioavailability with formulation advancement.....	21
Table 6. Average percentages of neral and geranial retained in varied Q ₁₀ H ₂ formulations during 25 °C storage period.	45
Table 7. Properties of model synthetic and natural emulsifiers used for comparison.	61
Table 8. Mean particle size increments (nm) of citral-loaded emulsion systems stored at 25 °C and 50 °C after 60 days.	69
Table 9. Properties of four different lipid candidates as oil phase.	90
Table 10. Pharmacokinetic parameters of Q ₁₀ formulations after oral administration. .	110

LIST OF FIGURES

Figure 1. Schematic diagram of the instability mechanisms that occur in emulsions and nanoemulsions. (Reprinted from Ref. 10)	3
Figure 2. Mechanical devices or instruments that can produce nanoemulsions using high-energy approach: high pressure valve homogenizer, microfluidizer, ultrasonic jet homogenizer and ultrasonic probe homogenizer. (Reprinted from Ref. 14).....	5
Figure 3. United States functional drinks market value: \$ million, 2009-2013. (Reprinted from Ref. 40)	14
Figure 4. Chemical structures of citral's two geometrical isomers: neral and geranial. ..	14
Figure 5. A proposed mechanism of free radical and oxidation products from citral's degradation. (Reprinted from Ref. 53)	15
Figure 6. Chemical structures of three redox states of Coenzyme Q ₁₀	20
Figure 7. Definition of bioavailability as a sum of bioaccessibility and bioactivity. Physiochemical events involved in each stage. (Reprinted from Ref. 96)	25
Figure 8. pH-stat <i>in vitro</i> model for characterization of lipid digestion and bioaccessibility of lipophilic nutraceuticals.....	27
Figure 9. Schematic overview of the setup of the upper gastrointestinal trace model (TIM-1) and human colon model (TIM-2). (Reprinted from Ref. 104)	29
Figure 10. Mean emulsion particle size changes for citral-loaded emulsions with different concentrations of Q ₁₀ H ₂ stored at 25 °C (a) and 45 °C (b). Data represent the mean ± standard deviation (n=3).	43
Figure 11. Degradation profiles of neral (a) and geranial (b) in emulsions with different concentrations of Q ₁₀ H ₂ stored at 25°C in comparison with the control.	46

Figure 12. Degradation profiles of neral (a) and geranial (b) in emulsions with different concentrations of Q ₁₀ H ₂ stored at 45°C in comparison with the control.	50
Figure 13. Degradation profiles of neral (a) and geranial (b) in emulsions with 0.10 wt% of Q ₁₀ stored at 25°C in comparison with the control.	52
Figure 14. Degradation profiles of neral (a) and geranial (b) in emulsions with 0.10 wt% of Q ₁₀ stored at 45°C in comparison with the control.	53
Figure 15. Generation profiles of four major citral degradation off-flavors in the emulsions stored at 45°C: (a) <i>p</i> -cresol; (b) α , <i>p</i> -dimethylstyrene; (c) <i>p</i> -mentha-1,5-dien-8-ol; (d) <i>p</i> -methylacetophenone.	56
Figure 16. Concentrations of lipid degradation products from the emulsions stored at 45°C for 30 days: (a) 2-heptanone; (b) 1-octen-3-ol; (c) butanoic acid.	57
Figure 17. Particle size distribution profiles of citral-loaded colloidal systems (Day 0): nanoemulsions stabilized with different emulsifiers (Tween 80, Q-Naturale, SMP, PC75, LPC20) and micelles formed by Tween 80 molecules.	66
Figure 18. Mean particle size changes of citral-loaded colloidal systems stored at 25 °C (a) and 50 °C (b) during 60 days. Data represent the mean \pm standard deviation (n=3)... ..	68
Figure 19. Droplet surface charge distributions and average zeta-potential of citral-loaded emulsions stabilized by different emulsifiers (day 0).	70
Figure 20. Degradation profiles of neral (a) and geranial (b) in micelle and emulsion systems during storage at 25 °C.	72
Figure 21. Degradation profiles of neral (a) and geranial (b) in micelle and emulsion systems during storage at 50 °C.	73

Figure 22. Levels of four major citral degradation off-odors in all tested colloidal systems stored at 50 °C for 35 days: (a) <i>p</i> -cresol, (b) α , <i>p</i> -dimethylstyrene, (c) <i>p</i> -mentha-1,5-dien-8-ol, (d) <i>p</i> -methylacetophenone.	76
Figure 23. Concentrations of lipid degradation products from all tested colloidal systems stored at 50 °C for 35 days: (a) heptanal; (b) pentanal.	79
Figure 24. The cabinet of the <i>in vitro</i> gastrointestinal model, TIM-1: (a) food inlet, (b) gastric compartment, (c) duodenum compartment, (d) jejunum compartment, (e) ileum compartment, (f) semi-permeable hollow fiber membrane, (g) pyloric sphincter, (h) peristaltic valve, (i) ileo-caecal sphincter.	87
Figure 25. (a) Lipolysis curves (digestion time vs. volume of NaOH consumed) of four lipids during 2 h of <i>in vitro</i> digestion; (b) the corresponding extents of lipolysis (%).	91
Figure 26. (a) pH-stat <i>in vitro</i> lipolysis digestion curve (extent of lipolysis) of Q ₁₀ nanoemulsion and Q ₁₀ oil dispersion samples; (b) The Q ₁₀ bioaccessibility (% of input) after lipolysis in Q ₁₀ nanoemulsion and Q ₁₀ oil dispersion samples.	94
Figure 27. Bioaccessible Q ₁₀ fraction (% of input) accumulated in every 30-min digestion period from different parts of the TIM-1 model. (a) Bioaccessible Q ₁₀ fraction in jejunum filtrates from nanoemulsion; (b) Bioaccessible Q ₁₀ fraction in ileum filtrates from nanoemulsion; (c) Total bioaccessible Q ₁₀ fraction in both jejunum and ileum filtrates from nanoemulsion; (d) Bioaccessible Q ₁₀ fraction in jejunum filtrates from oil dispersion; (e) Bioaccessible Q ₁₀ fraction in ileum filtrates from oil dispersion; (f) Total bioaccessible Q ₁₀ fraction in both jejunum and ileum filtrates from oil dispersion.	96
Figure 28. Cumulative Q ₁₀ bioaccessibility (% of input) recovered during the 4h of digestion in TIM-1 model for both Q ₁₀ nanoemulsion and Q ₁₀ oil dispersion. (a)	

Cumulative Q_{10} bioaccessibility in jejunum; (b) Cumulative Q_{10} bioaccessibility in ileum;	
(c) Overall cumulative Q_{10} bioaccessibility in both jejunum and ileum.....	98
Figure 29. Bioaccessibility of $Q_{10}H_2$ and Q_{10} in both oil dispersion and nanoemulsion forms determined by the pH-stat digestion model.....	102
Figure 30. Pharmacokinetics (PK) curves of Q_{10} in the testing formulations: nanoemulsion vs. oil dispersion.....	110
Figure 31. Q_{10} 's concentrations in major organ tissues after being fed with single dosage of nanoemulsion or oil dispersion for 12 hr and 24 hr.....	114

CHAPTER 1: BACKGROUND INTRODUCTION

1.1. Emulsion science and technology

Emulsion is generally known as a colloid system consisting of two immiscible phases with one dispersed as droplets within the other continuous phase (1). In food industry, the two most commonly used liquid phases are oil and water. Basically, when the oil phase is dispersed in the water, it is called oil-in-water (O/W) emulsion, for example, milk, cream, dressing, mayonnaise, beverages, etc. Similarly, in the other case, when water becomes the dispersed phase in the oil, it is then called water-in-oil (W/O) emulsion, such as margarine and butter. Nevertheless, other types of more complicated emulsions do exist if properly designed, i.e. water-in-oil-in-water (W/O/W) emulsion and oil-in-water-in-oil (O/W/O) emulsion (2). However, these “double emulsions” usually don’t have sufficient stability for commercial applications (3). As most of the food applications aimed at delivering functional lipids, flavors, or hydrophobic compounds into aqueous-based products, O/W emulsion is by far the predominant form being widely used in the food industry (4). Therefore, in this dissertation, the term “emulsion” is generally referred to O/W emulsion, unless otherwise specified. In recent decades, with the advancement of interface and colloid science, some new types of colloidal systems have also been developed for specific applications, such as liposomes (5, 6), phytosomes (7), colloidosomes (8), etc. However, in terms of versatility in food applications, emulsion is still being the most important delivery system among others.

1.1.1. Emulsion classification

According to particle size and thermodynamic stability, emulsion can be divided into three categories: regular emulsion, nanoemulsion and microemulsion (9). Their

properties and differences are summarized in **Table 1**.

Table 1. Classification of emulsion type based on diameter and thermodynamic stability.

Emulsion type	Diameter range	Thermodynamic stability	Appearance
Regular emulsion	> 200 nm	Metastable	Optically opaque
Nanoemulsion	< 200 nm	Metastable	Transparent or slightly turbid
Microemulsion	< 200 nm (normally < 100 nm)	Stable	Transparent or high optical clarity

The regular emulsion and nanoemulsion are kinetically stable, but thermodynamically unstable systems. They will tend to breakdown during the time of storage through a variety of instability mechanisms (**Fig. 1**), i.e. gravitational separation (sedimentation/creaming), flocculation, coalescence, Ostwald ripening and phase inversion (10). Therefore, emulsion and nanoemulsion systems must be carefully designed to inhibit these mechanisms and improve shelf life of products. The major difference between these two systems is the dispersed droplet sizes in nanoemulsions ($d < 200$ nm) are much smaller than that in conventional emulsions. Thus nanoemulsions have higher optical transparency which can be used for specific applications. And also, it is reported that higher bioavailability can be achieved by using nanoemulsions in delivering lipophilic bioactive ingredients (11). The microemulsions, on the other hand, are thermodynamically stable systems under specific environmental conditions. It also contains extra small particles ($d < 200$ nm, in most cases $d < 100$ nm) with an optical transparent appearance. While it should be noted that microemulsions may also become unstable if environmental conditions are altered, such as in diluted solutions or under elevated temperatures.

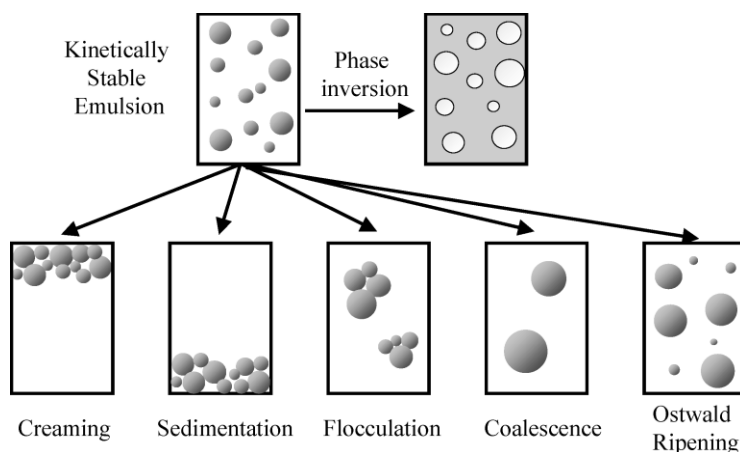


Figure 1. Schematic diagram of the instability mechanisms that occur in emulsions and nanoemulsions. (Reprinted from **Ref. 10**)

Due to structural and property similarity, there is considerable confusion between nanoemulsion and microemulsion. The major reason may lie in the prefixes used to denote them (12). As we know, “nano-” means 10^{-9} , which is smaller than the magnitude of 10^{-6} for “micro-”, therefore, people not in this area may think nanoemulsions should contain particles much smaller than microemulsions. However, this is not the case. Actually, microemulsions may have particles similar or in most of the cases even smaller than nanoemulsions. This is due to the historical development of these two systems, that the term “microemulsion” had already become well-established before the term “nanoemulsion” was introduced with the development of “nanotechnology” in the field of food science in about 15 years ago. And then the concept of “nanoemulsion” became widespread before being clearly defined and distinguished from “microemulsion”.

Theoretically, the “free energy theory” can be used to distinguish nanoemulsion from microemulsion (12). That is when comparing the free energy of both nanoemulsion and microemulsion to their phase separated states; microemulsion has a lower free energy

than the phase separated state that allows microemulsions to be formed spontaneously to favor system thermodynamic stability. Whereas nanoemulsion has a higher free energy level than phase separated state, which can only be made by energy input to overcome the activation energy differences.

In practice, however, it is still challenge to differentiate these two systems only by appearance or performance. Here gives some practical ways to distinguish them. If the sample information was given, one can refer to the emulsion composition and preparation method. Usually microemulsion requires much higher surfactant-to-oil ratio compared with nanoemulsion, but only needs simple preparation conditions, while nanoemulsion usually needs high energy input methods. While if no sample information is available for reference, one can determine the particle size distributions and particle shapes to tell the difference. Microemulsions usually show a single narrow peak in size distribution, and the particles can be spherical or non-spherical due to ultralow interfacial tension. But nanoemulsions may have single or multiple peaks with narrow or broad size distribution, while its particles are usually spherical due to Laplace pressure. More detailed information regarding the terminology, differences and similarities of nanoemulsion *versus* microemulsion can be referred to a systematic review by McClements (12).

1.1.2. Emulsion preparation methods

Generally, emulsions can be prepared with high-energy methods and low-energy methods depending on the system design and equipment availability. As mentioned, microemulsion usually can be formed spontaneously by self-assembly. Therefore, simple low-energy methods such as mild stir and agitation are sufficient to produce microemulsion. In contrast, nanoemulsion normally needs to be prepared using high-

energy methods, although it is also possible to use special low-energy methods (13).

Based on current state of the art, mechanical devices that are capable of producing nanoemulsions with extra small particle sizes are summarized in **Fig. 2** (14).

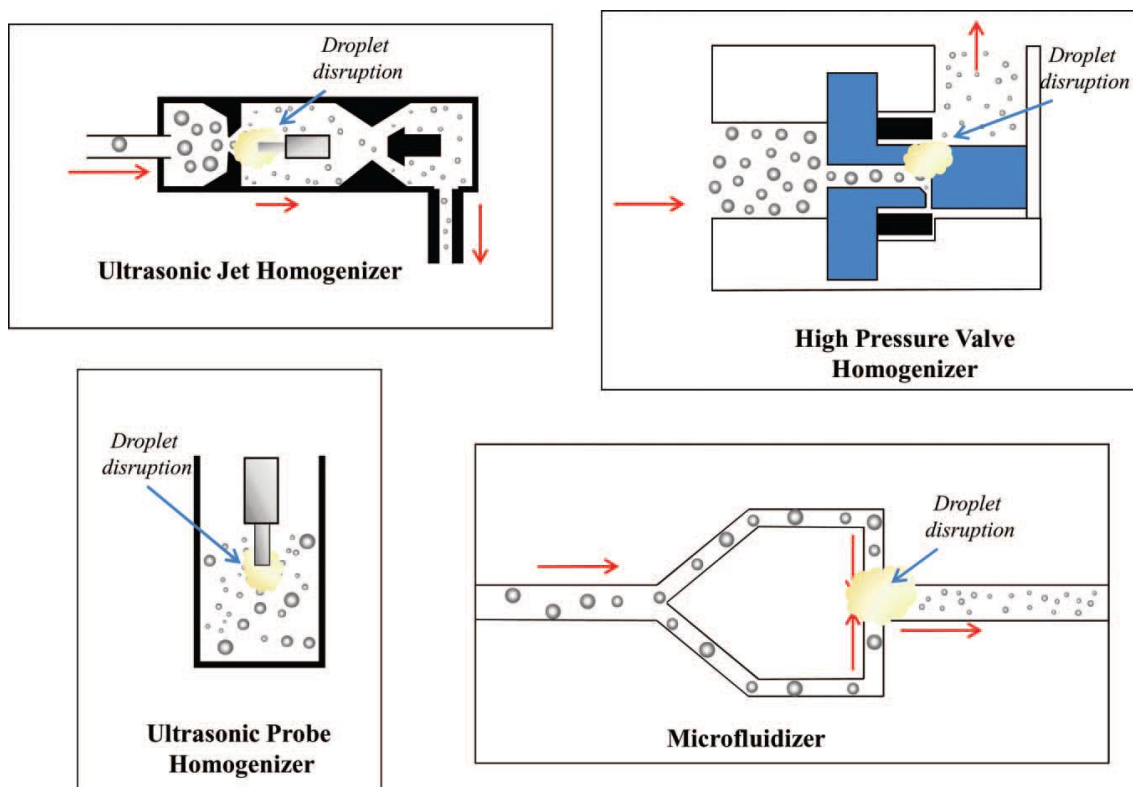


Figure 2. Mechanical devices or instruments that can produce nanoemulsions using high-energy approach: high pressure valve homogenizer, microfluidizer, ultrasonic jet homogenizer and ultrasonic probe homogenizer. (Reprinted from **Ref. 14**)

Among these devices, high pressure valve homogenizer is the most widely used one in producing both conventional emulsions and nanoemulsions (15, 16). Usually a two-step method is used to produce (nano-) emulsions. First a coarse emulsion is prepared using a high-shear/high-speed mixer, and then the emulsion pre-mix is fed into the inlet reservoir of the high pressure homogenizer for further processing. The coarse

emulsion will be pulled into the narrow chamber inside the homogenizer and passed through the valve with special design to experience intensive disruptive forces. The droplet size produced by high pressure valve homogenizer is usually correlated with the number of passes and/or the homogenization pressure applied, and also the viscosity ratio of the oil and water phases, emulsifier concentration and affinity to the interface (14, 17).

The basic principle of a microfluidizer is similar with a high pressure valve homogenizer, which also involves of using high pressure generated inside the instrument to efficiently facilitate droplet disruption. However, the design of channels through which the liquid flows is different. The microfluidizer divides the flow into two streams, with each of them passing through a narrow channel, and then impinge with each other in the interaction chamber. The intensive disruptive force will be generated when the two streams of fluid moved with ultrafast speed under high pressure. Actually, microfluidizers were traditionally used in pharmaceutical industry in earlier years (18, 19), but now have been more utilized in the food and beverage industry to produce emulsions and nanoemulsions (20-22). Recently, the success of using microfluidizer to make food-grade nanoemulsions by “one-step” method was reported (23). Without premixing the coarse emulsion, fine nanoemulsion can be directly made with oil and water phases in a single pass dual-channel processing, which is difficult to achieve by other devices.

Ultrasonic homogenizers utilize high-intensity ultrasonic waves to generate strong disruptive forces to produce ultra-small particles (24, 25). Usually the ultrasonic probe homogenizer is used in preparing bench scale or small quantity samples, while the ultrasonic jet homogenizer can be used to continuously produce relatively large-scale

products. In practice, the ultrasonic homogenizers are more suitable for low-viscosity fluids, but are less suitable for viscous systems. And there is also concern about the high local intensities involved in sonication may lead to polysaccharide de-polymerization, protein denaturation or lipid oxidation during homogenization (26).

Besides high-energy approaches, some low-energy approaches are also available to produce nanoemulsions and microemulsions, provided that the system composition was optimized, i.e. emulsifier, oil and water contents (27). The low-energy approaches will have special interest when considering the manufacturing cost, or dealing with some sensitive ingredients that are prone to degradation/oxidation. The two most commonly used methods are Spontaneous Emulsification and Phase Inversion. Detailed mechanisms and preparation methods of the current available low-energy approaches in producing emulsions and nanoemulsions are well summarized by McClements and co-workers (13, 14). It is worth mentioning that these low-energy approaches usually have limitations in starting materials and scaling up. For example, based on current knowledge, only small molecular surfactants are able to produce emulsions using spontaneous emulsification method. And the relative small production scale of low-energy approaches also limits their real applications in food and beverage industry.

1.2. Beverage Emulsion

Beverage emulsions are a special class of emulsions due to the fact that they are consumed in a highly diluted form rather than in the original concentrated form. Typically, the concentrate is diluted for 500-1000 times in a ready-to-drink (RTD) base that gives an oil concentration < 20 mg/L for the finished product (28). The final beverages can be either carbonated or not, and can be either re-homogenized or not.

Thus, the emulsions must have a high degree of stability in both concentrated and diluted forms. As mentioned in the previous session, there are many instability mechanisms of emulsions, among which, creaming is the most common phenomenon observed in diluted beverages. Beverage industry uses the term “ringing” for creaming in bottled soft drinks, because the flavor emulsion separate from the soda, floats onto the top and shows a white creamy ring or oily ring at the neck of the bottle (29).

1.2.1. Classification

It should be noted that emulsions, nanoemulsions and microemulsions can all be used as the concentrates for beverage applications, with each has its own advantages and limitations. While the classification of beverage emulsions is normally based on the functionality. Typically, beverage emulsions can be divided into two major categories: flavor emulsions and cloud emulsions (30).

The flavor emulsions provide beverages with flavors, colors, and cloudiness in some cases. A typical flavor emulsion is composed of flavor oils, antioxidant and weighting agents (if necessary) as the oil phase, and with emulsifier, coloring, sweetener, acidulant and preservatives in water phase. Flavor oils, such as orange, lemon-lime and grapefruit oils, are normally essential oils with intense flavor profiles. These flavor oils are commercially available in varying folds from different isolation and processing conditions. Usually the density, interfacial tension, viscosity, refractive index and flavor intensity increase as the oil folds increase (31).

The cloud emulsions provide only cloudiness usually with no flavor. And the oils used in cloud emulsions can be terpenes or vegetable oils (triglycerides) (32). Compared

with flavor oils, the clouding oils have extremely low water-solubility, thus are more stable to Ostwald ripening. As the main purpose of cloud oil is to produce droplets that can scatter light to give product a desirable turbidity, such as in the application of soft drinks. It becomes critical that the droplets of a cloud emulsion are within the size range where efficient light scattering occurs, while still remain good physical stability during storage, transportation and handling. Typically the desirable diameter of cloud oil droplets is around 200-500 nm (31).

1.2.2. Recent development and trends

Nowadays, consumers' choice for beverages are no longer simply dictated by a need for refreshment, but are more influenced by other factors, such as “low-calorie”, “no artificial favors/colors”, “no preservatives”, “all natural ingredients”, etc. (31) According to the regulations, some of the claims that can be made on beverages are given in **Table 2**. As a result, beverage innovators are under pressure to satisfy the evolving demands, more and more specially designed products are becoming available. Based on the current beverage market, the compositions and calorie contents of some popular commercial beverage products are summarized in **Table 3**.

Among these trends, the marketing of low calorie drinks is always a big one and has been implemented for many years. As obesity has become a global issue, people are more aware of the calorie (sugar) intake from the beverages (33, 34). In earlier years, the beverage manufacturer responded the market with a variety of low or zero-calorie products. However, problems were mainly related with the tastes, that many products failed due to low consumer acceptance (35). Recently, with the commercialization of some promising non-caloric sweeteners, together with the research progress made on

sweetness enhancers (36) and modulators (37), there have been renewed attempts for producing low-calorie beverages. Based on origins, the non-caloric sweeteners can be divided into synthetic and natural chemicals. Common synthetic sweeteners used in the beverage industry including saccharin, aspartame, acesulfame, sucralose, neotame, advantame, neohesperidin dihydrochalcone, etc. And current available natural sweeteners include stevia, mogroside, erythritol, glycyrrhizin, thaumatin, brazzein, monatin, etc. Each of these sweeteners has specific sensory properties and can be used alone or in combine with others for specific applications (38).

Besides low-calorie beverages, the “clean label” and “all-natural” products are also drawing huge attentions in recent years. It seems that any products with the “Natural” claim are always much attractive than others. As a trend, most synthetic flavors are being replaced with natural ones; synthetic colors are being removed with the introduction of natural alternatives, and many other ingredients (such as weighing agents, preservatives, antioxidants, etc.) are either being removed or listed as clean. However, problem of the natural ingredients is that they are normally less robust compared with the synthetic ones, and also being more expensive. For example, natural colors (such as carotenoids) may degrade rapidly when exposed under light and heat. And natural emulsifiers (such as proteins) are sensitive with the change of pH, heat and ionic conditions. Therefore, more factors need to be considered before an all-natural product being prototyped and launched. Though with challenges, all manufacturers are still making every possible effort to align their products with the explosively increasing “clean label” market.

Table 2. Claims and justifications that can be made on beverage products. (Reprinted from **Ref. 31**)

Claim	Justification	Regulation Source
“0 calorie”	Less than 5 cal per RACC.	21 CFR 101.60(b)
“All natural”	Undefined, but regarded as a product is free of any synthetic ingredients.	N/A
“Artificially flavored”	Any substance that impart flavor that is not derived from its natural source.	21 CFR 101.22(a)(1)
“Contains % juice”	For juice made from concentrate, calculated use percentage from the Brix table in 21 CFR 101.30(h)(1) as the basis for 100% juice.	21 CFR 101.30(j), 21 CFR 101.30(h)
“Excellent source of vitamin”	Contains 20% or more of the DV per RACC.	21 CFR 101.54(b)
“Good source of vitamin”	Contains 10%-19% of the DV per RACC.	21 CFR 101.54(e)
“Low calorie soda”	40 cal or less per RACC.	21 CFR 101.60(b)
“Low sodium”	140 mg or less per RACC.	21 CFR 101.61
“Natural and artificial flavor”	Contains natural and artificial flavors.	21 CFR 101.22(a)(1), 21 CFR 101.22(a)(3), 21CFR(g)101.22(3)
“Naturally flavored”	The flavor constituents function in the food as flavor, not solely as a source of nutrition is derived from its natural source in nature.	21 CFR 101.22(a)(3)
“No added sugar”	No sugar or sugar-containing ingredients are added during processing.	21 CFR 101.60(c)(2)
“No artificial colors”	Contains no colorant source outside the principal flavor components of beverage. Natural color is considered artificial color when used for colorant purposes.	21 CFR 101.22(k)(1)(2), 21 CFR 74
“No HFCS”	Cannot contain HFCS.	21 CFR 101.65(b)(1)(2)
“No preservatives”	Cannot contain preservatives.	21 CFR 101.65(b)(1)(2)
“No pulp”	Cannot contain pulp.	21 CFR 101.65(b)(1)(2)
“Reduced sugar”	At least 25% less sugars per RACC than an appropriate reference food.	21 CFR 101.60(c)

RACC: Reference amounts customarily consumed; DV: Daily values; HFCS: High fructose corn syrup; CFR: Code of Federal Regulations.

Table 3. Examples of the composition and calorie content of some commercial beverage products currently on the market. (Adapted from **Ref. 31**)

Product	Brand	Manufacturer	Sweetener	Calories (per 8 oz.)	Emulsifier	Weighting agent	Natural claim
Half & Half Iced Tea Lemonade	Arnold Palmer	AriZona	HFCS, Sucralose, Ace- K	50	GA	None	No
Half & Half Iced Tea Lemonade	Arnold Palmer Zero	AriZona	Sucralose	0	GA	None	No
Cherry Citrus	BodyArmor	Body Armor Nutrition	Cane Sugar	70	GA	EG	Yes
Tropical Mandarin	BodyArmor	Body Armor Nutrition	Cane Sugar	70	GA	EG	Yes
Lemon Lime	Xion4 (Powerade)	Coca-Cola	HFCS	80	GA	EG	No
Orange	Xion4 (Powerade)	Coca-Cola	HFCS	80	GA	EG	No
Sour Melon	Xion4 (Powerade)	Coca-Cola	HFCS	80	M-FS	SAIB	No
Orange Soda	Fanta	Coca-Cola	HFCS	120	M-FS	EG, BVO	No
Original Citrus	Fresca	Coca-Cola	APM, Ace-K	0	GA	EG, BVO	No
Energy - Tropical Citrus	Vitamin Water	Coca-Cola	Fructose, Cane Sugar	120	GA	EG	No
Essential Orange - Orange	Vitamin Water	Coca-Cola	Fructose, Cane Sugar	120	GA, M-FS	EG	No
Squeezed Lemonade	Vitamin Water Zero	Coca-Cola	Erythritol, Rebiana	0	GA	EG	No
Orange Soda	Sunkist	Dr. Pepper Snapple	HFCS	110	M-FS	EG	No
Orange	Diet Crush	Dr. Pepper Snapple	APM, Ace-K	0	GA	EG	No
Citrus Soda	Sun Drop	Dr. Pepper Snapple	HFCS	120	GA	EG, BVO	No
Pineapple Orange Guava	Nantucket Nectar's	Dr. Pepper Snapple	Sucrose	120	GA	None	Yes
Orange Mango	Nantucket Nectar's	Dr. Pepper Snapple	Sucrose	120	GA	None	Yes
Strawberry Kiwi	Snapple	Dr. Pepper Snapple	Sucrose	100	GA	EG	Yes
Lemonade	Gatorade G- Series	PepsiCo	Sucrose	80	GA	EG, SAIB	No
Lemon-Lime	Gatorade G- Series	PepsiCo	Sucrose	80	GA	EG	No
Orange	Gatorade G- Series	PepsiCo	Sucrose	80	GA	EG, BVO	No
Citrus Soda	Mtn Dew	PepsiCo	HFCS	110	GA	BVO	No
Citrus Soda	Mtn Dew Diet	PepsiCo	APM, Ace-K	0	GA	BVO	No
Lemon	Nature's Blend	Poland Spring	Cane Sugar	50	GA	EG	Yes

Ace-K: Acesulfame Potassium; APM: Aspartame; BVO: Brominated vegetable oil; EG: Ester Gum; GA: Gum acacia; HFCS: High fructose corn syrup; M-FS: Modified-food starch; SAIB: Sucrose acetate isobutyrate.

1.3. Functional beverage

Functional beverage is a subsector of functional food, and is by far the most active form of food that can be consumed anytime, anywhere with convenience to meet consumer demands (39). Like functional food, there is no officially announced definition for functional beverage. Generally, it can be considered as a type of non-alcoholic drinks that can provide additional health benefits beyond satisfying the basic sensory needs. For example, they can be specially designed to improve heart health, immune wellness, digestion, joint health, or have the effect of energy-boosting by fortifying specific functional ingredients, including but not limited to vitamins, minerals, herbs, nutraceuticals or additional raw fruits and vegetables.

There was a very fast growing speed for the functional beverages market values in recent years. According to a newly released industry profile report (40), the United States functional drinks market grew by 7.4% in 2013 to reach a value of \$27,049.6 million (**Fig. 3**). And in 2018, it is forecast to reach the value of \$41,292.6 million, an increase of 52.7% since 2013. PepsiCo, Coca-Cola, Red Bull and Monster Beverage being the four biggest industrial leaders share majority of the market. And among the launched functional beverage products, energy drinks share the highest (63.8%) market, followed by sports drinks (32.3%), and nutraceutical drinks (3.9%).

Therefore, more researches on beverage emulsions, especially nutraceutical emulsions are needed to supply the market with more innovative products. Recently, many researches on designing functional emulsion systems with potential applications in beverages were reported. Many vitamins or nutraceuticals, including Vitamin E (41), β -carotene (42, 43), curcumin (44), ω -3 fatty acids (45), were successfully fortified into the

emulsion formulations with increased stability, dosage, or bioavailability.

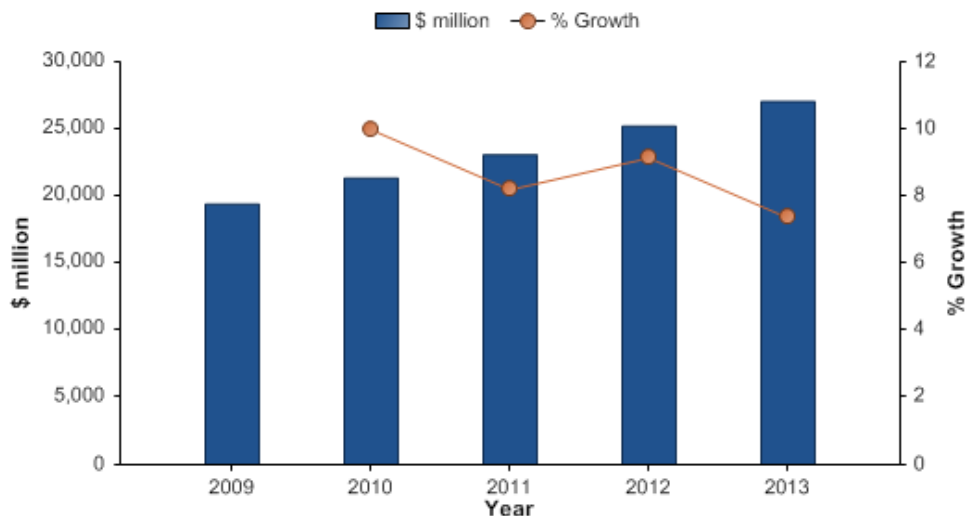


Figure 3. United States functional drinks market value: \$ million, 2009-2013. (Reprinted from Ref. 40)

1.4. Citral

Citral, one of the most important flavoring compounds with strong lemon aroma and high consumer acceptance, is widely used as an additive in foods, beverages and perfumery industries (46). Chemically, it is a 3,7-dimethyl-2,6-octadienal, with two geometrical isomers (Fig. 4): neral (*Z*-configuration) and geranial (*E*-configuration). The natural occurring ratio of neral and geranial in citral is about 2:3.

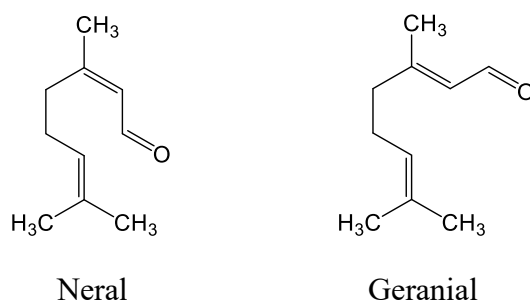


Figure 4. Chemical structures of citral's two geometrical isomers: neral and geranial.

1.4.1. Challenges with citral's application

The long existing problem that limits citral's application is its rapid degradation and oxidation under acid catalization and oxidative stress during processing and storage in acidic beverages (47, 48). The degradation of citral leads to the major loss of the lemon-like aroma and also the generation of many undesired off-flavors (49-51). The complicated degradation mechanism of citral is not completely established and understood by far. A previously proposed free radical and oxidation products formed from citral is presented in **Fig. 5** (52, 53). Among all types of degradation products from citral, some of the acid-catalyzed isomerization compounds such as *p*-cymene, *p*-cymene-8-ol and its dehydration product, α ,*p*-dimethylstyrene were previously postulated to contribute to the major potent off-odors (49, 50). But later studies further claimed some autoxidation compounds like *p*-cresol and *p*-methylacetophenone, which have lower odor thresholds of 0.3-1.0 ng/L and 2.7-10.8 ng/L in air respectively, to be more responsible for the undesired odorant (51, 52).

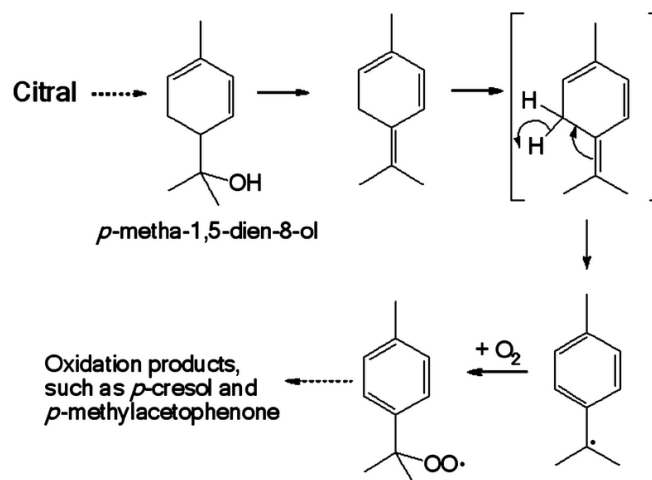


Figure 5. A proposed mechanism of free radical and oxidation products from citral's degradation. (Reprinted from **Ref. 53**)

1.4.2. Strategies to prevent citral from degradation

To protect citral from rapid degradation and minimize the major potent off-flavor generation, many strategies have been investigated by using food chemistry and engineering principles, including spray drying encapsulation, micelles and reverse micelles systems, emulsion and nanoemulsion systems, surface modification of the emulsion droplets, multi-layer emulsions, addition of varying antioxidants, etc. An overview of the recent development of strategies in protecting citral from degradation is summarized in **Table 4**.

Table 4. Recent progress in protecting citral and similar monoterpene derivatives from degradation in model systems.

Reference	System	Design	Results
Kimura <i>et al.</i> (49)	Aqueous solvent system with antioxidant	BHT, BHA, α -tocopherol, Eucalyptus leaves extract, etc. as antioxidant	None of the tested compounds was effective in decreasing the generation of oxidative products.
Peacock <i>et al.</i> (50)	Carbonated beverage system with antioxidant	Iso-ascorbic acid as antioxidant	Iso-ascorbic acid could react with oxidizing agents, and inhibited the formation of α - <i>p</i> -dimethylstyrene and <i>p</i> -cymen-8-ol.
Bertolini <i>et al.</i> (54)	Spray dry encapsulation	Gum arabic as wall material	Citral stability was improved with the protection of wall material.
Liang <i>et al.</i> (55)	Aqueous buffer system with antioxidant	Grape seed, pomegranate seed, green tea and black tea extracts as antioxidant	The added phenolic extracts could not inhibit citral degradation, but significantly inhibited <i>p</i> -methylacetophenone formation.
Ueno <i>et al.</i> (56)	Aqueous buffer system with antioxidant	Black tea theaflavins as antioxidant	Theaflavins showed inhibitory effects on the formation of <i>p</i> -cresol and <i>p</i> -methylacetophenone.
Djordjevic <i>et al.</i> (57)	Emulsion	SDS-chitosan and gum arabic as emulsifier	Citral degraded less in gum arabic stabilized emulsion, but formation of <i>p</i> -cymene was less in SDS-chitosan stabilized emulsion.
Djordjevic <i>et al.</i> (58)	Emulsion	WPI and gum arabic as emulsifier	Citral degraded less in gum arabic stabilized emulsion, but formation of <i>p</i> -cymene was less in WPI stabilized emulsion.
Choi <i>et al.</i> (59)	Emulsion /	MCT and triacetin as oil phase, stabilized by	Incorporation of both oil phases in the emulsion system protected citral

	microemulsion	Brij 35 as emulsifier	from degradation.
Mei <i>et al.</i> (60)	Emulsion / solid lipid emulsion	Liquid and solid octadecane as lipid phase	Crystallization of solid lipid increased citral's partition into aqueous phase, thus resulted in faster degradation of citral.
Choi <i>et al.</i> (61)	Emulsion	Lauryl alginate (cationic), Brij 35 (non-ionic), and SDS (anionic) as emulsifier	Anionic surfactant stabilized emulsion attracted high concentration of protons thus promoted citral's degradation.
Choi <i>et al.</i> (62)	Micelle / reverse micelle	Tween 80 and PGPR as amphiphilic agent	Formation of both micelles and reverse micelles increased citral's stability.
Strassburger <i>et al.</i> (63)	Microemulsion in juice beverages	Cyclodextrins as encapsulation agent	Citral's chemical stability improved in the tested system.
Rungsardthong <i>et al.</i> (64)	Molecular complex	α -, β -, and 2-hydroxypropyl- β -cyclodextrin as encapsulation agent	Citral's stability improved when incorporated in cyclodextrin matrix.
Rosa <i>et al.</i> (65)	Spray dry encapsulation	Sucrose and trehalose as matrix	Citral retention was similar for matrices containing either trehalose or sucrose.
Yang <i>et al.</i> (53)	Nanoemulsion combined with antioxidant	Black tea extract, ascorbic acid, naringenin, tangeretin, β -carotene, and tanshinone as antioxidant	Addition of appropriate lipophilic antioxidants (β -carotene, tanshinone, black tea extract) could enhance citral's chemical stability.
Yang <i>et al.</i> (66)	Multilayer emulsion	Chitosan and ϵ -polylysine as coatings added to primary emulsion droplets	Addition of chitosan layer improved the stability of citral, while adverse effect was found in the ϵ -polylysine coated system.
Zhao <i>et al.</i> (67)	Nanoemulsion combined with antioxidant	Ubiquinol of different concentrations as antioxidant	Appropriate concentration of ubiquinol can effectively improve citral's stability in nanoemulsion.
Maswal <i>et al.</i> (68)	Micelle in aqueous system	Brij 30 and Brij 35 as amphiphilic agent	Chemical degradation of citral found to be reduced within the micelle systems.
Park <i>et al.</i> (69)	Micelle in aqueous system	Brij 35, 58, 78, and 700 as amphiphilic agent	No significant difference of citral degradation rate in Brij micelles formed with different hydrophobic tail length and hydrophilic head.
Yang <i>et al.</i> (70)	Emulsion	Soy protein-polysaccharides Maillard reaction product as emulsifier	Citral's stability was improved with better physical stability of emulsion prepared.
Xiang <i>et al.</i> (71)	Multilayer emulsion	Milk proteins and beet pectin as emulsifier	Secondary emulsion had better physical stability and protected citral better than primary emulsion.

BHT: 2,6-di-tert-butyl-*p*-cresol; BHA: 3-tert-butyl-4-hydroxyanisoles; SDS: sodium dodecyl sulfate; WPI: whey protein isolate; Brij: polyoxyethylene lauryl ether; PGPR: polyglycerol polyricinoleate.

Although many of the above mentioned studies reported improved citral stability or inhibited degradation products generation in tested systems, still many unsolved issues need to be further studied and improved. For instance, spray drying will protect citral from degradation within the capsule. However, when the spray-dried flavor powders are applied in the liquid beverages, the instability problem of citral recurs. Indeed, emulsion is the most widely used delivery system of citral or lemon oil for beverage applications. Most studies only focused on citral's stability in concentrated emulsion systems, while it might be another case when the emulsion concentrates get diluted in the final products, as the oil concentration becomes much lower and that might facilitate citral's partitioning into the aqueous phase and become unstable. The concept of multilayer emulsion seems rewarding, but the coating of additional layers usually produces relatively big emulsion droplets with limited applications and extra cost. Moreover, it is important to select proper emulsifiers and other ingredients for the citral-loaded systems, such as switching some of synthetic emulsifiers and antioxidants into natural/organic alternatives for clean label purpose. Last but not least, it is worth mentioning that protein based ingredients are generally not appropriate to stabilize citral. Because most proteins are known to either reversibly (physicochemically) or irreversibly (chemically) interact with flavors, and result in the reduction of flavor intensity (flavor fade) (72). As citral is an aldehyde, theoretically it will form covalent bonds (Schiff-bases) with the amide side chains of proteins, which affects citral's release, perception and analysis.

Obviously, some of the previous work need to be better designed and more systematic work should be proposed and conducted for better understanding of citral's degradation kinetics and applications in beverage systems.

1.5. Coenzyme Q₁₀

Coenzyme Q₁₀, also known as CoQ₁₀ or Q₁₀, is a group of lipid soluble, vitamin-like compounds essential for the electron transport chain in mitochondria for energy (ATP) production (73). Chemically, it is a 2,3-dimethoxy-5-methyl-6-decaprenyl-1,4-benzoquinone. Because of its ubiquitous distribution in nature, it is also named as ubiquinone. CoQ₁₀ has been recognized for its potential benefits particularly in reference to cardiovascular and neurodegenerative diseases (74-76).

CoQ₁₀ is also an essential and potent antioxidant in human body that scavenges free radicals generated under oxidative stress. It exists in three redox states (**Fig. 6**) (77): the fully oxidized ubiquinone (Q₁₀); partially reduced ubisemiquinone (Q₁₀^{•-}); and fully reduced ubiquinol (Q₁₀H₂). These compounds can be recycled *in vivo* by the mitochondrial respiratory chain. Ubiquinol (Q₁₀H₂) is the “activated” form responsible for the antioxidant and health promoting properties. In contrast to other antioxidants, this compound inhibits both the initiation and the propagation of lipid and protein oxidation (78) and is capable of regenerating other antioxidants such as α -tocopherol (77). Recent studies also revealed its functions in lipoprotein protection, gene expression involved in human cell signaling, metabolism and transport. Although CoQ₁₀ can be biosynthesized *in vivo*, age-related decline in human body will cause accelerated aging and diminished energy levels. Therefore, CoQ₁₀ is now a commercialized nutraceutical in many dietary supplements on the market, and is gaining more attention as well as consumer acceptance. Furthermore, the addition of CoQ₁₀ as a functional nutraceutical in beverage products, such as energy drinks, is a promising and appreciable trend.

Coenzyme Q₁₀

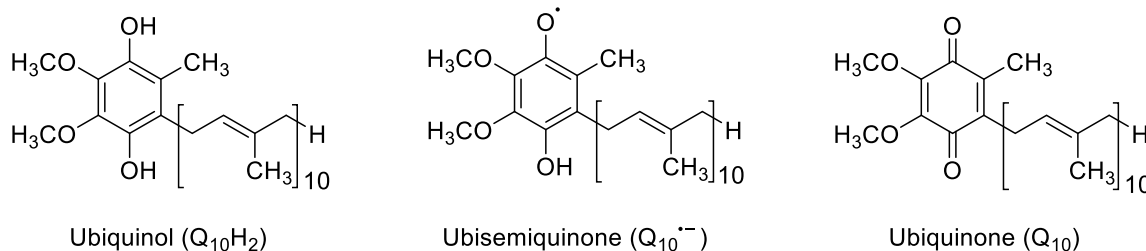


Figure 6. Chemical structures of three redox states of Coenzyme Q₁₀.

1.5.1. Problems associated with CoQ₁₀ as dietary supplement

Due to high molecular weight (863.34 g/mol) and poor water solubility, CoQ₁₀ has very limited oral bioavailability. The concept and factors related with bioavailability will be systematically introduced in the next session. In simple words, CoQ₁₀ is difficult to be absorbed by gastrointestinal tract and then becomes available for utilization in human body when ingested orally.

Currently, most of the commercially available CoQ₁₀ supplements are oil-based suspensions in softgel capsules and powder-filled hardshell capsules or tablets. However, many animal or human trials indicated low bioavailability of CoQ₁₀ in these products. Weis *et al.* (79) tested the bioavailability of four oral CoQ₁₀ formulations (one hard gelatin capsule and three soft gelatin capsules) in healthy volunteers. No significant difference was observed except for a formula with soybean oil suspension of CoQ₁₀. Nevertheless, all tested formulations still had very low bioavailability of CoQ₁₀. Miles *et al.* (80) also reported the bioequivalence of CoQ₁₀ from some over-the-counter supplements in an study with nine health adults, and found a non-solubilized powder product was minimally absorbed. While the results showed some solubilized products

had improved bioavailability compared with the reference.

Overall, it is still a challenge to design novel formulations of CoQ₁₀ supplements with high bioavailability at current stage, especially when considering the source of ingredients, and versatility of applications.

1.5.2. Strategies to improve CoQ₁₀'s bioavailability

In recent years, some solubilized forms of CoQ₁₀ were developed and launched by different companies, which were claimed to have improved bioavailability. Other approaches and systems for delivering CoQ₁₀ were also reported, such as using solid dispersion, microspheres, nanoparticles, nanoemulsions, liposomes, self-emulsifying drug delivery systems (SEDDS), molecular complexation with cyclodextrin, and many other patented hydrocolloid systems (81). A brief summary of recent work related with formulation development to improve CoQ₁₀'s bioavailability is summarized in **Table 5**.

Table 5. Recent progress in probing or improving CoQ₁₀'s bioavailability with formulation advancement.

Reference	System	Formulation Design	Testing Model	Conclusion
Kommuru <i>et al.</i> (82)	SEDDS	Labrasol as emulsifiers, lauroglycol as cosurfactant, and Myvacet 9-45 as oil.	Dog	A two-fold increase in bioavailability was observed for SEDDS compared to a powder formulation.
Zaghloul <i>et al.</i> (83)	Q-Gel [®] Q-NoI [™]	Patented soft gelatin capsules containing MCT sorbitol and sorbitan monooleate.	Dog	The relative bioavailability of Q-Gel [®] and Q-NoI [™] were 3.6 and 6.2-fold higher than that of a powder-filled capsule.
Schulz <i>et al.</i> (84)	Solu [™] Q ₁₀	Patented soft gel capsule with MCT and polysorbate-80.	Human	Better bioavailability of Solu [™] Q ₁₀ observed compared with oil dispersions and crystalline forms of CoQ ₁₀ .
Terao <i>et al.</i> (85)	Complex with γ -CD	Molecular encapsulation of CoQ ₁₀ by complexation with γ -CD, compared with	Human	Bioavailability significantly increased after single administration of CoQ ₁₀ - γ -CD

		CoQ ₁₀ with MCC.		than CoQ ₁₀ -MCC formulation.
Hosoe <i>et al.</i> (86)	Kaneka QH™	Soft gelatin capsules containing ubiquinol emulsified with diglycerol monooleate, rapeseed oil, lecithin and beeswax.	Human	Significantly improved plasma concentration of ubiquinol was observed after single and multiple doses of ingestion.
Hatanaka <i>et al.</i> (87)	Nanoemulsion (NE), dry-emulsion (DE)	NE made with MCT and surfactants; DE made with gum arabic and sugar alcohol by spray dry.	Rat	NE was most effective for improving the bioavailability of CoQ ₁₀ in all tested formulations.
Liu <i>et al.</i> (88)	CoQsource®	A commercial self-assembling colloidal system - VESIsorb®.	Human	Significantly improved bioavailability was observed in tested formulation compared with a CoQ ₁₀ oil suspension.
Ok <i>et al.</i> (89)	Nanoparticle (NQ20)	Emulsified with a sucrose fatty acid ester, poly-glycerin fatty acid ester, and sucrose.	Rat	Increased plasma CoQ ₁₀ levels were observed when NQ20 was administered compared to an oil suspension.
Cho <i>et al.</i> (90)	Emulsion	Emulsion stabilized by Tween 80 with different particle sizes.	Rat	CoQ ₁₀ level was highest in small intestinal tissues when ingested with emulsion of smallest particle size.
Zhou <i>et al.</i> (91)	Lipid free Nano-vehicle	CoQ ₁₀ stabilized by different surfactants: TPGS, Cremophor RH40, PSAE, etc. in glycerol aqueous solution.	Rat	Compared with CoQ ₁₀ suspension, nano-CoQ ₁₀ modified with surfactants significantly increased plasma concentration and AUC.

MCT: medium chain triglyceride; γ -CD: γ -cyclodextrin; MCC: microcrystalline cellulose; TPGS: D- α -Tocopherol polyethylene glycol 1000 succinate; PSAE: polyglycerol 10 stearic acid ester.

Among these studies, majority of designed colloid systems improved the bioavailability of CoQ₁₀ by increasing its solubility, or reducing the droplet size of vehicles. However, most of the above mentioned CoQ₁₀ formulations are pharmaceutical grade made with synthetic or non-food ingredients. Not much work has been done to fortify CoQ₁₀ with food-grade or natural ingredients, especially for functional beverage and drink applications. Therefore, more efforts should further be addressed to develop and investigate food-grade delivery systems for solubilized form of CoQ₁₀ using novel ingredients and techniques.

1.6. Bioavailability

The term bioavailability is a central concept in designing and evaluating bioactive ingredients or nutraceuticals fortified in functional foods. Depending on the research area, bioavailability has several working definitions (92). In pharmacology, bioavailability is a measurement of the rate and extent to which a drug reaches the systemic circulation (93). Theoretically, when a drug is administered intravenously, it will have 100% bioavailability. However, when it is administered through other routes, such as orally or parenterally, its bioavailability generally decreases and varies from one to another due to physiological and physiochemical barriers. In food and nutritional sciences, the final nutrient or dietary ingredient concentration at the site of action, which may be utilized for the desired physiological functions, defines bioavailability (94).

Usually, oral route is most considered for bioavailability studies, as many medications and almost all foods are ingested from mouth. However, due to the physiological complexity of digestive system and numerous biological interactions and chemical reactions involved, it is difficult to predict the oral bioavailability of nutrients and bioactives. As we know, human digestive system consists of gastrointestinal (GI) tract together with many accessory organs, including salivary glands, pancreas, liver, and gallbladder (95). Take a chewable dietary supplement for example. Its journey through the digestive system starts in mouth, where it is masticated into small pieces (bolus) with the action of teeth, and its digestion is initiated with enzymes in saliva. Then the bolus passes down through esophagus and enters into stomach, where the gastric juice continues digestion process to further breakdown bolus into chyme with the help of peristalsis and enzymes. At certain gastric emptying rate, chyme is then transported into

small intestine through pylorus. Small intestine, including duodenum, jejunum, and ileum, is the region in GI tract where digestion and absorption of most lipids, nutrients, or bioactive ingredients take place. The material that is not absorbed in small intestine will then go into large intestine for further fermentation. Some becomes fecal matter and is finally eliminated from the body.

In both pharmacology and food nutrition sciences, oral bioavailability is usually determined with *in vivo* tests using different subjects, including clinical trials and different animal models, such as dogs, rats, mice etc., depending on the system design and resources availability. Area under curve (AUC) plotted with the blood concentration of tested compound versus the defined testing time after ingestion is usually calculated to indicate and compare its relative bioavailability in tested formulations.

However, as using *in vivo* models can be practically and ethically complex, measuring the *in vitro* bioaccessibility of a compound is a simplified alternative, and is gaining popularity especially in food and nutrition researches for rapid screening of formulations (96). Bioaccessibility is defined as the fraction of a compound released from its matrix in the gastrointestinal tract and becomes available for absorption (97). In brief, bioaccessibility includes the events that take place during the digestion of food matrix into a form that can be potentially assimilated by the body, but not including systemic bioactivities associated with its post-intestinal absorption, such as transportation and target delivery of the compound; interaction, biotransformation, and metabolism that it may undergo; also the generation of biomarkers and the related physiological responses (96). Therefore, bioavailability can also be defined as a sum of both bioaccessibility and bioactivity (**Fig. 7**). The fraction of a compound that is bioaccessible does not necessarily

mean it will finally become bioavailable. Nevertheless, oral bioavailability is positively correlated with the bioaccessibility, together with the subsequent bioactivities associated with transport efficiency and metabolism resistibility.

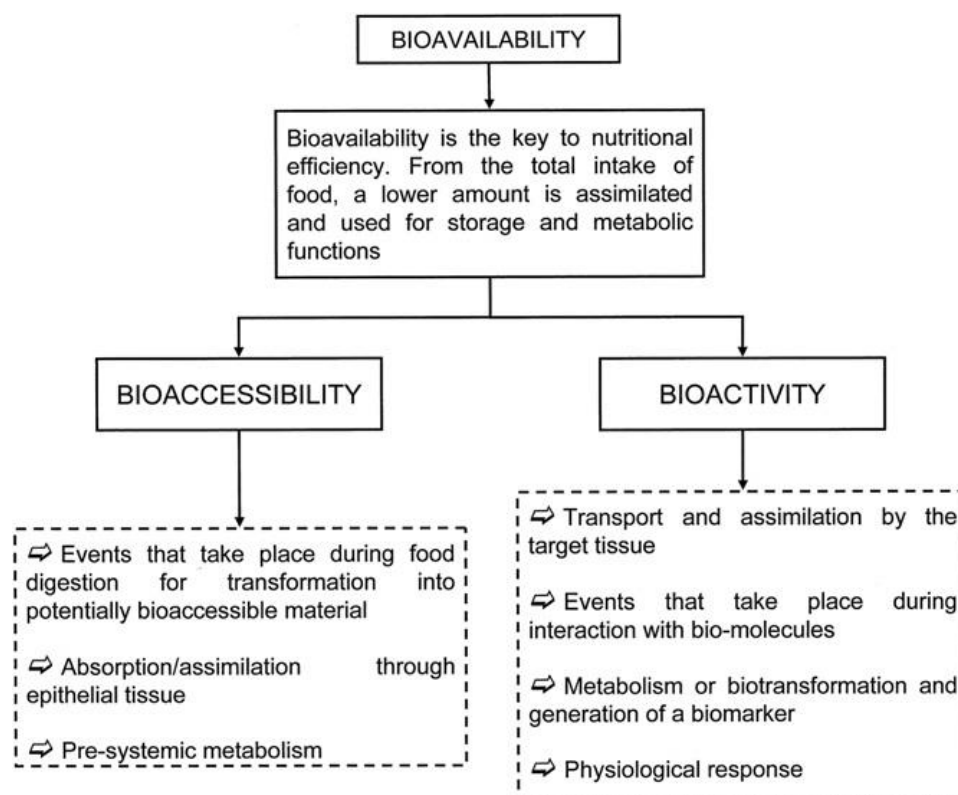


Figure 7. Definition of bioavailability as a sum of bioaccessibility and bioactivity. Physiochemical events involved in each stage. (Reprinted from **Ref. 96**)

1.6.1. Bioaccessibility and common *in vitro* models

Basically, to gain information of a compound's bioaccessibility, it is critical to learn its digestion kinetics in the GI tract. Currently, a number of *in vitro* models are available to simulate the digestive process, where researchers have garnered information regarding the bioaccessibility of nutraceuticals (98). Based on design, these *in vitro* models can be generally divided into single-step and multi-step models. Single-step

models only consider one specific region of the GI tract, such as stomach, small intestine or colon, with the small intestine conditions being mostly simulated. While multi-step models are usually more complicated, and consider two or more regions of the GI tract.

❖ pH-stat model

The pH-stat model is widely used in the pharmaceutical and nutraceutical research for *in vitro* bioaccessibility characterization of lipophilic drugs or nutraceuticals based on the process of lipid digestion (99, 100). It mimics digestion with simulated small intestinal fluid (SSIF) containing lipase, bile salts, phospholipids and other ingredients in a stable intestinal pH and temperature condition. In brief, when testing sample is exposed with SSIF, lipid digestion is largely initiated by the action of lipase. Drugs or nutraceuticals will release from the lipid phase and a certain fraction of them will migrate into the hydrophobic core of micellar structures formed by lipid digestion products and bile salts, thus becomes bioaccessible. Although experimental details may differ slightly based on design and condition, the theory and fundamental principles are analogous. Basically, it assumes that upon digestion, one mol of triglyceride releases two mols of free fatty acids (FFAs) and consumes two mols of NaOH for neutralization to maintain the pH. The extent of lipolysis, defined as the percentage of triglycerides digested during lipolysis, can be determined from the amount of NaOH consumed during the real-time lipolysis digestion. And the bioaccessible fraction of drugs or nutraceuticals can be determined by analyzing their concentrations in the solubilized micellar phase after lipolysis. The setup of pH-stat *in vitro* model and associated information are shown in **Fig. 8**.

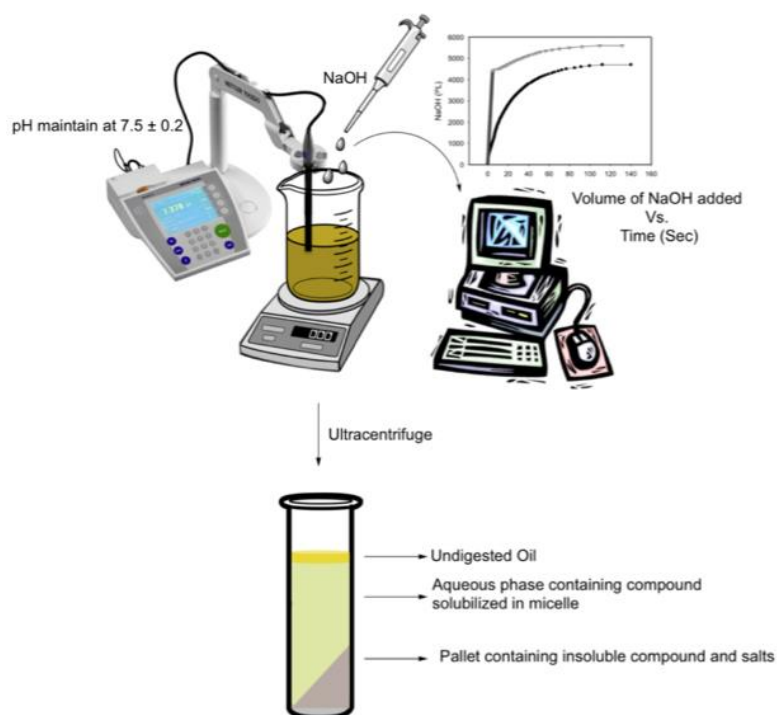


Figure 8. pH-stat *in vitro* model for characterization of lipid digestion and bioaccessibility of lipophilic nutraceuticals.

It should be noted that the pH-stat model only simulates digestion condition in small intestine. However it can also be upgraded into multi-step models by combining with the simulation of other regions of GI tract, such as mouth, stomach (101, 102). But regardless of number of factors considered, the pH-stat model and its derivatives are considered as static models, due to the fact that they are not able to mimic dynamic physical conditions in GI tract (103), such as peristalsis motion, transitional change in physiological environment, etc.

❖ TNO gastro-intestinal model (TIM)

The TNO gastro-Intestinal Model (TIM) developed by TNO Quality of Life (Zeist,

The Netherlands) is a more sophisticated dynamic *in vitro* digestion system. According to the region of GI tract it stimulates, there are two TIM systems. TIM-1 mimics the upper GI tract including stomach and small intestine and TIM-2 mimics the large intestine (104). Schematic setup of both TIM-1 and TIM-2 systems are shown in **Fig. 9**.

For digestion and bioaccessibility study, TIM-1 system is by far the most complicated and precise model. It simulates the successive dynamic events occurring in the lumen of the stomach (monogastric) and small intestine. For small intestine, it further subdivided into the duodenum, jejunum and ileum. This computer-controlled *in vitro* model controls temperature, pH conditions in stomach and different compartments of the small intestine, concentrations of gastric and intestinal enzymes, levels of bile salts in different parts of the gut, etc. It is a dynamic multi-step model that can also mimic the peristalsis motion in GI tract, gastric emptying, and transition of chyme. The bioaccessible fraction is determined by continuous sampling from jejunum and ileum compartments over a preset time period. Quite a few validation studies using the TIM-1 have been done focusing on the bioaccessibility of fat soluble vitamins (104, 105), water soluble phytonutrients (106-108), and several pharma studies (109, 110) demonstrating excellent correlations with *in vivo* data.

The TIM-2 system is more focused on understanding the metabolism of certain active compounds that escapes from the digestion in the upper GI tract and enters into large intestine (111), investigating the undigested fraction and its further digestion and fermentation on the activity and composition of the gut microbiota (112, 113), or testing the prebiotic activity of non-digestible carbohydrate compounds (114).

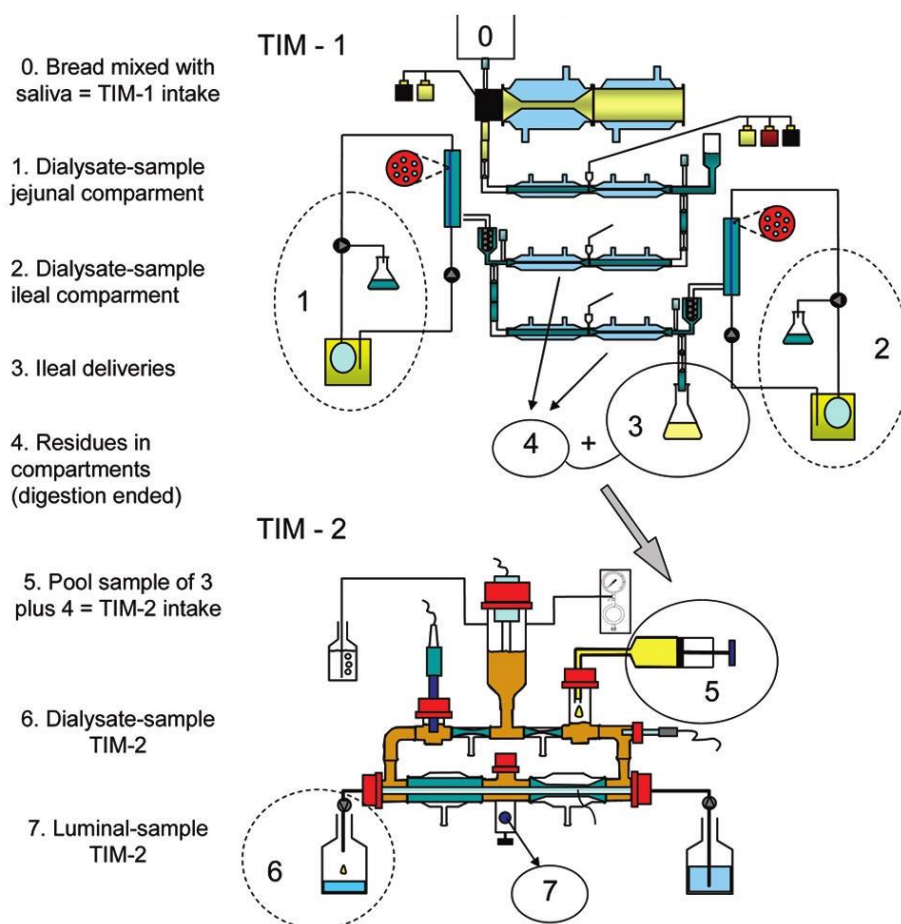


Figure 9. Schematic overview of the setup of the upper gastrointestinal trace model (TIM-1) and human colon model (TIM-2). (Reprinted from **Ref. 104**)

1.6.2. Transport coefficient

After a hydrophobic compound becomes solubilized in bile salts micelles and vesicles, it has to go through a mucous layer before reaching the surface of small intestine epithelial cells (115). Then absorption of the compound through small intestine occurs through two routes, transcellular and paracellular. Usually small molecules ($M_w < 200$) might be able to go paracellularly through tight junction and do not go through the enterocytes, and thus can escape from the intestinal cellular metabolism (116). While majority of compound transportation uses the transcellular route. The compound with its

vehicles is absorbed into the enterocytes through either passive diffusion, which is driven by concentration gradient, or active transport through specific protein channels on the surface of the epithelial cells (103).

Since the transportation coefficient of a compound through the enterocytes is limited by its permeability, interaction with enterocytes, and resistibility to cellular metabolism, a model only considering of the physicochemical factors is usually not sufficient to stimulate this process. The most widely used *in vitro* model is the Caco-2 cell model, which also takes biological factors during permeation into account. Caco-2 model is a single layer of properly differentiated human colon carcinoma cells into phenotype with the similar physiological functions of the enterocytes (117). It is a well-established model for prediction of the transport coefficient of a compound through small intestine and becomes available for further absorption to portal blood or lymphatic circulation (118-120).

1.6.3. Systemic metabolism

Once a compound transports through the enterocytes, it will be absorbed from the intestinal portal vein system, and undergoes first-pass metabolism in the liver before entering into the systemic circulation. Liver is known to be the major organ for biotransformation of xenobiotics and the rate-limiting factors that reduce the system bioavailability of drugs and nutraceuticals. Among the enzymes associated with biotransformation and metabolism, Cytochrome P450 (CYPs), especially the CYP1, CYP2, and CYP3 gene families, catalyze more than 75% of the endogenous compounds by oxidation, hydroxylation, and demethylation (121, 122). As CYPs are highly abundant in liver, the biotransformation of drugs and nutraceuticals can be characterized with the

isolated liver microsomes as an *in vitro* model. Researchers can select microsome lots based on the enzyme activity level of specific CYPs, and use such systems for studying enzyme inhibition, clearance, and metabolite identification based on varying analytical techniques. However, it should be noted that the expression of CYPs can be variable among donor species and is also dependent on the incubation and sampling interval.

Current knowledge on the *in vivo* metabolism of CoQ₁₀ is limited. Only few literatures reported the observation of CoQ₁₀'s metabolic pathway and associated metabolites by using radioactive compounds in animal models, such as rats and guinea pigs. Generally, CoQ₁₀ is considered to be absorbed via the lymphatics and concentrated mainly in the liver and then excreted via bile, urine and feces. The fecal excretion was the main route of elimination (123, 124). In an early study, the metabolic fate of CoQ was investigated in rats by using methoxy-¹⁴C-labeled ubiquinone-7 as the model compound (125). Two radioactive metabolites were isolated and identified from urine and feces, with both excreted as conjugates. The structure of the major metabolite is 2,3-dimethoxy-5-methyl-6-(3'-carboxypropyl-3'-methyl)-1,4-benzoquinone, which accounted for about a half of the urinary metabolites, whereas the other one is γ -lactone of 2,3-dimethoxy-5-methyl-6-(5'-carboxypentyl-3'-hydroxy-3'-methyl)-1,4-benzoquinone. Overall, oxidative shortening of the side chain appeared to be the main metabolic transformation of ubiquinone-7. Later, Nakamura *et al.* (126) examined the biliary and urinary metabolites of ¹⁴C-CoQ₁₀ in guinea pigs after intravenous administration. The main metabolites were assumed to be glucuronide of 2,3-dimethoxy-5-methyl-6-(3'-methyl-5'-carboxy-2'-pentenyl)-1,4-benzohydroquinone (Q acid-I) and 2,3-dimethoxy-5-methyl-6-(3'-carboxypropyl)-1,4-benzoquinone (Q acid-II) in free and corresponding hydroquinone

conjugate forms. More recently, Bentinger *et al.* (127) had some interesting observations using ^3H -labeled compound with more retained radioactivity in tracing the metabolic pathway of CoQ₁₀ in rats. The major metabolites were purified from the urine, and the mass spectrometric fragmentation showed that these compounds contained the ring structure with a short side chain and were phosphorylated. They demonstrated that CoQ₁₀ is metabolized in all tissues, and the metabolites are phosphorylated in the cells, transported in the blood to the kidney, and excreted into the urine.

1.6.4. *In vitro* and *in vivo* correlations

Although *in vitro* models provide a rapid and cost-effective alternative for the *in vivo* studies in predicting and determining the oral bioavailability of nutraceuticals, they cannot fully reflect the real events happening *in vivo*. Therefore, for many studies, the *in vitro* models are only used as a screening tool to compare and identify promising candidates for next step studies, especially when a large sample pool is presented. However, if the accurate bioavailability needs to be determined, an *in vivo* test is still advisable. And it has becoming critically important to establish the *in vitro* and *in vivo* correlations (IVIVC) to better designing *in vitro* models for prediction of the corresponding *in vivo* performances.

Notably, lots of efforts have been made to develop more accurate *in vitro* models in simulating the human digestive system. Singh's group established a simulated gastric model, and utilized computational fluid dynamics techniques to obtain unique insight and quantitative characterization of the 3-D dynamics of gastric contents during digestion (128, 129). This model showed promising results in determining and modeling the disintegration rate of different food structures, under different physiological conditions.

Tharakan *et al.* designed an *in vitro* small intestinal model, which simulated the dimension, peristalsis and segmentation motion of small intestine (130). The authors studied mass transport phenomena occurring in the lumen and their potential effect on the concentration of nutrients available for absorption, provided a fundamental understanding of the behavior of food structures and absorption *in vivo*. Also, as mentioned earlier, the TIM models are by far the most advanced *in vitro* models for characterizing upper GI pre-absorption (TIM-1) and lower bowel post-absorption (TIM-2) events. The TIM systems were built and validated on abundant *in vivo* data, and thus showed optimistic results for IVIVC.

On the other hand, results obtained from multiple *in vivo* models may also vary from each other, due to factor of interspecies differences. It is predictable that data obtained from rats and dogs might be different even tested with the same experimental groups. Ultimately, only clinical trials indicate the most accurate physiological events associated with digestion and absorption of foods and nutrients in humans.

Therefore, taken all possible factors into consideration, the following mathematical expression was recently proposed by Ting *et al.* (103) to more accurately predict the oral bioavailability of nutraceuticals:

$$F_{oral} = F_B \times F_T \times F_M \times C_A \times C_S$$

The equation reveals a future perspective that the prediction of human oral bioavailability can be projected using only *in vitro* modeling systems. In this equation, the fractions of bioaccessibility (F_B), transport coefficient (F_T), and resistibility to systemic metabolism (F_M) can all be determined by appropriate *in vitro* studies. And the

other two factors are IVIVC coefficient (C_A) and interspecies scaling coefficient (C_S).

Obviously, to accurately determine C_A and C_S , much more work needs to be done. Comprehensive investigations among different models and species should be carefully carried out. Overall, with the development of modeling systems covering more aspects of physiological and physicochemical events, together with improvement of IVIVC and interspecies validation, it is possible to evaluate the oral bioavailability of nutraceuticals more efficiently and accurately.

CHAPTER 2: HYPOTHESIS AND OBJECTIVES

2.1. Hypothesis

The general scope of this dissertation was to develop a novel functional beverage system to better protect sensitive flavors and improve the oral bioavailability of nutraceutical ingredients. Accordingly, citral was selected as the model flavor compound for study due to its high popularity and the long existing instability problem. And CoQ₁₀ was picked as the targeting nutraceutical compound to be incorporated into the beverage system because of its promising health benefits but limited bioavailability.

Emulsion is by far the dominating colloidal system to incorporate hydrophobic components (such as flavor oils, lipophilic nutraceuticals, etc.) into beverage products. Desired shelf-life and physical stability can be achieved by proper designing of the emulsion composition, interfacial structure, and droplet size. As a consequence, the lipophilic compounds trapped in the lipid core are protected, and can be delivered in a solubilized form. Moreover, emulsions with extra small particle sizes have the advantage of being easily and rapidly absorbed when subjected to digestion in the GI tract.

Based on the given rationale and background information, I hypothesize that **both citral stability and CoQ₁₀ bioavailability can be greatly improved by properly designing nanoemulsion based delivery systems with food-grade/natural ingredients.**

2.2. Objectives

To test the hypothesis, four specific objectives will be investigated:

(I). Test the antioxidant effect of CoQ₁₀ on citral stability and off-flavor formation in emulsion systems.

It is widely accepted that there are free radicals generated during citral degradation as well as lipid oxidation in the emulsion systems. CoQ₁₀, besides its health promoting effects, is also known as a potent lipophilic antioxidant that can quench oxidative stresses. While the antioxidant property of CoQ₁₀ in inhibiting citral's degradation and off-flavor generation in the emulsion system was never tested and validated. The reduced form of CoQ₁₀, known as ubiquinol, is considered to be the activated form responsible for the antioxidant properties. In the designed experiments, both the reduced (ubiquinol) and oxidized (ubiquinone) forms of CoQ₁₀ will be tested. Moreover, different concentrations of ubiquinol in the formulation will also be tested and optimized.

(II). Design emulsion formulations with natural/clean ingredients, then test and compare citral stability in these systems.

Little work has been done to systematically compare the stability of citral in beverage emulsions stabilized by different emulsifiers. Currently the food industry is trying to replace all the synthetic ingredients including emulsifiers with natural source alternatives, thus to claim clean label products. Several groups of synthetic & natural emulsifiers that have been widely used or relatively new in the food industry, with varying structures and molecular weights will be studied and compared for stabilizing

citral in emulsion systems.

(III). Evaluate the bioaccessibility of CoQ₁₀ in optimized formulations using *in vitro* models.

The CoQ₁₀ loaded nanoemulsion formulation will be compared with the unformulated CoQ₁₀ oil dispersion as the control. Two *in vitro* models (pH-stat & TIM-1) will be used to evaluate the bioaccessibility of CoQ₁₀ in tested formulations.

(IV). Evaluate the oral bioavailability and biodistribution of CoQ₁₀ in optimized formulations using *in vivo* models (animal study).

In vivo pharmacokinetic parameters (C_{\max} , T_{\max} , AUC) and the relative bioavailability of CoQ₁₀ will be determined and compared among the tested formulations using animal models. Moreover, tissue uptake of CoQ₁₀ in major organs will be evaluated to better understand its physiological distribution after dosing, and to see if our developed formulation improved CoQ₁₀'s levels in targeted tissues.

CHAPTER 3: EFFECT OF COENZYME Q10 ON CITRAL STABILITY AND OFF-FLAVOR FORMATION IN NANOEMULSIONS

The work in this chapter has been published in the title of “Effect of Ubiquinol-10 on Citral Stability and Off-Flavor Formation in Oil-in-Water (O/W) Nanoemulsions” in Journal of Agricultural and Food Chemistry (Volume 61, Issue 31, Pages from 7462 to 7469) in August 2013.

3.1. Introduction

To protect citral from degradation, two major approaches can be generally considered. First, to design delivery systems that can isolate or minimize the contact of citral with oxidative stresses and acidic conditions. Alternatively, to load antioxidants that can effectively protect citral from rapid oxidation. More recently, the promising effects of adding antioxidants, especially naturally occurring ones, into emulsion systems loaded with citral, has drawn increasing attention. Yang *et al.* (53) from our group systematically investigated the effects of six different natural antioxidants on the stability of citral in O/W nanoemulsions and found that β -carotene, tanshinone, and black tea extract could greatly enhance citral's chemical stability during the storage as well as inhibiting some of the potent off-flavor compounds. However, some antioxidants used in the study are commercially unavailable or cost-ineffective, which hinders their real application in the food industry at the current stage. Some carotenoids and tea extracts have their own taste profiles and intense colors that will also pose a problem in the lemon-flavored beverages. Therefore, it is still necessary to find more suitable antioxidants that can effectively inhibit citral degradation and the off-flavor formation.

Considering the fact that CoQ₁₀ will be incorporated into our functional beverage

system as a nutraceutical, we naturally came up with the idea to test and see if CoQ₁₀ can function as an antioxidant in the emulsion systems. The antioxidant property of CoQ₁₀ in inhibiting citral's degradation and off-flavor generation was never tested and validated. As we know, CoQ₁₀ exists in multiple redox states. The reduced form of CoQ₁₀, known as ubiquinol or Q₁₀H₂, is considered to be the activated form responsible for the antioxidant properties. The aim of this work was then to test the effect of Q₁₀H₂ as an antioxidant in the O/W nanoemulsion system to protect citral from chemical degradation and off-flavor generation. The effect of different concentrations of Q₁₀H₂ in the formulation was tested and discussed.

3.2. Materials and methods

3.2.1. Materials

Neobee 1053 medium-chain triacylglycerol (MCT) consists of 55% caprylic and 44% capric triglycerides was obtained from Stepan Company (Northfield, IL). Alcolac PC75 (phosphatidylcholine enriched) soy lecithin containing *ca* 76% unsaturated and 24% saturated fatty acids was a gift from American Lecithin Company (Oxford, CT). Q₁₀H₂ (95%, UV) was purchased from Hangzhou Joymore Technology Co., Ltd. China. All other chemicals and supplies were purchased from Sigma-Aldrich (St. Louis, MO) and used without further purification and treatment.

3.2.2. Emulsion preparation and storage

The oil-in-water (O/W) nanoemulsions were prepared by using 10 wt% of MCT as the oil phase, 85 wt% of pH 3.0 buffer solution (10 mM citric acid/ sodium hydroxide/ sodium chloride) as the water phase, and 5 wt% of PC75 soy lecithin as the emulsifier which can be dispersed in water phase. For each emulsion sample, 0.1 wt% (1000 ppm)

citral and 0.01 wt % (100 ppm) undecane (internal standard) were dissolved in the lipid phase, and $Q_{10}H_2$ with different concentrations (0.01 wt%, 0.05 wt%, 0.1 wt%, and 0.2 wt%) were also added into the oil phase before homogenization, respectively. Then the aqueous phase and oil phase were thoroughly mixed and homogenized using an Ultra-Turrax T-25 high speed homogenizer (IKA Works Inc., Wilmington, DE) at 24,000 rpm for 5 min followed by a high pressure homogenizer (EmulsiFlex-C3, Avestin Inc., Ottawa, Canada) for six cycles with the pressure of 150 MPa. 10 grams of each emulsion sample was weighted and stored in a 20 mL amber glass vial (Supelco Analytical) with screw cap (PTFE/silicone septum, Supelco Analytical) designed for Solid Phase Microextraction (SPME) immediately after preparation. All the vials with emulsion samples were divided into two groups, with one stored at 25 °C, and the other stored at 45 °C, both under dark conditions throughout the experiments.

3.2.3. Particle size measurement

The mean hydrodynamic emulsion particle size and distributions were measured using a BIC 90 plus particle size analyzer equipped with a Brookhaven BI-9000 AT digital correlator (Brookhaven Instrument Corp., New York) based on dynamic light scattering. The light source is a solid-state laser operating at 658 nm with 30mW power, and the signals were detected by a high-sensitivity avalanche photodiode detector. Emulsion samples stored at 25 °C and 45 °C were diluted 100× with Milli-Q water and well mixed prior to the measurement to prevent multiple scattering effects. All the measurements were conducted in triplicate at a fixed scattering angle of 90° at 25±1 °C. The mean diameter of each sample was determined by Cumulant analysis of the intensity-intensity autocorrelation function, $G(q, t)$.

3.2.4. Measurement of citral

An Agilent 6850 gas chromatography was used to quantify citral's two isomers and various degradation products during the storage. The GC was equipped with a J&W DB-5MS capillary column (30 m \times 0.25 mm i.d.; 0.25 μ m film thickness) and connected with a flame ionization detector (FID). The FID temperature was set at 250 °C. And the oven temperature profile was programmed as follows: there was a 4 °C/min increment from 60 °C to 150 °C at first stage, and then further increased to 230 °C at the rate of 20 °C/min, finally held at 230 °C for 5 min with the total program timing of 31.5 min. The flow rate of hydrogen as the flame gas was controlled at 40.0 mL/min, air flow at 45 mL/min, and helium as the carrier gas flow at 45.0 mL/min. The injection port was equipped with a 0.75 mm inner diameter SPME injection sleeve to minimize the broadening effect. And for the SPME extraction, a manual sampling SPME fiber holder with a 65 μ m PDMS/DVB fiber (needle size 23 ga) was employed. The SPME fiber was exposed in the headspace of the amber glass vials with emulsion samples under constant magnetic stirring for 40 min for adsorption equilibrium at 50 °C. Then, it was inserted into the injection sleeve immediately and held for 5 min for complete desorption. Internal standard (undecane) was used to quantify citral's two isomers and the degradation products.

3.2.5. GC-Mass analysis of citral's degradation products

An Agilent 6890 gas chromatograph equipped with an Agilent 5973 mass detector and a J&W DB-5MS capillary column (30 m \times 0.25 mm i.d.; 0.25 μ m film thickness) was used. The temperature programming and gas flow rates were kept the same as the above described GC measurements. The ionization voltage was held at 70 eV and the ion

temperature was 280 °C. Authentic compounds for major degradation products of citral (*p*-cresol, α ,*p*-dimethylstyrene, *p*-metha-1,5-dien-8-ol and *p*-methylacetophenone) were purchased from Sigma Aldrich (St. Louis, MO) for matching the mass spectrum and retention index.

3.2.6. Statistical analysis

All experiments were conducted twice in duplicate, and all data were expressed as means \pm standard deviations. Where appropriate, data were analyzed using t-test by SigmaPlot 12.0 software, significant difference was defined at $p < 0.05$.

3.3. Results and discussion

3.3.1. Physical stability of citral-loaded emulsions with and without Q₁₀H₂

The physical stability of O/W nanoemulsions under the storage temperatures of 25 °C and 45 °C were evaluated by the particle size profile of each sample in 10 day intervals throughout the storage time. The mean particle sizes of the different emulsion formulations were calculated by cumulant method and are shown in (Fig. 10). After high-speed and high-pressure homogenization processing in the same conditions, fresh nanoemulsions with particle sizes in the range of 98 nm to 120 nm were obtained. Among which, the control (without Q₁₀H₂) had the smallest particle size of 98 nm. The addition of Q₁₀H₂ to the oil phase had varied impact on the particle size. And during the storage time, the particle size of emulsions stored at 25 °C increased very slowly. All the emulsions had an increment of 25-40 nm in particle sizes during the 40 day storage time. The particle sizes of emulsions stored at 45 °C, in contrast, showed a faster and sharper increase due to the greater thermodynamic moving rate of particles. Approximately 70-95 nm increment range was observed for all the tested emulsion samples after 40 days. All

the samples showed the similar trend of increment profile, and none of them were observed with having phase separation or creaming during the storage period at either temperature. Visual observation also indicated good kinetic stability of all the citral-loaded lecithin stabilized nanoemulsions.

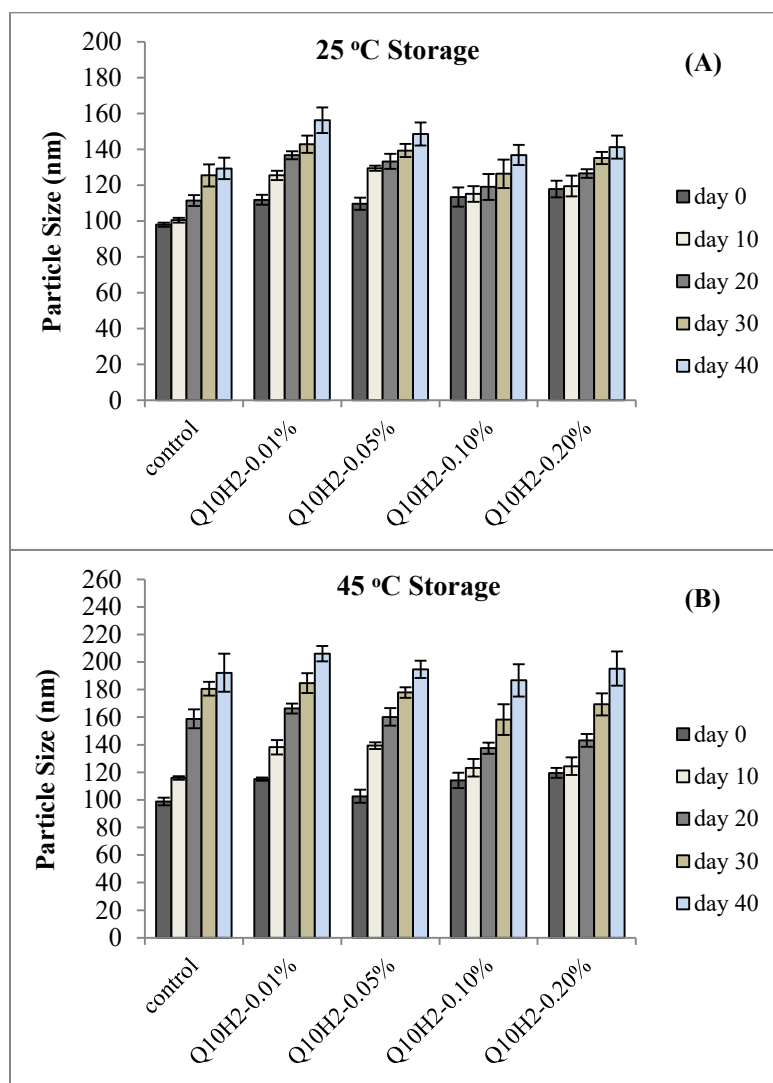


Figure 10. Mean emulsion particle size changes for citral-loaded emulsions with different concentrations of Q₁₀H₂ stored at 25 °C (a) and 45 °C (b). Data represent the mean \pm standard deviation (n=3).

3.3.2. Stability of citral in emulsions with and with Q₁₀H₂

The two isomers of citral, neral and geranial, naturally occur in the ratio of 2:3. In this study, both the degradation rate of neral and geranial were measured to indicate citral's loss during storage at 25 °C and 45 °C for 40 days. From the degradation rate profiles, neral and geranial behaved similarly in terms of degradation trends. Under the storage temperature of 25 °C (**Fig. 11**), control (without Q₁₀H₂) had 53.8% neral and 49.3% geranial left after 15 days. After 40 days of storage, there was 29.2% neral and 27.3% geranial left. Both neral and geranial showed a relatively fast degradation rate at earlier stages (day 0 - day 15), and slower rates were observed afterwards.

Adding different concentrations of Q₁₀H₂ into the citral-loaded emulsions caused different and complicated effects. Data that shows the average percentage of citral remaining and statistical significance compared to control is presented in table format (**Table 6**). With 0.01 wt% concentration of Q₁₀H₂ (Q₁₀H₂/citral ratio 1:10) in the system, surprisingly, more rapid degradation of both neral and geranial were observed in contrast with control. Only 47.9% neral and 42.4% geranial remained after 15 days, and at the end of 40 days, 19.3% neral and 16% geranial were left. However, when the concentrations of Q₁₀H₂ were increased to 0.05 wt% (Q₁₀H₂/citral ratio 1:2) and 0.10 wt% (Q₁₀H₂/citral ratio 1:1), the inhibition effects of both neral and geranial's degradations were observed, especially at early storage time. Specifically, the sample with 0.05 wt% Q₁₀H₂ retained 62.7% of neral and 60.2% of geranial on day 15. And 0.10 wt% Q₁₀H₂ greatly inhibited citral from degradation compared to the control. Around 77.3% neral and 74.2% geranial were still left after 15 days, which showed significant difference compared to control and the best effect among all the tested formulations. However, the emulsions with Q₁₀H₂ in

the formulations showed more linear citral degradation rates. At the end of the 40 day storage period, 26.8% of neral and 25.9% geranial were left in the sample with 0.05 wt% Q₁₀H₂, which was slightly lower than the control. The sample with 0.10 wt% Q₁₀H₂ still retained 35.3% neral and 34.6% geranial after 40 days. Compared to the values of control, this was about an increase of 20.9% neral and 26.7% of geranial retention. Complicated results were observed when the Q₁₀H₂ concentration was further increased to 0.20% (Q₁₀H₂/citral ratio 2:1). From the quantification of the GC data, there was 56.2% of neral and 52.0% of geranial on day 15 remaining, and 26.6% neral and 24.8% geranial left after 40 days, which was slightly better than the 0.05 wt% Q₁₀H₂ sample but less effective than the 0.10 wt% sample during the early stage of storage period. Overall, the sample with 0.10 wt% Q₁₀H₂ formulated into the system showed the best effect to inhibit degradation of both neral and geranial at the 25 °C storage conditions.

Table 6. Average percentages of neral and geranial retained in varied Q₁₀H₂ formulations during 25 °C storage period.

Sample		Day 7	Day 15	Day 23	Day 31	Day 40
Control	Neral	83.48±2.94	53.75±2.17	43.75±3.16	37.90±0.84	29.24±2.84
	Geranial	77.43±6.03	49.31±1.35	40.77±4.16	33.78±3.29	27.29±3.86
Q ₁₀ H ₂ - 0.01%	Neral	71.70±2.18 ^a	47.91±0.90	30.42±1.08 ^a	23.45±0.66 ^a	19.26±2.37
	Geranial	67.03±1.66 ^a	42.36±1.21 ^a	27.11±0.07 ^a	20.94±0.76 ^a	15.98±1.98
Q ₁₀ H ₂ - 0.05%	Neral	83.13±0.03	62.73±0.57 ^a	49.21±1.07 ^a	36.75±2.18	26.76±1.87
	Geranial	82.10±1.10	60.24±2.73 ^a	46.87±1.20	35.87±1.78	25.88±2.16
Q ₁₀ H ₂ - 0.10%	Neral	89.58±2.10	77.34±0.53 ^a	62.24±0.58 ^a	48.89±1.81 ^a	35.28±0.84 ^a
	Geranial	90.86±5.69	74.23±3.70 ^a	58.38±0.86 ^a	45.37±2.49 ^a	34.58±1.07
Q ₁₀ H ₂ - 0.20%	Neral	86.12±5.68	68.80±2.65 ^a	56.19±2.88 ^a	41.05±2.25	26.64±0.74
	Geranial	86.02±6.25	65.21±2.11 ^a	52.02±3.65 ^a	38.02±2.93	24.75±0.10

^a statistically significant difference from control

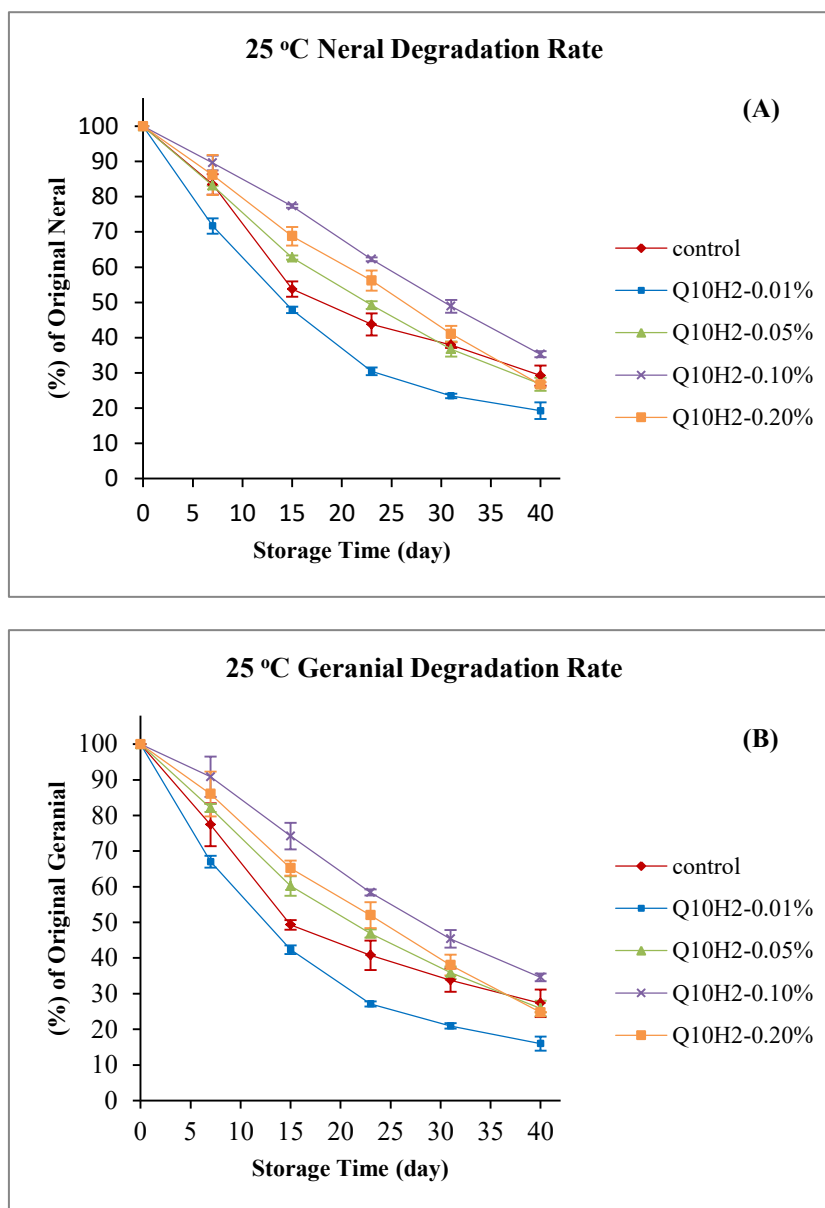


Figure 11. Degradation profiles of neral (a) and geranial (b) in emulsions with different concentrations of Q₁₀H₂ stored at 25°C in comparison with the control.

From the results of the 25 °C degradation, it can be tentatively concluded that concentration of Q₁₀H₂ played an important role in protecting citral from degradation in the O/W nanoemulsions. With low concentration of Q₁₀H₂ (0.01 wt%) in the formulation, it was ineffective at protecting the citral from degradation. Adversely, it promoted citral to degrade in a faster rate than the control. By increasing the Q₁₀H₂ concentration to higher levels, inhibition effects were observed. But beyond a certain level (e.g. 0.20 wt% in our formulations), the inhibition will be adversely suppressed. One possible reason may be due to the complexity of the citral-loaded emulsion system, which involved both lipid oxidation and citral degradation/oxidation over the storage period. Q₁₀H₂ as an antioxidant could theoretically scavenge free radicals and retard oxidation. However, it has been implied before that the antioxidant functions of ubiquinol are mainly encompassed by the QH₂→Q^{•-} redox transition, whereas their pro-oxidant character will also arise from O₂ reduction coupled to the Q^{•-}→Q reaction (131). The context of the redox transitions of ubiquinol conducted by Rich *et al.* (132) and Swallow *et al.* (133) allowed one to use relevant reduction potentials to view the reactivity of ubiquinols with nitrogen- and oxygen-containing free radicals on thermodynamic grounds. From which, the E (QH₂/Q^{•-}, 2H⁺) and E (Q^{•-}/Q) values are +190 mV and -220 mV, respectively. Overall, it appears that the ubiquinol/ubisemiquinone transition may be associated with antioxidant functions, whereas the ubisemiquinone/ubiquinone redox reaction may be endowed with pro-oxidant properties. So, when low concentration of Q₁₀H₂ presented in the system, most of them were autoxidized into Q₁₀^{•-} and were further fully coupled by O₂ to form Q₁₀ and O₂^{•-} at the early stage of storage, from which most Q₁₀H₂ were ‘sacrificed and wasted’. The superoxide radicals formed can further oxidize Q₁₀H₂ or

other compounds to form different radicals which can have possible pro-oxidant properties thus promote citral from degradation and oxidation. An increased level of $Q_{10}H_2$ worked better as a real antioxidant probably due to the majority of $QH_2/Q^{\bullet -}$ transition occurring at early stages to facilitate its antioxidant properties other than the minor $Q^{\bullet -}/Q$ redox reaction when $Q_{10}H_2$ was abundant in the early stage. The phenomenon of further increasing the concentration of $Q_{10}H_2$ to 0.20 wt% showed a decreased inhibition effect was also interesting. It seems that antioxidant property of $Q_{10}H_2$ is not proportionally linked with its dosage, while it is mostly dependent on the complexity of the system involved and environment encountered. As we know, quenching of an oxidizing radical always produces another radical and so may produce a pro-oxidant. Whether or not the overall effect of different concentrations of ubiquinol-10 worked as antioxidant or pro-oxidant depends on combination of the properties (reduction potential and lifetime) of the various radicals involved in the whole process in the specific environment. Clearly, it is not easy to predict and hence, our observations may be only a reported phenomenon that specifically occurred in our tested systems. Although it is difficult to elucidate the detailed mechanism associated by far, many previous studies and reviews (134-136) also addressed the similar phenomena on other antioxidants like carotenoids. Thus the importance of antioxidant concentration should be emphasized with a switch from anti- to pro-oxidation observed in several systems as its concentration increases beyond certain value.

While at 45 °C (**Fig. 12**) storage temperature, both neral and geranial showed more rapid degradation rates in all the tested formulations. Although data were partially overlapped and showed no statistical significance, minor differences of both neral and

geranial retentions can still be observed. After first three days of storage, around 65-72% neral and 60-65% geranial were left in different formulations. The sample with 0.01 wt% Q₁₀H₂ showed a relatively faster degradation rate than others after day ten. And the 0.10 wt% Q₁₀H₂ sample had a slightly slower rate of degradation for both neral and geranial compared to the control. Other two Q₁₀H₂ concentrations also showed minor effect at early storage period. However, at later stages (i.e. after 10 days) they were proven to be not effective in protecting citral from degradation and even had little promotion effect. After 20 days of storage at 45 °C, only about 5% to 14% of neral, and 4%-12% geranial was left among all the formulations. At the end of the 40 days, almost all the neral and geranial were degraded. As under high temperature condition, the degradation was more rapid and complicated to compare, the purpose of the high temperature storage was to investigate the off-flavor compounds produced by citral degradation, the detailed results and discussions will be shown in later session.

Due to different formulations, extraction methods, and storage conditions, it is difficult for direct and quantitative comparisons between our data with previous work. But the lecithin stabilized emulsions did show better protection on citral's chemical degradation under similar storage time and conditions. For instance, Djordjevic *et al.* (57) prepared sodium dodecyl sulfate-chitosan (SDS-CS) and gum arabic (GA) stabilized emulsions to test their efficacy on the stability of citral. Almost all the neral and geranial were lost only after six days of storage at 37 °C in the SDS-CS stabilized emulsion, and around 35% of neral and geranial was left of the GA stabilized one. In contrast, our formulation with lecithin PC75 as the emulsifier showed better protection at the even harsher conditions of 45 °C storage. In which, after seven days, there were still around

40% neral and 36% geranial left for the sample without antioxidant.

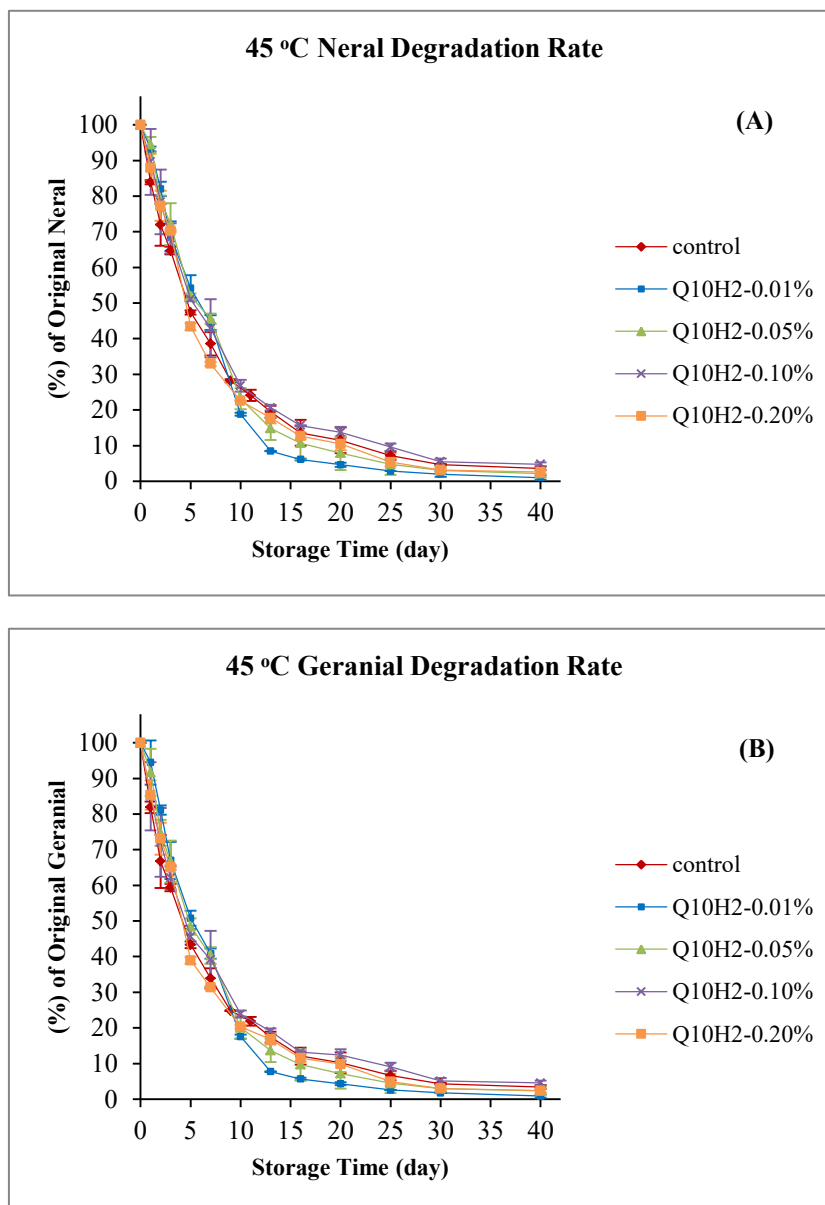


Figure 12. Degradation profiles of neral (a) and geranial (b) in emulsions with different concentrations of Q₁₀H₂ stored at 45°C in comparison with the control.

3.3.3. Comparison between ubiquinol-10 and ubiquinone-10

A previous study (77) indicated that ubiquinone-10 (Q_{10}), unlike $Q_{10}H_2$, exerts no antioxidant activity to inhibit lipid peroxidation in vitro. In order to systematically investigate the effect of Q_{10} on inhibition of citral's degradation, a set of experiments were also conducted to compare 0.10 wt% of Q_{10} in the emulsion formulation and the one with same concentration of $Q_{10}H_2$ as previously tested. Similar emulsion particle size distributions and profiles were recorded for the formulation with 0.10 wt% Q_{10} . The freshly-prepared citral nanoemulsion had a mean particle size of 107.0 ± 1.6 nm. After 40 days of storage, a slight increment of 26 nm was observed at 25 °C. In the 45 °C storage condition, the emulsion particle size increased by about 75 nm to a value of 182.0 ± 9.6 nm (data not shown), which was in the same range as the control and other formulations with differing concentrations of $Q_{10}H_2$. To investigate the effect of Q_{10} on citral's stability, GC measurements of both neral and geranial's degradation rates during the storage time were also obtained under 25 °C (**Fig. 13**) and 45 °C (**Fig. 14**) storage conditions. With the incorporation of 0.10 wt% Q_{10} , no significant difference was observed in neral and geranial degradation compared with control under 25 °C, and less effective as the same concentration of $Q_{10}H_2$, indicating Q_{10} could not protect citral from chemical degradation, though it will neither promote the degradation. While under 45 °C storage condition, citral degraded slightly faster in the sample with Q_{10} than in the control.

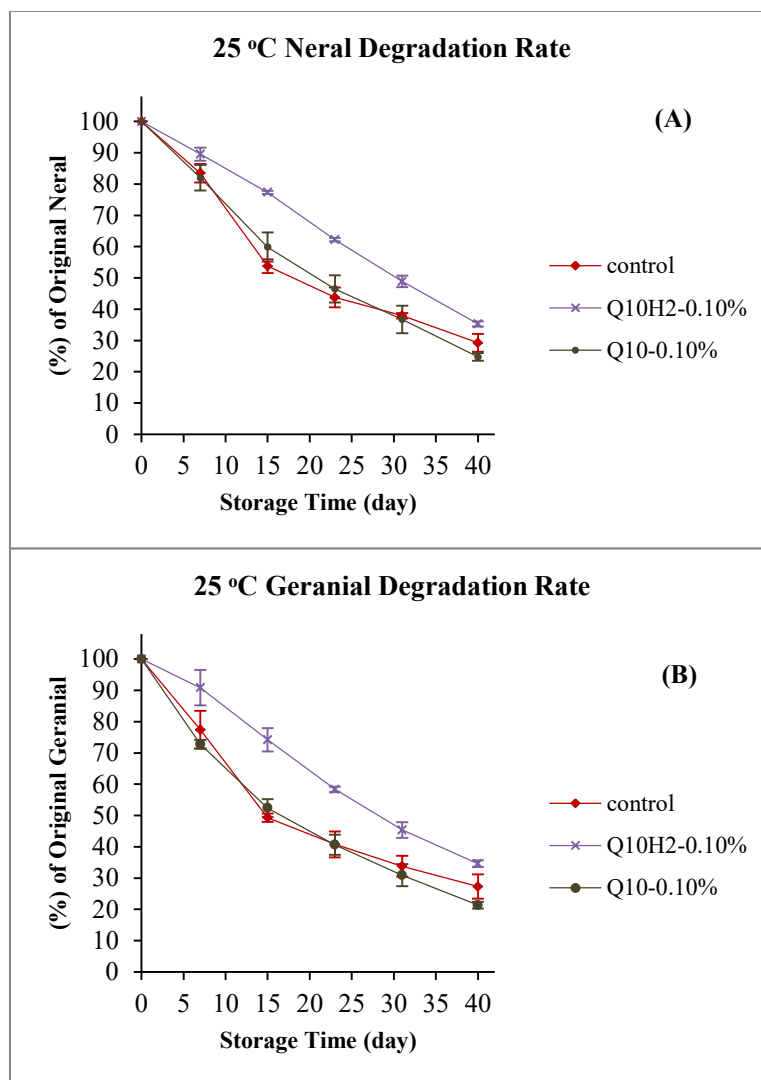


Figure 13. Degradation profiles of neral (a) and geranial (b) in emulsions with 0.10 wt% of Q₁₀ stored at 25°C in comparison with the control.

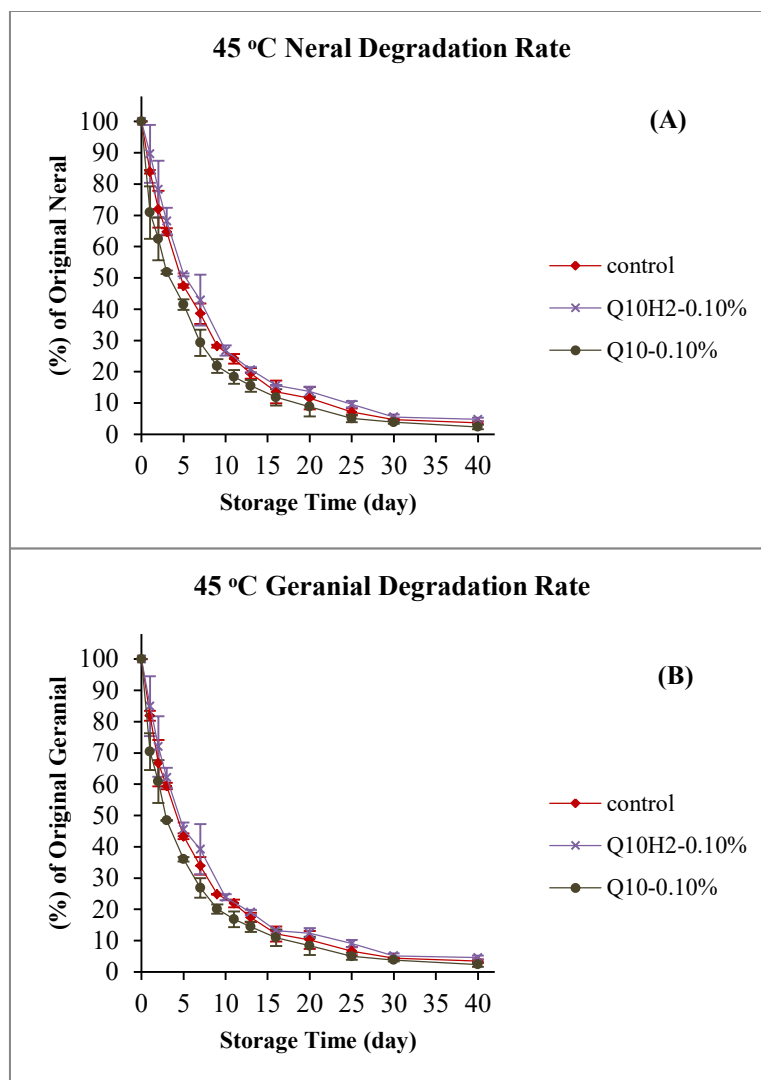


Figure 14. Degradation profiles of neral (a) and geranial (b) in emulsions with 0.10 wt% of Q₁₀ stored at 45°C in comparison with the control.

3.3.4. Evaluation of the major citral degradation compounds

Citral was completely degraded after 40 days of storage at 45 °C. Four major citral degradation products (*p*-cresol, α ,*p*-dimethylstyrene, *p*-mentha-1,5-dien-8-ol, and *p*-methylacetophenone) were detected and quantified throughout the storage period, with mass spectrum and retention index that agrees with authentic compounds purchased from Sigma-Aldrich (St. Louis, MO). Among which, three of them were oxidation products, only *p*-mentha-1,5-dien-8-ol was the acid-catalyzed reaction products (56). Moreover, some other degradation products like *p*-cymene, *p*-cymen-8-ol, and many monoterpene alcohols could not be detected. Therefore, it can be concluded that encapsulation of citral in oil phase of nanoemulsion can effectively isolate protons in the acidic aqueous phase, thus inhibits acid-catalyzed degradation reactions as we previously observed (53). The detailed generation profiles of the four detected off-flavors during the storage were shown in **Fig. 15** (a–d).

However, for the acid-catalyzed degradation product, *p*-mentha-1,5-dien-8-ol (c), adding Q₁₀H₂ could not effectively inhibit its formation, instead, the control showed the minimum levels throughout the storage time. And for the three oxidation products, different concentrations of Q₁₀H₂ had different effects on their generations. For *p*-cresol (a), only 0.10 wt% of Q₁₀H₂ slightly inhibited the formation of it compared to control. Others, especially the sample with 0.01 wt% Q₁₀H₂ actually increased the formation of *p*-cresol to a higher level of 7.7 ± 0.26 ppm on day 30 in contrast with 3.4 ± 0.38 ppm of the control. For *p*-methylacetophenone (d), similar results were observed, with the 0.10 wt% Q₁₀H₂ showing the minimum detectable levels throughout the storage period. The 0.05 wt% sample was fluctuating around comparable with the control and showed negligible

difference. Low (0.01%) and high (0.20%) concentration samples both promoted the generation of *p*-methylacetophenone to higher levels. Finally, it seems that the generation of α ,*p*-dimethylstyrene (b), can be inhibited to certain levels by adding appropriate concentrations of Q₁₀H₂ (0.05%, 0.10% and 0.20%). Among which, 0.10% always showed the best performance. Only the 0.01% sample had slightly higher levels than the control. The observed results were in well accordance with the citral degradation profiles though. The sample (0.10 % Q₁₀H₂) with slowest degradation rate of both neral and geranial performed best in the off-flavor generation. Although some concentrations of Q₁₀H₂ (0.05% and 0.20%) showed some protection effect on citral's degradation under 25 °C, it turns out that they could not effectively inhibit the potent off-flavors like *p*-cresol and *p*-methylacetophenone under 45 °C. Also from the degradation profiles of both neral and geranial under 45 °C, faster degradation rates were observed of the emulsions with certain concentrations of Q₁₀H₂, only the 0.10% sample showed the inhibited rate compared with the control. These results, on the other hand, demonstrated the importance of the concentration of Q₁₀H₂ in the emulsion system to protect citral from degradation and the relevant off-flavors generation.

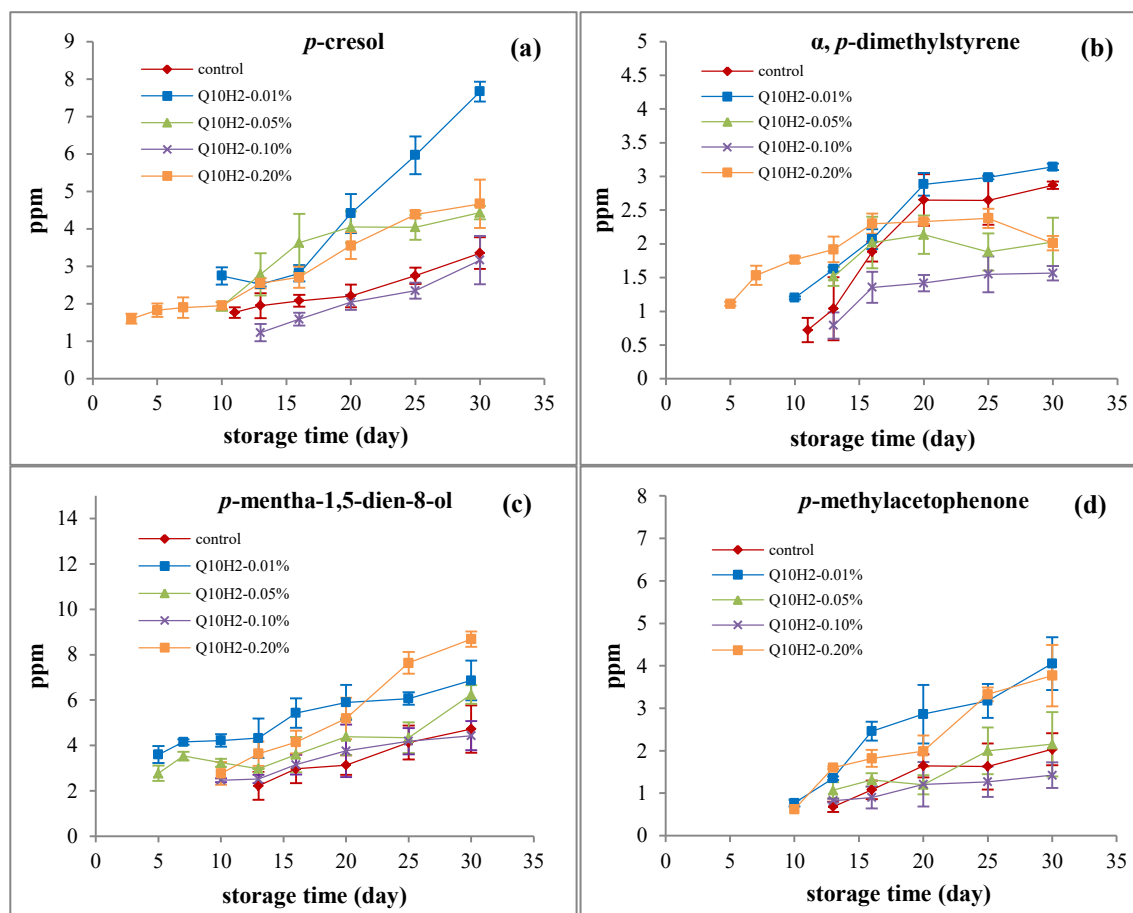


Figure 15. Generation profiles of four major citral degradation off-flavors in the emulsions stored at 45°C: (a) *p*-cresol; (b) α ,*p*-dimethylstyrene; (c) *p*-mentha-1,5-dien-8-ol; (d) *p*-methylacetophenone.

3.3.5. Effect of ubiquinol-10 on lipid oxidation

Although lipid oxidation is not the main topic of this work, some of the lipid degradation products were detected during the storage tests due to the incorporation of MCT and lecithin in the emulsion formulations, such as 2-heptanone, 1-octen-3-*ol* and butanoic acid. The concentrations of the above mentioned degradation compounds on day 30 (45 °C storage condition) were shown in **Fig. 16**. Incorporation of Q₁₀H₂ decreased the level of 2-heptanone, with the sample of 0.10% showing the minimum. For 1-octen-3-*ol*, only the 0.10% sample showed a decreased level. Other formulations all had relatively higher values than the control. The data of butanoic acid showed the sample with 0.01% Q₁₀H₂ had higher amounts than the control, and others all worked better than the control. These results were complicated and need more interpretations and support to better define the effect of Q₁₀H₂ and role of its concentrations on lipid oxidation. It is widely accepted that addition of antioxidants into emulsions would retard lipid oxidation through inactivating free radicals, scavenging oxygen, and other oxidative molecules, while the concentration of antioxidant in specific system and the potential switch from anti- to pro-oxidant at critical levels should be drawn more attention according to this research.

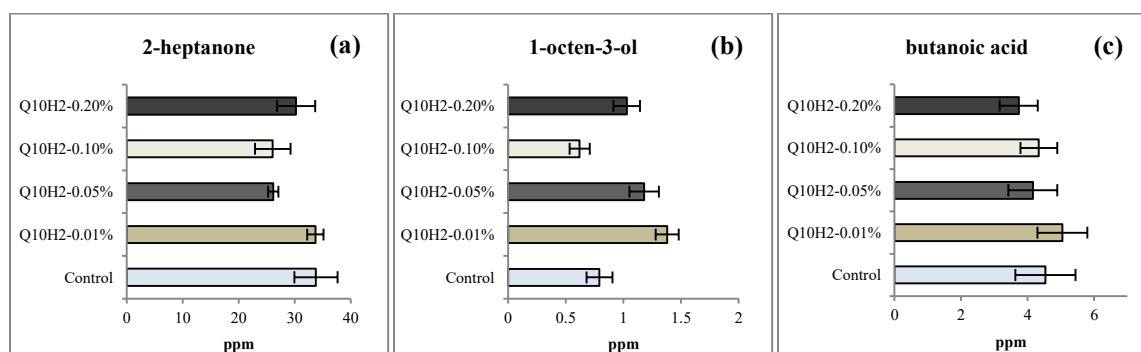


Figure 16. Concentrations of lipid degradation products from the emulsions stored at 45°C for 30 days: (a) 2-heptanone; (b) 1-octen-3-*ol*; (c) butanoic acid.

3.4. Conclusions

In summary, the effects of different concentrations of Q₁₀H₂ on citral's stability were systematically investigated and compared in the citral-loaded oil-in-water (O/W) nanoemulsions. Among all the tested formulations, the optimum concentration of Q₁₀H₂ was determined to be 0.10 wt% (Q₁₀H₂/citral ratio 1:1), which can effectively protect citral from chemical degradation and oxidation in the system. However, 0.01 wt% Q₁₀H₂ was proven to have no protection effect, and may induce the Q₁₀[•]/Q₁₀ redox transition, which gave Q₁₀H₂ pro-oxidant properties. Further increasing Q₁₀H₂ concentration beyond a certain value (e.g. 0.20 wt%) also hindered its efficacy. Major off-flavor compounds from citral degradation were monitored throughout the storage, and the major oxidation products, i.e., *p*-cresol, *p*-methylacetophenone, α ,*p*-dimethylstyrene, and some of the lipid degradation products could be properly inhibited with the optimum Q₁₀H₂ concentration. The oxidized form of Q₁₀ was determined to have no protection effect on citral's chemical stability and the off-flavor generation. This study provided detailed and quantitative data for reference of the CoQ₁₀ incorporated emulsion systems in inhibiting citral degradation and preventing the corresponding off-flavor generation. Besides the chemical antioxidant property in protecting sensitive flavor compounds, CoQ₁₀ can also serve as a functional ingredient to improve human health. Thus new strategies can be inspired for food industry to develop multi-functional food products with improved sensory and human health.

CHAPTER 4: EFFECT OF EMULSIFIER TYPE ON THE FORMATION OF NANOEMULSION AND CITRAL STABILITY IN THESE SYSTEMS

4.1. Introduction

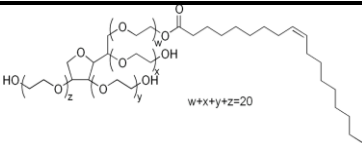
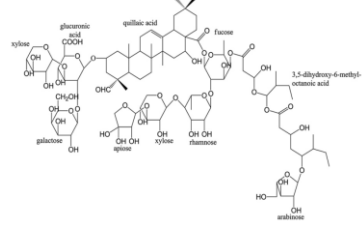
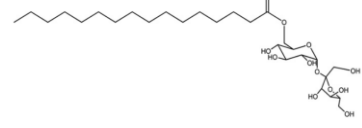
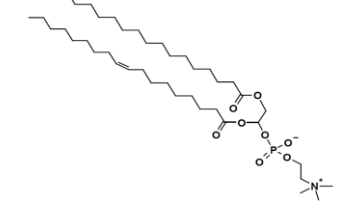
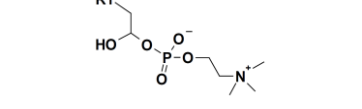
There has been increasing consumer demand for clean label products made with more natural, sustainable ingredients in the food industry. Being an integral part of emulsion, emulsifier is also experiencing its transition from synthetic to natural alternatives to align this big trend. However, due to limitation in performance, versatility and cost, the real application of natural emulsifier is still very limited. Synthetic surfactants such as Tweens and Spans together with some animal protein based emulsifiers are still the predominant candidates for various food product applications. Obviously, more studies on comparing and identifying promising natural emulsifiers for specific food applications need to be performed. Up to now, no comprehensive research has been published regarding citral's stability and off-flavor generation in emulsions stabilized by different types of emulsifiers. Only few reported the influence of some biopolymer stabilized emulsions on the stability of citral (57, 58). The purpose of this study was therefore to directly compare the effects of some promising natural emulsifiers with synthetic surfactants in stabilizing O/W emulsions, and with specific interest in investigating citral's stability in these systems.

Currently, the candidate pool of natural emulsifier is limited compared with the synthetic materials. Only four categories of natural amphiphilic ingredients are recognized, including proteins, polysaccharides, saponins and phospholipids (137). However since most natural emulsifiers cannot be used to form emulsions using low-energy approaches, we selected candidates based on its compatibility with high-energy

approaches in assembling nanoemulsions. Common proteins (lactoglobulin, serum albumin, casein etc.) and polysaccharides (gum arabic, pectin etc.) can form regular emulsions, but are more challengeable to produce emulsions with particle size smaller than 200 nm (*d*), due to relative big molecular size of these biopolymers and high surfactant-to-oil ratio (SOR) needed to stabilize emulsion droplets. Moreover, polysaccharides and proteins may be depolymerized or denatured with the high local temperature and pressure generated by high-energy methods, which can adversely affect their functionality. Therefore, in the current study, we focused on evaluating the performances of small molecular surfactants, which can achieve much reduced SOR and particle size with high-energy methods.

If brief, five types of highly recognized and promising natural and synthetic emulsifiers were selected for evaluation and comparison: polysorbate, saponin, sugar ester, lecithin and lyso-lecithin. Correspondingly, model compounds were identified for representing each of these categories, including Tween 80, Q-Naturale, sucrose monopalmitate (SMP), PC75 lecithin and LPC20 lyso-lecithin. Among them, polysorbate 80 and SMP are synthetic, while Q-Naturale, PC75 and LPC20 are considered to be natural or natural derived. The detailed information of these five surfactants is summarized in **Table 7**. Based on similarity in their molecular weights, Tween 80 was coupled with Q-Naturale[®] for comparison, and SMP was evaluated against PC75 and LPC20. The overall performances of these compounds in stabilizing nanoemulsion and citral were systematically investigated and elucidated.

Table 7. Properties of model synthetic and natural emulsifiers used for comparison.

Emulsifier	Category	Source	HLB	Charge	Mw (g/mol)	Molecular Structure
Tween 80	Polysorbate	Synthetic	15	Non-ionic	1310	
Q-Naturale	Saponin	Natural	13.5	Ionic	~1650-2000	
Sucrose Monopalmitate (SMP)	Sugar ester	Synthetic	18	Non-ionic	580	
PC75	Lecithin	Natural	9	Ionic	~760-800 *	
LPC20	Lyso-lecithin	Natural derived/ Clean label	12	Ionic	~500 *	

* Molecular weights of PC75 and LPC20 were estimated based on pure phosphatidylcholine (PC) and pure lyso-PC. A palmitoyl/oleoyl (C16:0/C18:1) -PC was shown to represent the molecular structure of PC75.

4.2. Materials and methods

4.2.1. Materials

Tween 80 was purchased from Sigma-Aldrich (St. Louis, MO); Q-Naturale[®] 200 was provided by Ingredion Inc. (Bridgewater, NJ); Habo Monoester P90 containing 90% of sucrose monopalmitate was obtained from Compass Foods (Singapore); PC75 and LPC20 were kindly provided by American Lecithin Company (Oxford, CT). Neobee 1053 MCT was obtained from Stepan Co. (Northfield, IL). Citral (mixture of neral and

geranial, 95% pure), undecane, and other chemicals and suppliers were purchased from Sigma-Aldrich (St. Louis, MO). Milli-Q water was used throughout the experiments when needed.

4.2.2. Nanoemulsion preparation

In brief, five citral-loaded (0.1 wt%) nanoemulsions were made with each of the above mentioned emulsifiers. For nanoemulsion systems, the water phase was composed of pH 3.5 citric acid buffer (88.34 wt%) and emulsifier (1.5 wt%), together with EDTA (0.05 wt%) as chelating agent. Since the commercial Q-Naturale[®] 200 product only contains 14% of the Quillaja extract (active ingredient), therefore 10.7 wt% of Q-Naturale[®] was added in 79.14 wt% buffer, which gives the equivalent amount of 1.5 wt% of emulsifier in the final composition. The oil phase was composed of MCT (10 wt%), citral (0.1 wt%) and undecane as internal standard (0.01 wt%). The mixture of each water and oil phase was then passed through a pre-optimized homogenization treatment: high-shear (Ultra-Turrax T-25, IKA Works Inc.) at 15,000 rpm for 3 min, followed by high-pressure homogenization (EmulsiFlex-C3, Avestin Inc.) at 10,000 psi for 5 cycles. Fine nanoemulsions stabilized with different emulsifiers were produced after the processing.

4.2.3. Control group preparation

Besides emulsion systems, other researchers indicated micellar structures can also help to protect citral from degradation (68, 69). Therefore, in this study, the control group was citral-loaded micelle system formed by self-assembly of Tween 80 molecules. In detail, 1.5 wt% of Tween 80 was dissolved in the pH 3.5 citric acid buffer before 0.1 wt% citral was added. Then the system was stirred for 12 h at 4 °C until citral became

solubilized in the Tween 80 micellar structures in the buffer system. Citral's stability was compared among all the tested nanoemulsions and the control group during the storage.

4.2.4. Storage tests

For each emulsion and the control micelle solution containing citral, 10 grams of sample was weighed and transferred into a 20 mL amber glass vial with screw cap (PTFE/silicone septum, Supelco Analytical) designed for SPME immediately after preparation. All vials with emulsion samples were divided into two groups, with one stored at 25 °C, and the other stored at 50 °C, both kept under dark conditions throughout the experiments. During the storage, physical stability of emulsions was evaluated by monitoring mean particle sizes, distribution profiles and surface charges of the emulsion droplets. Citral's stability was assessed by measuring both neral and geranial's degradation trends in all tested samples.

4.2.5. Particle size distribution and zeta potential measurements

The particle sizes distributions were measured by Dynamic light scattering (DLS) using a Zetasizer Nano ZS (Malvern Instruments, U.K.) with a 3 mW He-Ne laser at 633 nm. The unit collects light back-scattered at an angle of 173°. Citral-loaded emulsion samples together with micelle solutions were diluted with pH 3.5 buffers for 100 times before analyzing. After thermal equilibration of the sample, autocorrelation functions were collected using acquisition times of 30 - 60 s per correlation function. Measured autocorrelation functions were converted into particle size distribution and z-average size by using the "narrow modes" algorithm.

Zeta-potential measurement of the citral-loaded emulsion systems were performed using the same Zetasizer instrument with micro-electrophoresis. The instrument uses a Phase Analysis Light Scattering method to measure the electrophoretic mobility of particles in solution. The Smoluchowshi equation is used to calculate the zeta potential of the particles in solution. Emulsion samples were diluted 100× with pH 3.5 buffer in disposable capillary cells and measured by a ZEN1002 type Dip cell probe with electrode. Measurements were performed in triplicate.

4.2.6. Measurement of citral

To measure citral's two isomers (neral & geranial) and different degradation compounds, we used an Agilent 6850 gas chromatography equipped with a J&W DB-5MS capillary column (30 m × 0.25 mm i.d.; 0.25 μm film thickness) and a flame ionization detector (FID). The program of GC was set to our previous optimized conditions as mentioned in Section 3.2.4. For extraction of neral, geranial and volatile degradation compounds, a manual sampling SPME fiber holder with a 65 μm PDMS/DVB fiber (needle size 23 ga) was used. The SPME fiber was exposed in the headspace of the amber glass vials with emulsion samples under constant magnetic stirring for 40 min at 50 °C until adsorption equilibrium reached. Then, it was inserted into the injection sleeve immediately and held for 5 min for complete desorption. Undecane was used as an internal standard to quantify neral, geranial and the degradation compounds.

4.2.7. GC-Mass analysis of degradation products

To determine key degradation products of citral and some lipid oxidation products, we used an Agilent 6890 GC equipped with an Agilent 5973 mass detector and

a capillary column with the same specification of the GC measurements. The oven temperature program and gas flow rates were also kept the same as described above. The ionization voltage was held at 70 eV and the ion temperature was set at 280 °C. Authentic compounds for major citral degradation products (*p*-cresol, α ,*p*-dimethylstyrene, *p*-metha-1,5-dien-8-ol and *p*-methylacetophenone) and lipid degradation products (heptanal, pentanal) were purchased from Sigma Aldrich (St. Louis, MO) for matching the mass spectrum and retention index.

4.2.8. Statistical analysis

All measurements regarding citral's degradation and off-flavor generation were duplicated. The mean and standard deviation were calculated from these measurements. When necessary, we analyzed data with t-test by SigmaPlot 12.0 software to define significant difference ($p < 0.05$).

4.3. Results and discussion

4.3.1. Physical stability of citral-loaded colloidal systems during storage

The physical stability of all citral-loaded emulsions together with the micelle system (control group) were monitored for particle sizes and surface charges (zeta-potential) during a 60-day storage test at both 25 and 50 °C. **Fig. 17** shows the particle size distribution profiles together with the mean sizes for each of the fresh made (Day 0) emulsions and micelles. From the results, citral-loaded micelles formed by Tween 80 showed an average size of 11.05 nm, significantly smaller than all the emulsion droplets. Which is predictable, since micelles assembled by polysorbate molecules usually result in particle sizes around 5-10 nm in aqueous systems, with citral molecules aligned or incorporated within its hydrophobic region, the micelle size slightly increases. While all

the emulsions stabilized by different emulsifiers had similar distributions and mean particle sizes (140 - 160 nm range), indicating that the tested compounds had similar emulsifying properties under our defined processing condition, which produced small-size, monomodal distribution nanoemulsions. Among which, the LPC20 (141.9 nm) and Q-Naturale (144.4 nm) stabilized nanoemulsions produced relatively smaller sizes compared with others.

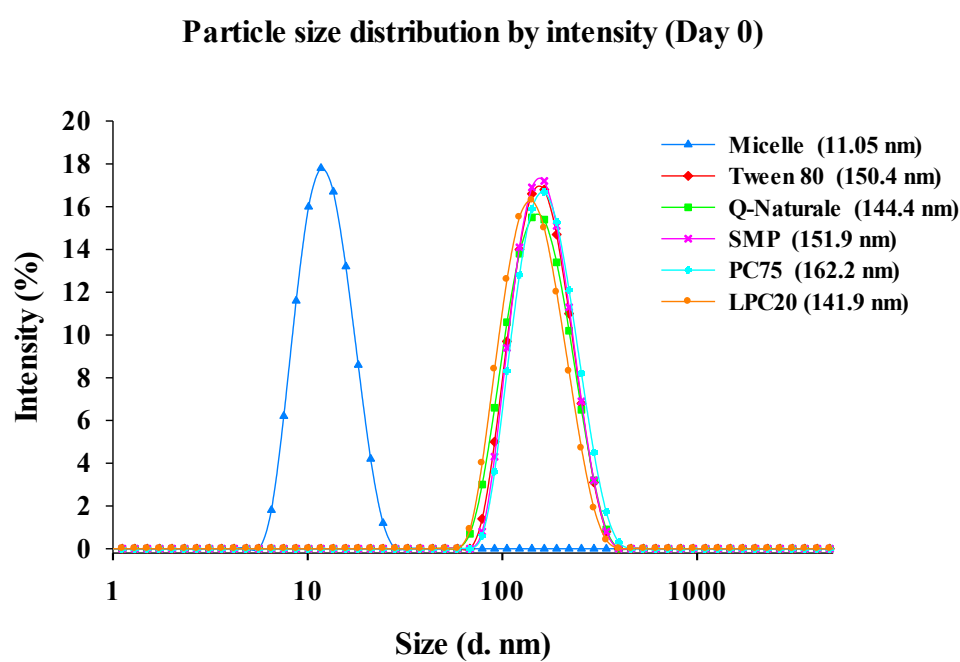


Figure 17. Particle size distribution profiles of citral-loaded colloidal systems (Day 0): nanoemulsions stabilized with different emulsifiers (Tween 80, Q-Naturale, SMP, PC75, LPC20) and micelles formed by Tween 80 molecules.

Then, all these colloidal systems were continuously monitored with their particle size changes for 60 days. Results were summarized in **Fig. 18**. The size of citral-loaded micelles didn't change much during the entire storage time, which fluctuated around 10-13 nm. However, the particle sizes of all the nanoemulsions generally increased during

the storage at both temperature conditions. **Fig. 18 (a)** shows the particle size changes monitored at 25 °C storage, and **Fig. 18 (b)** indicates the 50 °C storage results. At 25 °C, the particle sizes of emulsions increased slightly. All the emulsions had a slow growth of about 25-50 nm in particle sizes after 60 day storage. While at elevated temperature (50 °C), an approximately 40-85 nm increment was observed with much faster rates for all samples due to the greater thermodynamic moving rates of particles. Quantitative results of the differences in mean particle size of emulsions after 60 days of storage were summarized in **Table 8**. Among all tested emulsifiers, Q-Naturale stabilized emulsions had the minimum size growth at both temperature conditions after 60 days, followed by LPC20, SMP, and Tween 80 stabilized emulsions. The PC75 stabilized emulsion, however, showed relatively higher increment at both storages conditions. Nevertheless, all emulsions showed relatively good physical stability during the storage at both temperature conditions, no phase separation or creaming occurred in any samples after 60 days. The particle size distributions still maintained monomodal but were slightly shifted to higher size range and broader distributions were observed (data not shown).

It is widely accepted that the physical stability of emulsions are strongly correlated with the dispersed particle stability against flocculation and coalescence. Obviously, the smaller initial size and more stable of particles against growth, the higher physical stability of emulsion would be. Therefore, based on the observed trends, the physical stabilities of all nanoemulsions stabilized with the five tested emulsifiers were ranked in decreasing sequences as follows: Q-Naturale > LPC20 > SMP > Tween 80 > PC75.

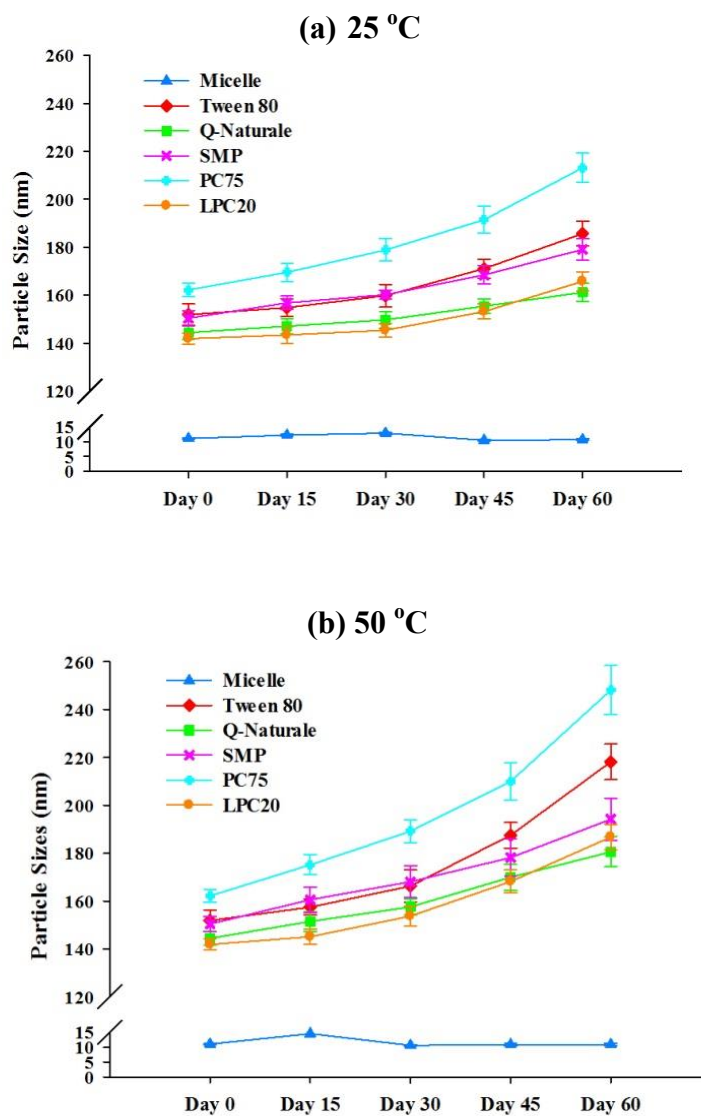


Figure 18. Mean particle size changes of citral-loaded colloidal systems stored at 25 °C (a) and 50 °C (b) during 60 days. Data represent the mean \pm standard deviation (n=3).

Table 8. Mean particle size increments (nm) of citral-loaded emulsion systems stored at 25 °C and 50 °C after 60 days.

		Tween 80	Q-Naturale	SMP	PC75	LPC20
25 °C	Day 0	151.9	144.4	150.4	162.2	141.9
	Day 60	185.7	161.2	179.1	213.2	165.8
	Difference	33.8	16.8	28.7	51.0	23.9
50 °C	Day 0	151.9	144.4	150.4	162.2	141.9
	Day 60	218.2	180.6	194.2	248.3	186.8
	Difference	66.3	36.2	43.8	86.1	44.9

At the same time during the storage, we also measured the surface charge (zeta-potential) of all the emulsion droplets stabilized by different emulsifiers. **Fig. 19** shows the results of the surface charge distributions of freshly made emulsion droplets at day 0. Due to the ionic nature of some molecules, emulsions stabilized by LPC20, PC75 and Q-Naturale showed highly negative charges at pH 3.5 (greater than -30 mV); with LPC20 stabilized one had the most negative charge of -48.6 mV. Tween 80 is non-ionic, therefore the average zeta-potential was close to zero. Interestingly, emulsion droplets stabilized by non-ionic SMP also carried slightly negative charge (-11.0 mV), probably due to the presence of some impurities, such as free fatty acids in the SMP samples, since the SMP is only 90 % pure. It is worth mentioning that the zeta-potential of all samples didn't change significantly during storage, though the negatively charged emulsions became slightly more negative after 60 days of storage (data not shown).

Usually, high surface charge indicates strong electrostatic repulsions existing between droplets, which prevent them from flocculation and coalescence. Therefore, the surface charge can also be used as a reference to indicate the stability of colloidal systems. However, no correlation was found from our results of surface charge with

emulsion stability. Especially for the PC75 stabilized emulsion, which carried highly negative charges, however, was less stability compared with others. Therefore, there must be other factors involved in the instability of emulsions, which will be raised and explained in the later session.

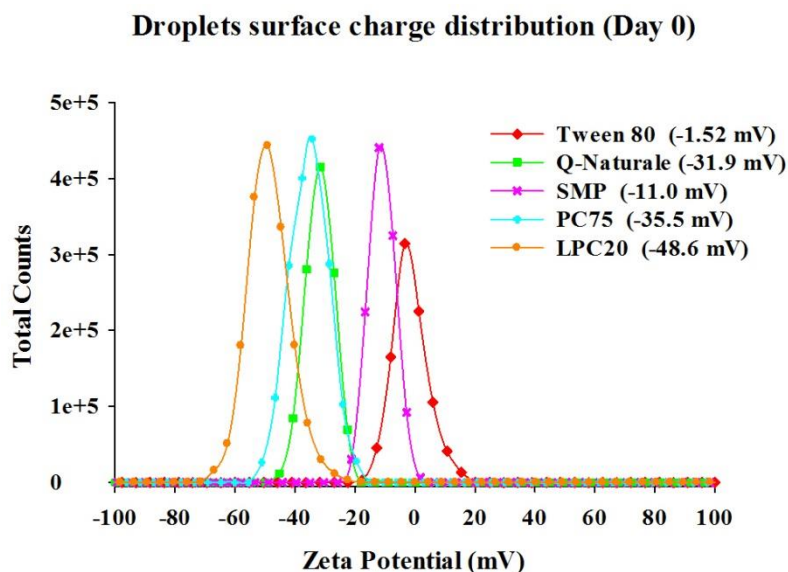


Figure 19. Droplet surface charge distributions and average zeta-potential of citral-loaded emulsions stabilized by different emulsifiers (day 0).

4.3.2. Stability of citral in micelle and emulsion systems

Citral's chemical stability was determined by measuring both neral and geranial's contents in all tested formulations at 25 °C and 50 °C storage for 35 days. **Fig. 20** shows the results of 25 °C storage. At 25 °C, both neral and geranial showed similar degradation trends, with neral degraded slightly faster than geranial. Among tested formulations, micelle system was proved to be least effective in protecting citral from degradation. After 1 week storage at 25 °C, only about 41.2% of neral and 72.2% of geranial were left. And by the end of 35 days storage, levels of neral and geranial further dropped to 12.3%

and 29.8% respectively. Compared with micelle, much higher levels of neral and geranial were retained in all tested emulsion systems. Among them, the one stabilized with Q-Naturale showed the best and superior effect in maintaining citral's stability. Results indicated more than 70% of neral and 92% of geranial were still left after 35 days storage at 25 °C. LPC20 and SMP stabilized emulsions had similar but slightly faster citral degradation rates compared with Q-Naturale. Followed next was the Tween 80 stabilized one, which showed even more accelerated rates. And finally, the PC75 stabilized emulsion had the fastest degradation trends of both neral and geranial among all tested emulsion systems. By the end of storage test, only 46.2% of neral and 61.5% of geranial were left. While under the 50 °C storage, much increased degradation rates of both neral and geranial in all systems were observed (**Fig. 21**). However, the trends were generally the same as the 25 °C storage. As shown in the plot, citral in micelle system degraded most rapidly. Only 8.2% of neral and 20.3% of geranial were left after 7 days storage at 50 °C. And by the end of 35 days, all neral and geranial were completely gone. For emulsion systems, Q-Naturale stabilized one continuously performed the best among others. With more than 36.1% of neral and 68.2% of geranial remained after 35 days, Q-Naturale emulsion significantly improved citral's stability even at elevated temperature condition. Besides Q-Naturale, LPC20 emulsion was ranked as the second in terms of citral's stability. The results for other three emulsion groups were more complicated at 50 °C storage. At early stages, relatively faster degradation rates were observed in PC75 stabilized emulsion than the SMP and Tween 80 ones. While by the end of storage on day 35, similar levels of neral and geranial were detected in these three systems.

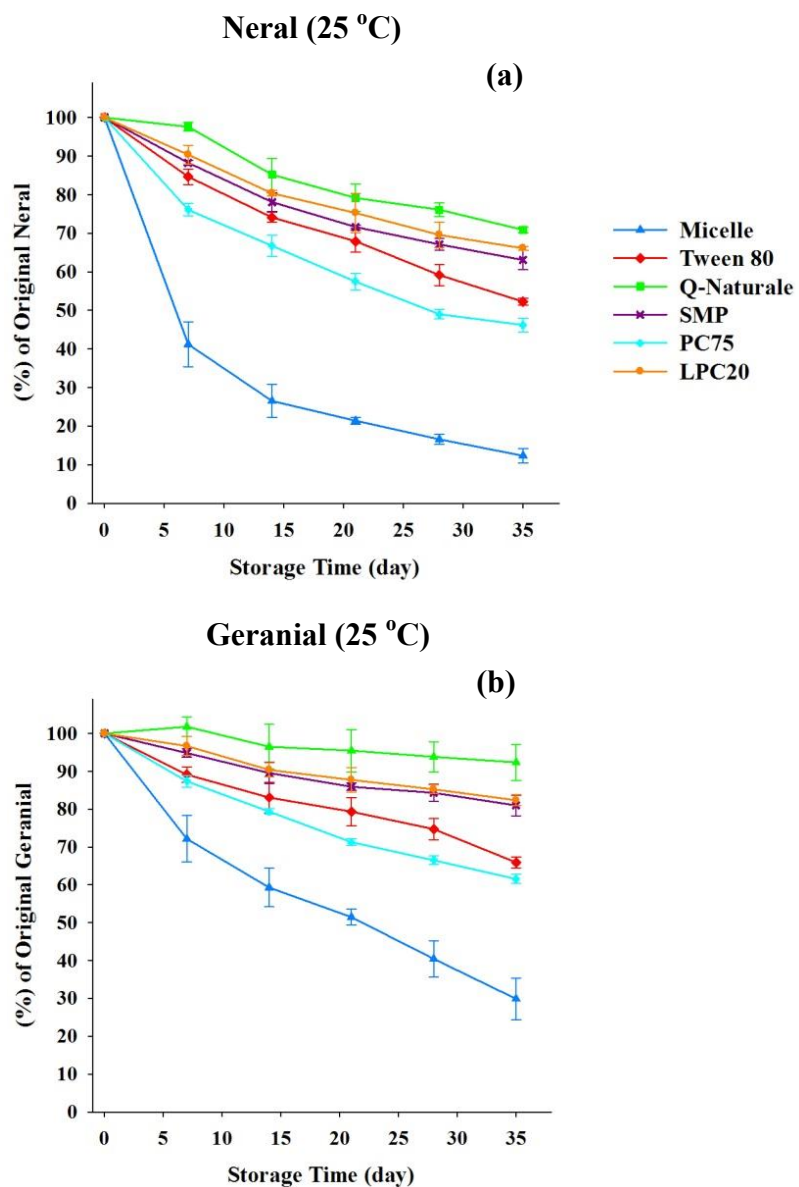


Figure 20. Degradation profiles of neral (a) and geranial (b) in micelle and emulsion systems during storage at 25 °C.

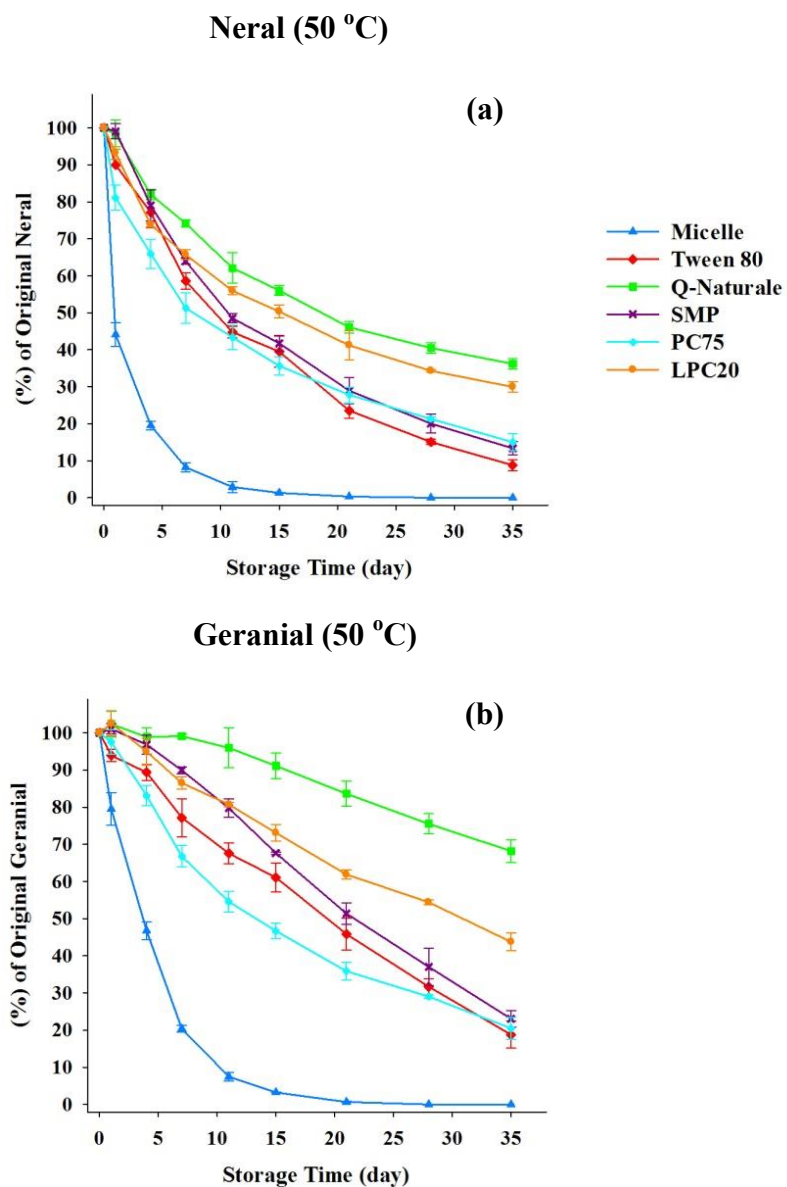


Figure 21. Degradation profiles of neral (a) and geranial (b) in micelle and emulsion systems during storage at 50 °C.

We observed that the results of citral's stability correlated well with emulsion physical stability as we summarized in section 4.3.1. Which is easy to understand, because citral has very limited water solubility, it may predominantly distributed at the oil-water interface or within the oil phase of emulsions, therefore more stable the emulsion was, more stable citral would be in the system. While the superior performance of Q-Naturale in protecting citral from degradation still intrigued us, since the results observed here was even better than some of our previous findings with addition of antioxidants in the emulsion systems (53, 67), although conditions were slightly different. There might be other factors involved beyond considering the physical stability of emulsions. We speculated that Q-Naturale may also contain antioxidant properties with some free radical scavenging abilities, which effectively protected citral from being oxidized. This hypothesis was strongly supported by a recent study by Uluata *et al.* (138), who compared the physical stability, autoxidation and photosensitized oxidation of ω -3 oils in nanoemulsions prepared with different surfactants including quillaja saponin. The authors found the free radical scavenge capacity of quillaja saponin (55.6 μ M Trolox equivalents/ μ M surfactants) was significantly higher than other surfactants, as confirmed by ORAC assay. They also observed improved emulsion stability and inhibited lipid oxidation in the quillaja saponin stabilized emulsions. Their assumption was that the antioxidant property of quillaja saponin may come from the abundant hydroxyl groups distributed on its molecules. Moreover, saponins from soy had also been reported to be able to scavenge free radicals and superoxide anions previously (139). These existing evidences together with our current findings confirmed the excellent performance of saponin emulsifier in stabilizing emulsions and protecting oxidation sensitive ingredients.

4.3.3. Evaluation of the major citral degradation compounds

The degradation of citral will not only lead to loss of the pleasant lemon aroma, but also generate a lot of undesired off-odors. In this study, four major citral degradation products (*p*-cresol, α ,*p*-dimethylstyrene, *p*-mentha-1,5-dien-8-ol, *p*-methylacetophenone) were identified and detected during storage. The levels of these four key off-odors were shown in **Fig. 22** (a, b, c, d) after storage at 50 °C for 35 days. Among these four off-odors, only *p*-mentha-1,5-dien-8-ol is the acid-catalyzed reaction intermediate, other three compounds are oxidation products. From the results, significantly higher levels of three oxidative products were observed in the micelles system, and lowest levels were always observed with the emulsion stabilized by Q-Naturale, especially for *p*-cresol and *p*-methylacetophenone. These results were generally in consistency with the citral stability data, indicating higher amount of citral being degraded, higher levels of oxidative off-odors were generated, although some minor variations existed. Also, it confirmed that Q-Naturale had exceptional performances in protecting citral from degradation and inhibiting oxidative off-odors generation in the emulsion systems due to its excellent emulsifying and antioxidant properties.

However, for *p*-mentha-1,5-dien-8-ol, only trace amount was detected in the micelle system, while higher levels were found in other emulsion systems. The reason probably lies in the fact that *p*-mentha-1,5-dien-8-ol is an intermediate compound, which may be further degraded. While after about 21 days storage at 50 °C, all citral in the micelle system were completely degraded, therefore little or no intermediate compound can be detected by the end of 35 days storage at elevated temperature. However, considerable amounts of citral were still retained in emulsion systems. Therefore certain

levels of this intermediate could still be detected in them. It was also notable that levels of *p*-mentha-1,5-dien-8-ol detected in emulsions systems were not correlated well with other oxidative off-odors, with the highest level detected in LPC20 stabilized emulsion, followed by Q-Naturale and PC75. Tween 80 and SMP stabilized systems had similar and relatively low levels.

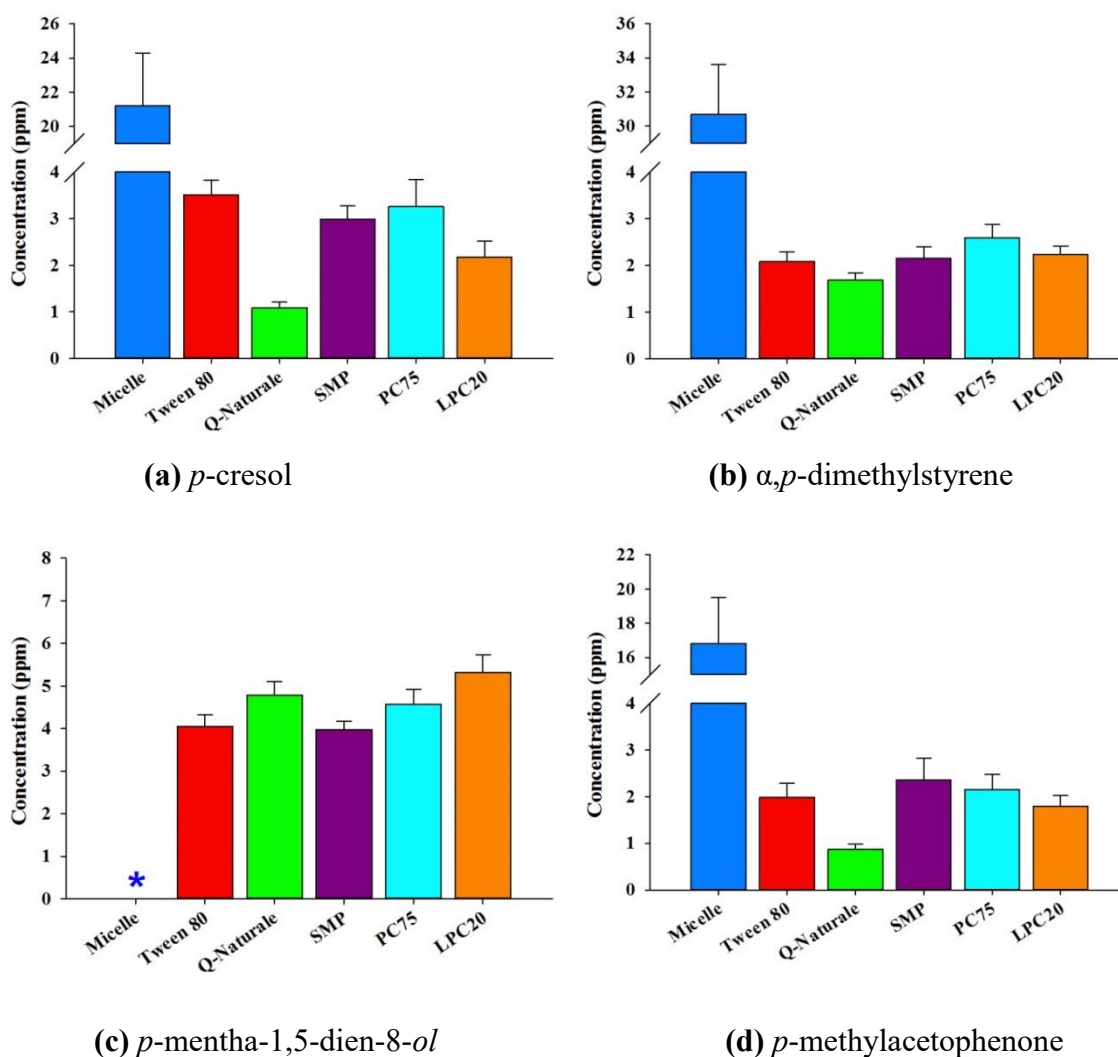


Figure 22. Levels of four major citral degradation off-odors in all tested colloidal systems stored at 50 °C for 35 days: (a) *p*-cresol, (b) α ,*p*-dimethylstyrene, (c) *p*-mentha-1,5-dien-8-ol, (d) *p*-methylacetophenone.

4.3.4. Evaluation of lipid degradation products

Besides monitoring citral's chemical stability and off-flavor generations, we were also able to detect some lipid oxidation/degradation products during the storage tests at elevated temperature condition. **Fig. 23** shows the detection levels of two key lipid oxidative degradation products (pentanal and heptanal) after storage at 50 °C for 35 days. Heptanal is usually derived from oxidation of n-9 mono-unsaturated fatty acid (e.g. oleic acid), and Pentanal is normally derived from oxidation of n-6 poly-unsaturated fatty acid (e.g. linoleic acid). However, we noticed that MCT, the oil phase used for this study, is mainly composed of saturated lipids. Thus there was low chance for MCT to be auto-oxidized and generate considerable amounts of these lipid degradation products. We then found clues by looking into the structures of emulsifiers used in this study. Tween 80 contains oleic acid (n-9) on its structure which might be prone to auto-oxidation and degradation at elevated temperatures. SMP itself doesn't contain unsaturated fats, while the impurities inside may have degradable fats. Lecithin products usually contain different levels of unsaturated fatty acids. PC75, as specified in product data sheet, contains ~70% of unsaturated fatty acids. In contrast, lyso-lecithin LPC20 has much less contents of unsaturated fatty acids as claimed. These unsaturated fat contents existed in emulsifier structures might be the main reason for the generation of these oxidative degradation products.

Based on the above information, reasonable explanation of the observed results can be deduced. Notably, highest amount of heptanal was observed in the PC75 stabilized emulsion, due to high amount of unsaturated fatty acids existed in PC75 phospholipids. Followed next was the LPC20 system, which had reduced levels of heptanal because of

lower amount of unsaturated fat content. Micelle system and Tween 80 stabilized emulsion were also detected with certain levels of heptanal, since polysorbate 80 molecules contain oleic acids. Then for the SMP system, very low level of heptanal was detected probably due to the contribution of impurities. While no heptanal (trace level lower than the detectable threshold) was found in Q-Naturale stabilized emulsion, since it is free from lipids that are prone to degradations. For Pantanal, however, only PC75 and LPC20 systems were detected after 35 days storage at elevated temperature, likely due to the presence of some n-6 poly-unsaturated fatty acids in lecithin and lyso-lecithin compositions, but not in other emulsifiers.

These results indicated unsaturated lecithin (PC75) was less stable against auto-oxidation compared with other emulsifiers during the storage. Moreover, this observation can also in turn to explain the observed inconsistency results of emulsion physical stabilities with the corresponding surface charges properties. The emulsion stabilized by PC75 had strong surface charge that could positively contribute to the emulsion stability but was proven to be least stable among tested formulations. The reason was probably due to the instability of PC75 molecules during the storage. The unsaturated fatty acids on PC75 were easily auto-oxidized and degraded. Therefore, decreased stability of the molecular structure impaired its emulsifying property and further lowered the stability of emulsion. However, lyso-lecithin (LPC20) was less affected due to the decreased level of unsaturated fatty acids. Although detected with certain levels of lipid degradation products, the performances of LPC20 in stabilizing citral-loaded emulsion and inhibiting the formation of off-flavor generation were still considered to be good among all tested emulsifiers, only next to Q-Naturale. Because compared with lecithin, lyso-lecithin only

contains one tail of fatty acids in the glycerol backbone, which makes it more hydrophilic (higher HLB values) and thus more efficient to stabilize O/W emulsions.

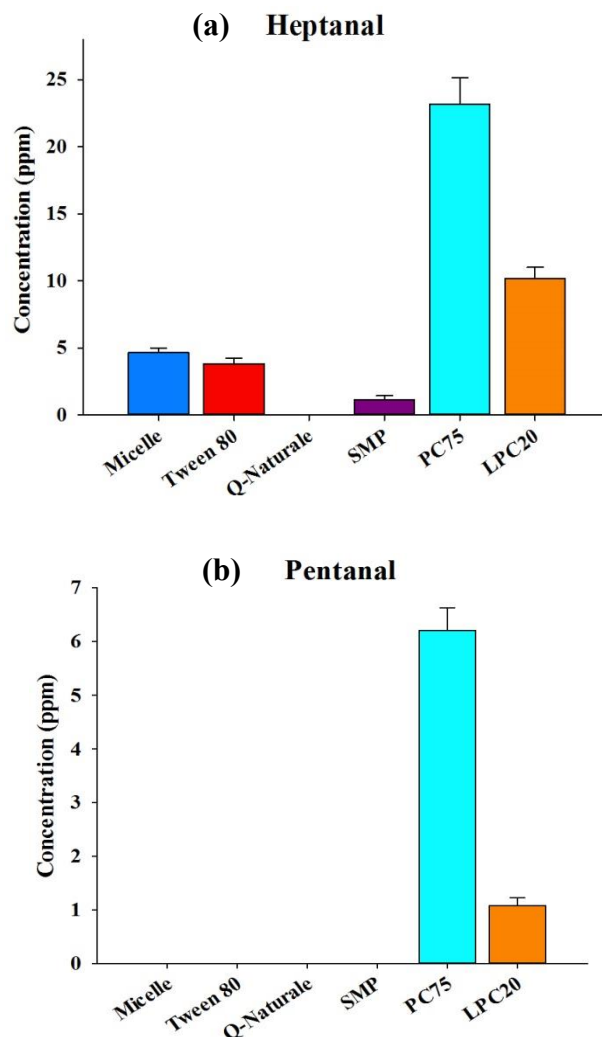


Figure 23. Concentrations of lipid degradation products from all tested colloidal systems stored at 50 °C for 35 days: (a) heptanal; (b) pentanal.

4.4. Conclusions

In summary, five different small molecular surfactants with synthetic or natural origins were tested and compared for their performances in stabilizing citral-loaded O/W nanoemulsions together with a micelle system composed of polysorbate 80 molecules.

Under our defined usage levels and processing conditions, all tested surfactants had analogous emulsifying properties to produce stable nanoemulsions with similar mean particle sizes and initial size distributions. Among them, Q-Naturale stabilized system performed slightly better than others in terms of physical stability during storage, followed by LPC20, SMP and Tween 80 systems. While PC75 stabilized emulsion showed less stability compared with others though it carried strong surface charges. As evidenced by the lipid degradation products generated, the reason was primarily due to the auto-oxidation of largely existing unsaturated fatty acids in lecithin molecules, which weakened its emulsifying properties and further impaired emulsion stability during storage. For citral's chemical stability, emulsions were proven to be more effective in protecting citral from degradation than the micelle system. The effects of different surfactants in protecting citral from degradation and inhibition of off-odors generations were generally correlated with the emulsion stability results, with the Q-Naturale stabilized emulsion had significantly better performance than others, even in elevated temperature conditions. The superior ability of Q-Naturale in stabilizing citral was not only attributed to its excellent ability to stabilize O/W emulsions, but also its potential antioxidant properties.

The current study confirmed promising effects of some natural emulsifiers, i.e. Q-Naturale and LPC20, in stabilizing O/W nanoemulsions and protecting sensitive aromas (citral) in the emulsion systems. Our results will be a meaningful reference for the food industry to select saponin and lyso-lecithin based natural emulsifiers in replacing the traditional synthetic surfactants for specific flavor and beverage applications. It is worth mentioning that there are different types of saponin, lecithin and lyso-lecithin emulsifiers,

our results were only based on one specific product of each of these emulsifier categories. More comprehensive studies need to be done in the future to systematically investigate other types of natural emulsifiers with different sources and compositions.

CHAPTER 5: IN VITRO DETERMINATION OF COENZYME Q10 BIOACCESSIBILITY

5.1. Introduction

Coenzyme Q₁₀, a lipid soluble, physiological important compound, was selected as the model nutraceutical for our functional beverage system. The aim of the current study was to improve its extra low bioavailability by using nanoemulsion as the delivery system. The bioavailability of Q₁₀ is predicted by its bioaccessibility, which can be obtained from simulated *in vitro* digestion models. Based on the formulation of citral-loaded nanoemulsions, we further optimized our nanoemulsion formulations for Q₁₀ delivery by screening different triglycerides as oil phases. Then we used two *in vitro* digestion models, pH-stat lipolysis and TIM-1 systems, to kinetically determine the bioaccessibility fraction of Q₁₀ in the testing formulations. Q₁₀ oil dispersion was used as the control group representing common oil-based CoQ₁₀ supplements, which will be compared with our optimized Q₁₀ nanoemulsion system.

Another objective of the current study was to determine the bioaccessibility differences of Q₁₀ versus Q₁₀H₂, two major redox states of CoQ₁₀, known as ubiquinone (oxidized form) and ubiquinol (reduced form) respectively. It is generally known that these two forms can be recycled *in vivo* within the mitochondrial respiratory chain by the action of endogenous enzymes. However, CoQ₁₀ in endo-membranes, plasma membranes is extensively in the reduced form, most of the CoQ₁₀ in serum and tissue is also in the reduced form (140, 141). Previous study also reported the conversion from Q₁₀ to Q₁₀H₂ took place in the enterocytes during its absorption (142). Therefore it is highly interesting to study the absorption kinetics of Q₁₀ and Q₁₀H₂, and investigate the bioavailability

differences by taking these two forms as supplements. Currently, ubiquinone and ubiquinol are both commercially marketed. As the reduced form, ubiquinol is being promoted as the active antioxidant/advanced form of CoQ₁₀. However, limited knowledge is garnered regarding the bioaccessibility and bioavailability differences of taking Q₁₀ versus Q₁₀H₂. In order to obtain more insights, we designed comparison studies to investigate the bioaccessibility of Q₁₀ and Q₁₀H₂ in our developed formulations by using pH-stat simulated digestion model.

5.2. Materials and methods

5.2.1. Materials

Coenzyme Q₁₀ was kindly provided by Advanced Orthomolecular Research Inc. (Calgary, Canada) and reduced form Q₁₀H₂ (95% UV) was purchased from Hangzhou Joymore Technology Co., Ltd. China. Coenzyme Q₈ was purchased from Avanti Polar Lipids (Alabaster, AL). Neobee 1053 medium-chain triacylglycerol (MCT) together with other triglycerides (Neobee 1095, Wecobee FS, Wecobee S) with different fatty acid chain lengths and compositions were provided by Stepan Co. (Northfield, IL). Alcolec LPC20 lyso-lecithin was a gift from American Lecithin Co. (Oxford, CT). Q-Naturale 200 was provided by Ingredion Inc. (Bridgewater, NJ). Sodium taurodeoxycholate (NaTDC) was purchased from CalBiochem (La Jolla, CA). Pancreatin with 8× USP specification, pepsin, trypsin, α -amylase and all other analytical chemicals and reagents were purchased from Sigma-Aldrich (St. Louis, MO). Fresh pig bile was obtained from Farm-to-Pharm (Warren, NJ). The bile was collected and standardized from a slaughterhouse, aliquoted for individual TIM experiments, and stored at -20 °C until use.

HPLC-grade methanol and ethyl alcohol were purchased from Pharmco-AAPER (Brookfield, CT). Milli-Q water was used throughout the experiments when needed.

5.2.2. Testing formulation preparation

A food-grade nanoemulsion was designed to encapsulate and solubilize Q₁₀, with the objective of improving its poor bioavailability. Based on the results from Chapter 4, we further fine-tuned the nanoemulsion formulation for Q₁₀ delivery. By dissolving 0.1-1.0 wt% of Q₁₀ in triglyceride (9.0-9.9 wt %), the oil phase was thoroughly mixed and homogenized with water phase containing emulsifier (5 wt%) using an Ultra-Turrax T-25 high-speed homogenizer (IKA Works Inc., Wilmington, DE) at 24,000 rpm for 3 min followed by homogenization using an EmulsiFlex-C3 high-pressure homogenizer (Avestin Inc., Ottawa, Canada) for 6 cycles at 150 MPa. The control group, Q₁₀ oil dispersion, was prepared at the same concentration in the oil phase as in the nanoemulsion representing the standard lipid-based Q₁₀ supplements.

5.2.3. Titration based pH-stat lipolysis model

The *in vitro* lipolysis model (fed-state) was carried out using the method described previously (143). In brief, the lipolysis buffer was composed of Tris maleate, NaCl, CaCl₂·H₂O, NaTDC, and phosphatidylcholine in concentrations of 50, 150, 5, 20, and 5 mM, respectively, to mimic the high concentrations of bile salts and endogenous phospholipids in the small intestine lumen. Pancreatin solution was prepared by mixing 1 g of pancreatin powder with 5 mL of the lipolysis buffer, followed by 15 min centrifugation at 2,000 rpm, collection of the supernatant was kept on ice until use. Samples containing 0.25 g of lipids were added to 9 mL lipolysis buffers. Then 1 mL pancreatin solution was added to initiate lipolysis under constant mixing. During the 2 h

simulated digestion, the system pH was controlled at 7.50 ± 0.02 by adding 0.25 mol/L NaOH at 37 °C. The NaOH concentration vs. time was recorded throughout the experiment, and the total NaOH consumed was obtained for final calculation. Upon completion, the whole lipolysis liquid was ultracentrifuged at 4 °C and 50,000 rpm for 1 h (Ti 60 rotor, Beckman Coulter). The middle aqueous phase of micellar Q₁₀ was collected and filtered using 0.22 µm filters before the HPLC analysis.

5.2.4. Determination of the extent of lipolysis and bioaccessibility

According to stoichiometric ratio, it assumes that upon digestion, one mol of triglyceride releases two mols of free fatty acids (FFAs) and consumes two mols of NaOH for neutralization to maintain the pH. The extent of lipolysis, defined as the percentage of triglycerides digested during lipolysis, may be determined from the total amount of NaOH consumed. A control was tested using either a water solution (for oil dispersion samples) or a corresponding emulsifier solution (for emulsion samples), and the amount of NaOH used for the mock lipolysis was subtracted from the Q₁₀ samples. The following equation describes the calculation of extent of lipolysis:

$$\text{Extent of Lipolysis} = \frac{V_{\text{NaOH}}(t) \times C_{\text{NaOH}} \times M_{\text{w,lipid}}}{2 \times m_{\text{lipid}}} \times 100\%$$

where $V_{\text{NaOH}}(t)$ is the volume of NaOH titrated into the reaction vessel at the digestion time (t) to neutralize the FFAs released. C_{NaOH} is the concentration of NaOH (mol/L), and $M_{\text{w,lipid}}$ is the average molecular weight of the lipid (g/mol). In this experiment, MCT has an average Mw of 503 g/mol and m_{lipid} is the total mass of digestible lipid added (g).

The corresponding Q₁₀ bioaccessibility of can be calculated as follows:

$$Q_{10} \text{ Bioaccessibility} = \frac{\text{Total mass of solubilized } Q_{10}}{\text{Total mass of } Q_{10} \text{ input}} \times 100\%$$

The mass of solubilized Q_{10} is calculated by the product of the concentration of Q_{10} in the aqueous phase and the total volume.

5.2.5. TIM-1 model

The schematic representation of the TIM-1 dynamic model is shown in **Fig. 24**. This *in vitro* gastrointestinal model mimics the digestive tract utilizing four compartments: stomach, duodenum, jejunum, and ileum. Each compartment is infused with defined start residues that resemble the actual physiological gastrointestinal conditions. In short, the formulations “meals” were tested during 4 h simulated digestions of the TIM-1 model in the fed-state. The “meal” (300 g) was prepared by combining 100 g sample (Q_{10} nanoemulsion or oil dispersion with same Q_{10} content), 95 g gastric electrolyte solution, 50 g water, 5 g gastric enzyme solution and 50 g water. Secretions of HCl (1M), sodium bicarbonate (1M), digestive fluids were modulated with pre-programmed flow rates, the pH curves, gastric emptying rates, and intestinal transit times. The surrounding water jackets controlled the temperature at 37 °C and simulated peristalsis by pressurizing the fluid. The Q_{10} in filtrates, passed through the capillary membranes (Spectrum Milikros modules M80S-300-01P, with 0.05 µm pore size) at the jejunum and ileum compartments, were defined as the soluble micellar fraction available for absorption, i.e. bioaccessible fraction. During the digestion, jejunum and ileum filtrates were collected in every 30 min fraction, and samples were immediately stored at -20 °C until analysis.

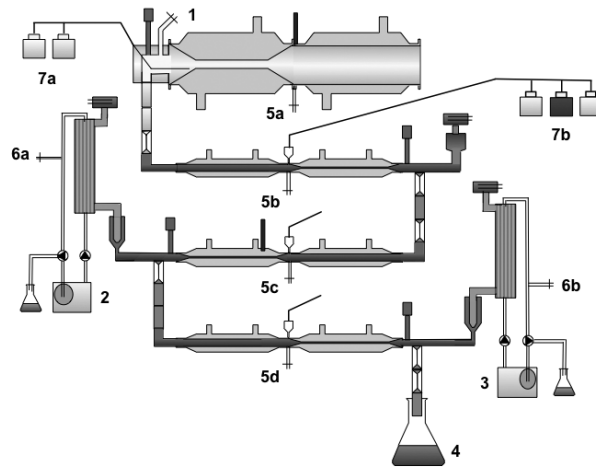
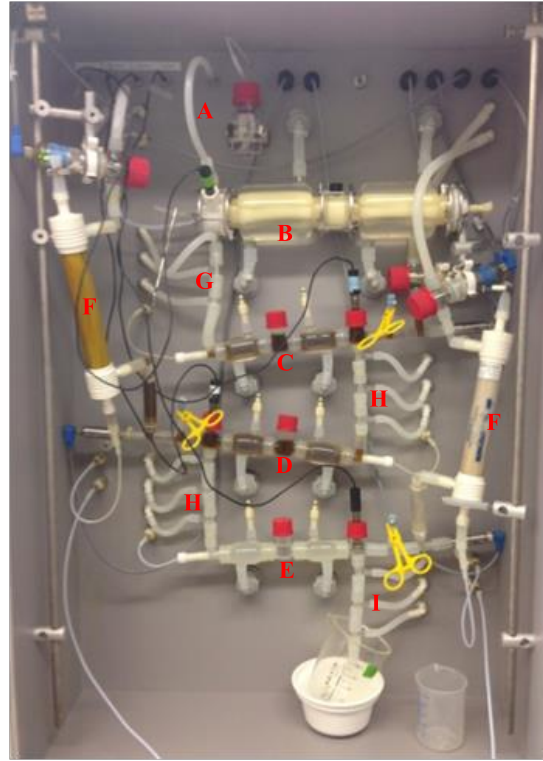


Figure 24. The cabinet of the *in vitro* gastrointestinal model, TIM-1: (a) food inlet, (b) gastric compartment, (c) duodenum compartment, (d) jejunum compartment, (e) ileum compartment, (f) semi-permeable hollow fiber membrane, (g) pyloric sphincter, (h) peristaltic valve, (i) ileo-caecal sphincter.

5.2.6. Extraction and analysis of Q₁₀

The concentration of Q₁₀ in the aqueous phases (pH-stat lipolysis) and filtrates (TIM-1) were determined using an UltiMate 3000 HPLC system (Dionex) with a UV-VIS absorption detector at 275 nm and a reverse phase Luna[®] 3 μ m C18, 150 \times 4.6 mm column (Phenomenex). The mobile phase was ethyl alcohol / methanol (60:40, v/v) with isocratic elution at a flow rate of 1 mL/min. For the pH-stat lipolysis samples, 200 μ L of the aqueous phase was filtered through a 0.22 μ m filter and mixed with 400 μ L ethanol for direct HPLC analysis. For the TIM-1 samples, upon thawing under room temperature and mixing the filtrates, 1 mL of each sample was transferred into small vials. Coenzyme Q₈ as the internal standard (I.S.) was added to the filtrates. Then 5 mL of *n*-hexane was added to each sample and vortex for 3 min to extract the Q₁₀ from the filtrates. After centrifugation, the top *n*-hexane layer was transferred into a new vial and then dried under nitrogen, reconstituted in ethanol, and analyzed by HPLC. To prevent Q₁₀ from photo degradation, all the procedures were conducted under dim light.

5.2.7. Measurements of the bioaccessibility of Q₁₀ versus Q₁₀H₂

Both oil dispersions and nanoemulsions were prepared using Q₁₀ and Q₁₀H₂ at the same level of 0.1 wt% for bioaccessibility determination using the pH-stat model. After simulated digestion, the bioaccessible fractions were quantitatively determined by HPLC. Due to the inevitable exposure of Q₁₀H₂ in the oxidative stress during sample preparation, such as homogenization and extraction, certain portion of Q₁₀H₂ might be oxidized into Q₁₀ before, during or after digestion. Therefore, for the bioaccessibility determination of Q₁₀H₂ formulas, reducing agent NaBH₄ was used to treat the samples before HPLC analysis.

5.2.8. Statistical analysis

The pH-stat lipolysis experiments were performed in triplicate for each sample. TIM-1 experiments were duplicated for each sample, and each sample duplicate was analyzed in two technical duplicates. All data were expressed as the mean \pm standard deviation. When appropriate, data were analyzed by SigmaPlot 12.0 software with a student t-test or one-way analysis of variance (ANOVA). Significant difference was defined at $p < 0.05$.

5.3. Results and discussion

5.3.1. Nanoemulsion formulation optimization for Q₁₀

Since Q₁₀ is a lipid soluble nutraceutical, the lipid phase of nanoemulsion was further investigated with different lipids. Four triglycerides with varying chain lengths and compositions were selected as the candidates for oil phase. The detailed physicochemical properties of these lipids are listed in **Table 9**. Among them, two Neobee oils are considered as medium chain triglycerides (MCT), and other two Wecobee oils are mixtures of long chain triglycerides (LCT). As a general rule, the melting point of a lipid is positively correlated with its chain length/molecular weight. And usually saturated fatty acids have higher melting points than the unsaturated fatty acids due to more linear molecular geometries, which allow the fatty acids molecules to be more closely stacked together, thus result in stronger intermolecular interactions and higher melting points. In this study, all the lipids are saturated triglycerides, and only Neobee 1053 MCT is liquid oil, other three lipids are considered as solid lipids under room temperature.

Table 9. Properties of four different lipid candidates as oil phase.

Triglycerides	Neobee 1053	Neobee 1095	Wecobee FS	Wecobee S
Composition	C8:0=55% C10:0=44%	C10:0=96%	C12:0=47.4%	C12:0=39.5%
			C14:0=15.3%	C14:0=12.9%
			C16:0=8.3%	C16:0=10.1%
			C18:0=19.4%	C18:0=26.5%
Melting Point °C (°F)	-5 (23)	32 (90)	39.8 (103.6)	44 (111)
Saponification Value	334	325	244	240

Then, the lipolysis raw curves of these four lipids (**Fig. 25 A**) were obtained by recording their corresponding digestion time vs. volumes of NaOH consumed. And the extent of lipolysis was calculated according to the above mentioned equation and shown in **Fig. 25 B**.

It is reported that the digestion rate of MCT was greater than LCT, and was independent of bile salt concentration (144). Our *in vitro* lipolysis results confirmed this observation, and further indicated that chain length of a lipid was negatively correlated with its rate and extent of digestion. Neobee 1053, being the shortest chain length lipid tested, had the fastest digestion rate and highest extent of lipolysis after 2 hours. Therefore, to accelerate digestion, we selected Neobee 1053 MCT, consisting of 55% caprylic and 44% capric triglyceride, as the oil phase to further prepare our Q₁₀ loaded oil-in-water (O/W) nanoemulsion.

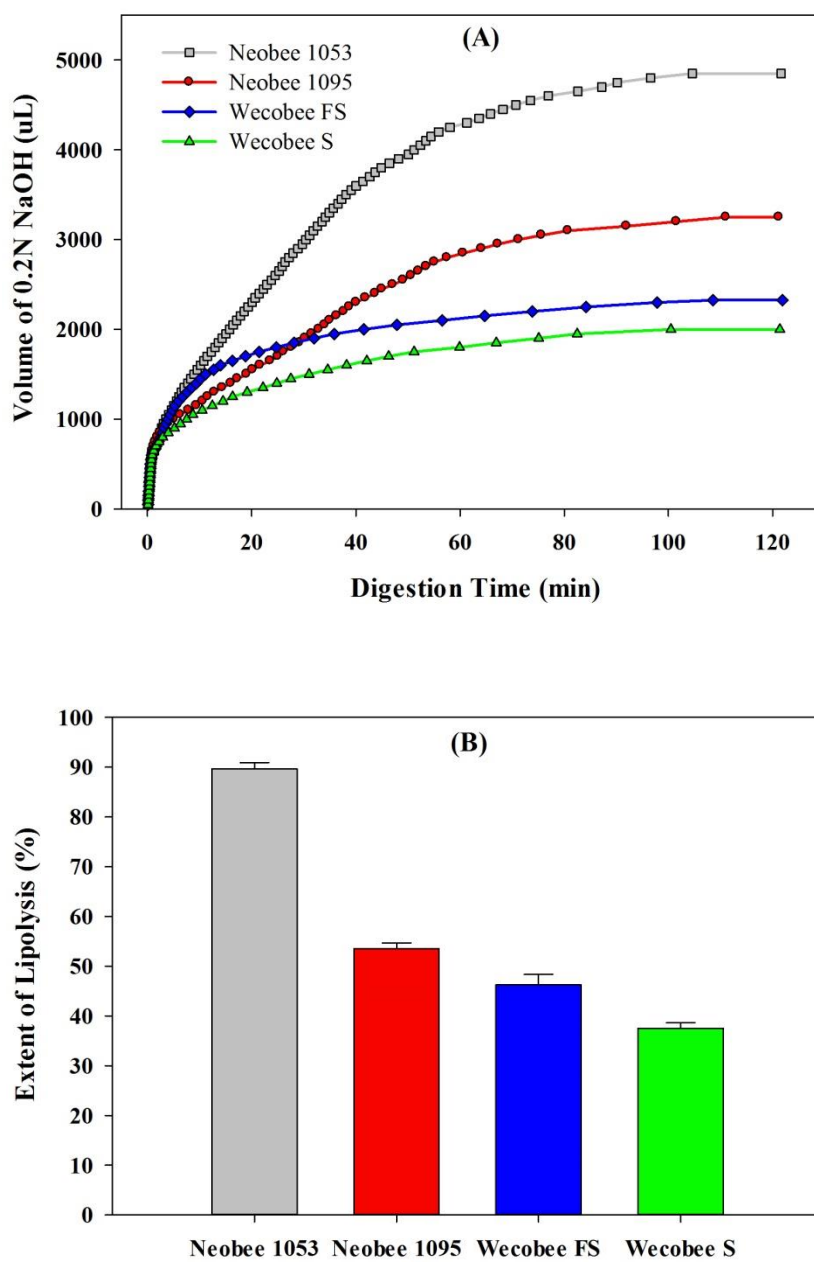


Figure 25. (a) Lipolysis curves (digestion time vs. volume of NaOH consumed) of four lipids during 2 h of *in vitro* digestion; (b) the corresponding extents of lipolysis (%).

Then, based on previous results from Chapter 4 for citral-loaded nanoemulsions, we selected Saponin (Q-Naturale 200) and lyso-lecithin (LPC20) as the candidates of emulsifiers for Q₁₀-loaded nanoemulsions. To be consistent with the previous developed formulas, we kept using 10 wt% of oil phase and aimed at stabilizing up to 1 wt% of Q₁₀ in the final formula. For low Q₁₀ dose (0.1 wt%), which was used for *in vitro* bioaccessibility characterization, both Q-Naturale and LPC20 performed well in stabilizing Q₁₀-loaded emulsions. However when Q₁₀ loading further increased to 1 wt% (used for next stage *in vivo* bioavailability characterization), LPC20 produced more stable nanoemulsion than Q-Naturale (data not shown). Moreover, considering the composition of cell membrane is phospholipid bilayer, using phospholipid based materials may have the merit of altering the membrane fluidity and potentially increase the transportation and bioavailability of delivered nutraceuticals. Given the above reasons, we selected LPC20 lyso-lecithin as the emulsifier for the Q₁₀-loaded nanoemulsions in experimental designs.

Therefore, the nanoemulsion formulation was optimized for CoQ₁₀ delivery, with 10% of Neobee 1053 MCT as the oil phase, 5% of lyso-lecithin as the emulsifier in the water phase, which was able to stable 0.1 - 1.0 wt% of CoQ₁₀. The optimized formulation can achieve the initial particle size of nanoemulsion to be ~105 nm after the defined homogenization conditions. And during a two-month storage test at 25 °C, only slight increase in particle size was recorded, no creaming or phase separation was observed (data not shown).

5.3.2. Using pH-stat model to determine the bioaccessibility of Q₁₀ formulations

Utilizing the pH-stat lipolysis model, both the Q₁₀ nanoemulsion and Q₁₀ oil dispersion had a high degree of lipolysis (**Figure 26A**). Lipids were readily digested to

free fatty acids during the 2 h lipolysis experiments for the nanoemulsion sample while about 90% of the triglycerides, in Q₁₀ oil dispersion were hydrolyzed after 2 h. Although the extent of lipolysis was not in huge different, the rate of lipolysis in the first 20 min was significantly higher for the nanoemulsion compared to the oil dispersion. In the first 5 min, approximately 70 % of lipids were rapidly digested in the nanoemulsion, while for the MCT dispersion only 24 % of oil was hydrolyzed. This observation is congruent with previous work (44), and can be possibly attributed to the larger oil-water interfacial area of nanoemulsion droplets compared with the bulk oil phase and thus facilitates lipase hydrolysis. The bioaccessible Q₁₀ fraction in the nanoemulsion was 77.11% and 16.35% in the oil dispersion (**Figure 26B**). The formulated nanoemulsion improved the bioaccessibility of Q₁₀ by a factor of nearly 5 compared with the oil dispersion sample.

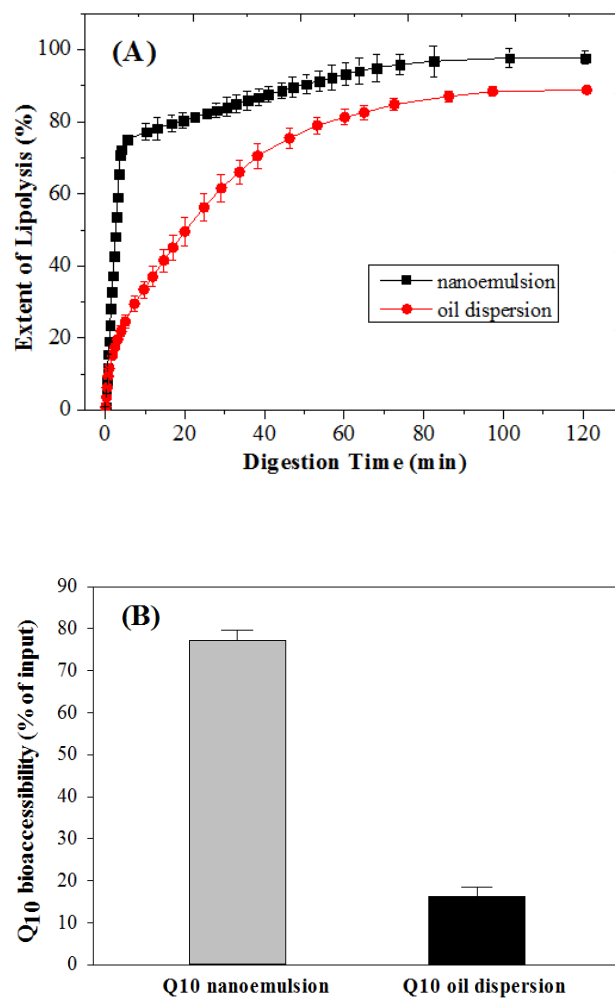


Figure 26. (a) pH-stat *in vitro* lipolysis digestion curve (extent of lipolysis) of Q₁₀ nanoemulsion and Q₁₀ oil dispersion samples; (b) The Q₁₀ bioaccessibility (% of input) after lipolysis in Q₁₀ nanoemulsion and Q₁₀ oil dispersion samples.

5.3.3. Using TIM-1 model to determine the bioaccessibility of Q₁₀ formulations

The aforementioned Q₁₀ nanoemulsion and oil dispersion were also tested using the TIM-1 model. The Q₁₀ concentrations in jejunum and ileum filtrates were analyzed and back calculated the Q₁₀ bioaccessibility at 30 min time intervals (**Fig. 27**). During the 4 h digestion, the bioaccessible fraction of Q₁₀ at each 30 min interval varied, but the general trends for the two formulations were with similar. For the nanoemulsion, negligible Q₁₀ was detected in jejunum filtrates during the first 30 min. After 30 min, the bioaccessible fraction increased gradually and the highest concentration was achieved between 150 and 180 min at 10.1% Q₁₀. The concentration then continually decreased until the end of digestion (**Fig. 27A**). Compared with jejunum, much lower concentration of Q₁₀ became bioaccessible in ileum (**Fig. 27B**), indicating that most of release of Q₁₀ was assembled into micellar form and readily absorbed in jejunum, while the remaining fraction was further assimilated in ileum. It was observed that the bioaccessible Q₁₀ in ileum increased with time fraction during the entire digestion process, which was in part due to the time lag of the chyme passing through the digestive tract. Being the latter part of the small intestine, the peak Q₁₀ concentration occurred later in ileum than in the jejunum. The overall Q₁₀ bioaccessibility was defined as the sum of bioaccessible fraction of Q₁₀ accumulated in both jejunum and ileum filtrates for the 4 hrs. The overall bioaccessibility of Q₁₀ from the nanoemulsion formulation was accumulated for each 30 min sample (**Fig. 27C**) and followed the trends seen in Fig 19A, with an increasing amount of Q₁₀ became bioaccessible at early stage of digestion, and the peak concentration observed between 150 and 180 min.

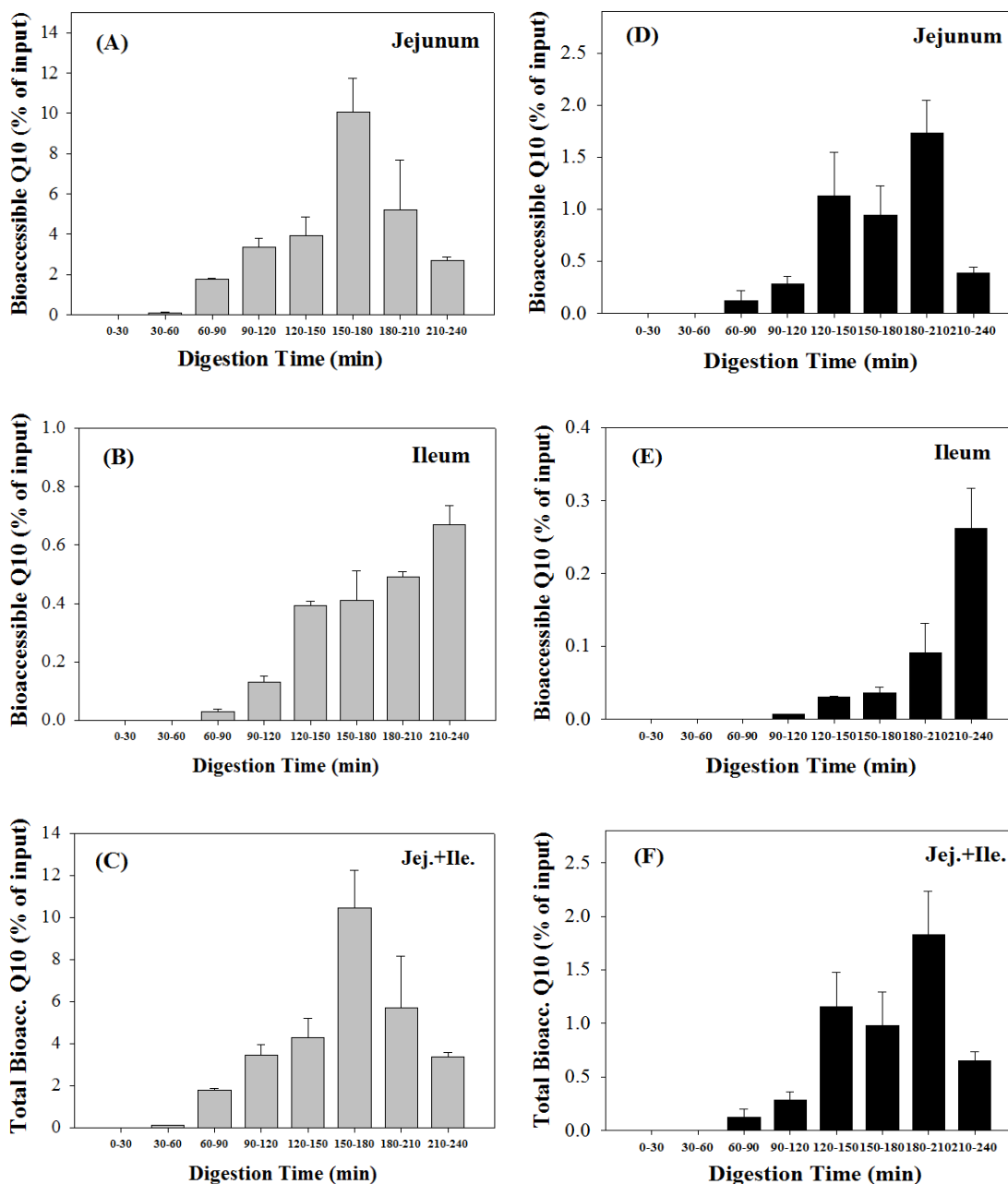


Figure 27. Bioaccessible Q₁₀ fraction (% of input) accumulated in every 30-min digestion period from different parts of the TIM-1 model. (a) Bioaccessible Q₁₀ fraction in jejunum filtrates from nanoemulsion; (b) Bioaccessible Q₁₀ fraction in ileum filtrates from nanoemulsion; (c) Total bioaccessible Q₁₀ fraction in both jejunum and ileum filtrates from nanoemulsion; (d) Bioaccessible Q₁₀ fraction in jejunum filtrates from oil

dispersion; (e) Bioaccessible Q₁₀ fraction in ileum filtrates from oil dispersion; (f) Total bioaccessible Q₁₀ fraction in both jejunum and ileum filtrates from oil dispersion.

In contract, the Q₁₀ oil dispersion showed decreased Q₁₀ bioaccessibility in both jejunum and ileum filtrates (**Fig. 27D, 27E**) and the overall bioaccessible fractions (**Fig. 27F**). The Q₁₀ concentration plateaued at 1.83% between 180 and 210 min. A delayed peak indicated a slower digestion of oil sample compared with nanoemulsion, which was in accordance with the results obtained using the pH-stat lipolysis curve. In a comparable overview, the accumulative Q₁₀ bioaccessibility of the two formulations in jejunum, ileum and the combined (jej.+ile.) total were plotted in **Fig. 28**. In the jejunum, the Q₁₀ bioaccessibility was 27.07% for the nanoemulsion compared to 4.59% for the oil dispersion (**Fig. 28A**). In the ileum it was 2.13% and 0.43% for the nanoemulsion and oil dispersion samples, respectively (**Fig. 28B**). Taken together (**Fig. 28C**), for the nanoemulsion, the total Q₁₀ bioaccessibility was 29.20% compared to 5.02% for the oil dispersion, indicating a nearly 6× increase in the bioaccessibility.

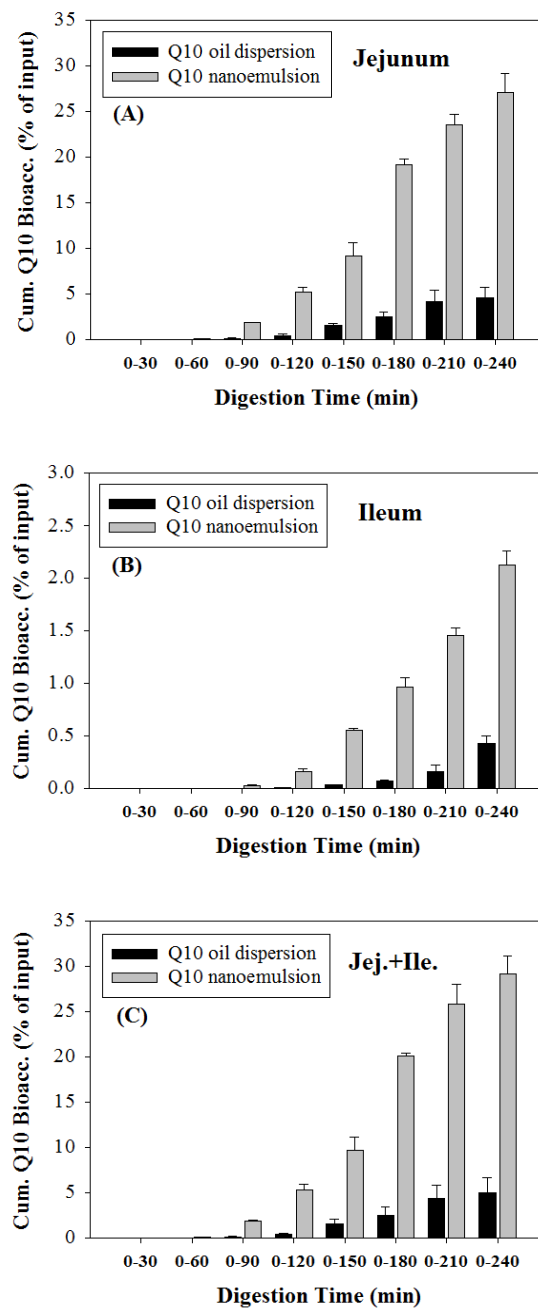


Figure 28. Cumulative Q₁₀ bioaccessibility (% of input) recovered during the 4h of digestion in TIM-1 model for both Q₁₀ nanoemulsion and Q₁₀ oil dispersion. (a) Cumulative Q₁₀ bioaccessibility in jejunum; (b) Cumulative Q₁₀ bioaccessibility in ileum; (c) Overall cumulative Q₁₀ bioaccessibility in both jejunum and ileum.

5.3.4. Discussion of the results obtained from two *in vitro* systems

Both *in vitro* systems indicated the nanoemulsion had a much higher (about 5~6×) bioaccessible Q_{10} fraction compared with oil dispersion. However, the absolute Q_{10} concentration obtained from TIM-1 model were considerably lower than pH-stat model. 29.20% of the inputted Q_{10} was recovered and determined bioaccessible in the TIM-1 for the nanoemulsion, this is in contrast to the 77.11% recovered in the pH-stat model. Similarly, there was a significant difference observed between of the oil dispersions in the two systems (TIM-1: 5.02%; pH-stat: 16.35%). The complexity and accuracy of the system designs and simulations account for the differences obtained. The pH-stat lipolysis model, as a simplified digestion model, only controlled temperature, pH, initial endogenous bile salts and phospholipid concentrations for digestion. Many of other important factors are overlooked. In most cases, a container with a stirrer surrounded by temperature control unit resembles the intestinal milieu in the pH-stat model poorly mimicking the physical conditions and the movement of digestive tract. Moreover, in the pH-stat model, the entire sample was completely exposed to the digestive solutions from the initial stage till the end of the digestion, with no defined gastric emptying, intestinal transit, nor dynamic secretions which modify the digestive rates. In contrast, the TIM-1 model more accurately simulates the upper GI tract considering more physiological conditions. Besides simulating the concentration of digestive enzymes, concentration of bile salts in different regions of gut and the transit of chyme, it also mimics peristaltic movements. More importantly, it allows for continual sampling throughout digestion at jejunum and ileum independently, which is significant for investigating the digestion kinetics. Obviously, the bioaccessibility data obtained from TIM-1 model is more

convincing and meaningful to act as a reference of further *in vivo* studies. While the pH-stat model may still provide some initial guidelines in the development of lipid based delivery systems for lipophilic nutraceuticals and drugs since it is a rapid, low cost method for assessing formulation.

It is also worth mentioning that all *in vitro* models only simulate processes occurring in the lumen and do not mimic biological activities associated with biotransformation or metabolism. The data gathered from these *in vitro* models overlook processes occurring in later stages of the absorption cascade that define true bioavailability, e.g. permeability through the gut wall by active transport, intra-enterocyte process, efflux transporters, lymphatic transport, and post-enterocyte processes including hepatic first pass metabolism. Therefore, more efforts to develop *in vitro-in vivo* correlations may aid in designing more accurate *in vitro* models.

5.3.5. Bioaccessibility of Q₁₀H₂ versus Q₁₀ determined by the pH-stat model

To better understand the differences in digestion/absorption kinetics between Q₁₀H₂ and Q₁₀, the bioaccessibility of Q₁₀H₂ was determined by the pH-stat model in both oil dispersions and nanoemulsions. Results were compared with the previously obtained Q₁₀'s bioaccessibility and summarized in **Fig. 29**. It was interesting that in the form of oil dispersion, 24.65% of Q₁₀H₂ became bioaccessible after simulated small intestine digestion, which was significantly higher than the 16.35% of bioaccessibility of Q₁₀. However, similar bioaccessibility of Q₁₀H₂ (78.21%) and Q₁₀ (77.11%) were observed in the delivery form of nanoemulsion. The increased bioaccessibility in oil dispersion indicated Q₁₀H₂ was more efficiently incorporated into mixed micelles compared with Q₁₀. This observation was in accordance with a recently published

research by Failla *et al* (145). Where the authors reported the increased bioavailability of ubiquinol compared to that of ubiquinone was due to more efficient micellarization and improved uptake of epithelial cells. While in the form of nanoemulsion, our results indicated the partitioning efficiencies of $Q_{10}H_2$ and Q_{10} into mixed micelles were similar probably due to significantly improved solubility of the lipophilic compound in emulsified nanoparticles which facilitated its digestion and releasing from the delivery matrix into mixed micelles. Moreover, it might be possible that the released emulsifier molecules, such as saponin and lecithin, contributed to the formation of mixed micelles, which further improved the bioaccessibility of CoQ_{10} . Therefore the differences of partitioning efficiencies into mixed micelles between $Q_{10}H_2$ and Q_{10} were not significant in this case. It should also be noted that extra processing (such as homogenization, extraction, etc.) of $Q_{10}H_2$ under the oxidative stress will make it more liable to be oxidized into Q_{10} . Therefore, for $Q_{10}H_2$'s bioaccessibility determination, sodium borohydride ($NaBH_4$) was used as a reducing agent to convert any oxidized Q_{10} back to $Q_{10}H_2$ before HPLC analysis.

Overall, our results confirmed the improved bioaccessibility of $Q_{10}H_2$ over Q_{10} in the oil dispersion when subjected to simulated digestion. While the importance of delivery systems in determining the bioaccessibility of lipophilic nutraceuticals should be highly addressed, as nanoemulsion can significantly improve the bioaccessibility of both $Q_{10}H_2$ and Q_{10} . No significant difference was observed for the bioaccessibility of $Q_{10}H_2$ and Q_{10} in nanoemulsion formulations.

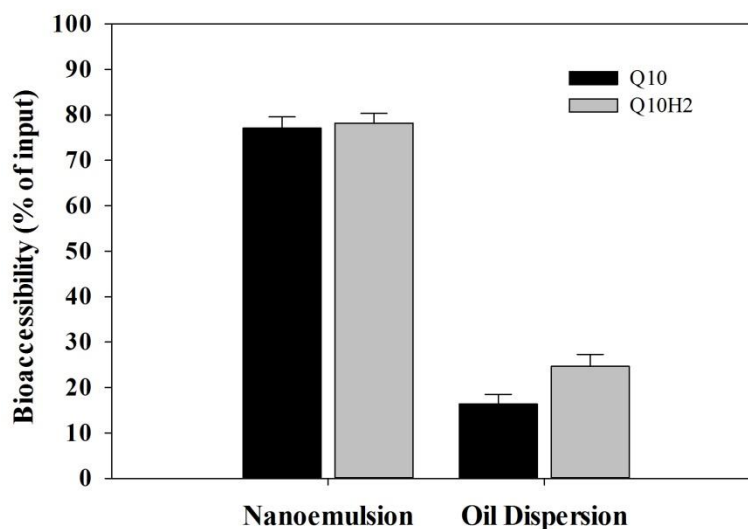


Figure 29. Bioaccessibility of Q₁₀H₂ and Q₁₀ in both oil dispersion and nanoemulsion forms determined by the pH-stat digestion model.

5.4. Conclusions

Nanoemulsion formulations for CoQ₁₀ delivery were tuned with oil phase and emulsifier selections based on previous citral stability work. The optimized CoQ₁₀ nanoemulsion was compared with the control oil dispersion group for bioaccessibility determination. Two *in vitro* models, pH-stat and TIM-1, were utilized to determine the bioaccessibility of Q₁₀. Results from both models confirmed a 5~6× improvement of Q₁₀ bioaccessibility for the nanoemulsion compared to the oil dispersion in the current study, indicating the importance of designing proper delivery systems for lipophilic nutraceuticals. While the absolute bioaccessibility values obtained from these two models were significantly different (i.e., the Q₁₀ bioaccessibility from pH-stat model was much greater than that obtained from the TIM-1 model). Considering the complexity of the GI track, the pH-stat model was over simplified system and it was suspected that an

overestimation of the bioaccessible fraction was observed. The TIM-1 model more adequately simulates the upper GI tract, increasing the control of the digestive fluids and conditions, and is more capable of delivering convincing *in vitro* bioaccessibility data. Still, the pH-stat model is a useful and rapid tool for initial formulation screening and comparison by providing relative bioaccessibility for proof of concept studies.

Moreover, we reported increased bioaccessibility of $Q_{10}H_2$ over Q_{10} evidenced by results from the pH-stat digestion model, especially in the oil dispersion form. The improved bioaccessibility was due to greater partitioning efficiency of $Q_{10}H_2$ into the mixed micelles formed during digestion. Again, nanoemulsions were shown to provide much higher bioaccessibility for both $Q_{10}H_2$ and Q_{10} compared with their oil dispersion forms, though no significant difference was observed for $Q_{10}H_2$ and Q_{10} in the nanoemulsion forms.

CHAPTER 6: IN VIVO DETERMINATION OF COENZYME Q10 BIOAVAILABILITY - PHARMACOKINETICS AND TISSUE DISTRIBUTION STUDIES

6.1. Introduction

To mediate its health-promoting effects, orally administered CoQ₁₀ must be bioavailable in systemic circulation and delivered to target tissues. As the bioavailability of CoQ₁₀ is not only determined by bioaccessibility results from *in vitro* models, but also other complicated bioactivities associated with absorption, transportation, metabolism, tissue uptake and distribution, etc. It is crucial to investigate the pharmacokinetics and tissue distribution of CoQ₁₀ after oral administration of the developed nanoemulsion formulations.

Pharmacokinetics (PK) study is a widely used method to access and indicate the relative bioavailability of drugs or nutraceuticals *in vivo*. There are quite a few reports on the pharmacokinetics of CoQ₁₀ in humans and in animal models. While different T_{\max} values (ranging from 2 h to 6 h or longer) and elimination half-life were reported with trials on different formulations and animal models. Also, in some studies, a second plasma CoQ₁₀ peak was observed at about 24 h following oral ingestion (124). Therefore, it is important to test the PK curve for CoQ₁₀ in our developed beverage emulsion formulations for better understanding of its relative bioavailability after consumption compared with the unformulated form.

After being available in blood for systemic circulation, CoQ₁₀ will be further delivered and accumulated in tissues and organs for potential physiological functions. There are literatures on the CoQ₁₀ distribution and redox states in various organs, while

few references can be found to indicate the change of levels of CoQ₁₀ in different tissue and organs after one time or chronic CoQ₁₀ supplement, probably due to the difficulty and complexity in conducting the experiments. It will be meaningful to collect these data by carefully designing animal experiments.

In this study, the plasma CoQ₁₀ responded to oral ingestion of both oil dispersion and nanoemulsion were examined and compared. Moreover, the distribution and uptake levels of CoQ₁₀ in major organ tissues were investigated after one time administration in both experimental and control groups.

6.2. Materials and methods

6.2.1. Materials

Coenzyme Q₁₀ was provided by Advanced Orthomolecular Research Inc. (Calgary, Canada). Coenzyme Q₈ was purchased from Avanti Polar Lipids (Alabaster, AL) as the internal standard. Neobee 1053 medium-chain triacylglycerol (MCT) were obtained from Stepan Co. (Northfield, IL). Alcolec LPC20 lyso-lecithin was a gift from American Lecithin Co. (Oxford, CT). HPLC-grade methanol and ethyl alcohol were purchased from Pharmco-AAPER (Brookfield, CT). Milli-Q water was used throughout the experiments when needed. All other chemicals and analytical supplies were purchased from Sigma-Aldrich (St. Louis, MO) and used without further purification and treatment.

6.2.2. Testing formulation preparation

CoQ₁₀ nanoemulsion was prepared according to the formulation developed in 5.2.2. By dispersing 1.0 wt% of Q₁₀ in 9.0 wt% Neobee 1053 MCT, the oil phase was

thoroughly mixed and homogenized with water phase containing 5.0 wt% of LPC20 lysolecithin using an Ultra-Turrax T-25 high-speed homogenizer (IKA Works Inc., Wilmington, DE) at 24,000 rpm for 3 min followed by homogenization using an EmulsiFlex-C3 high-pressure homogenizer (Avestin Inc., Ottawa, Canada) for 6 cycles at 150 MPa. The control group, Q₁₀ oil dispersion, was prepared at the same Q₁₀ concentration in the Neobee 1053, which represents common lipid-based Q₁₀ supplements.

6.2.3. Pharmacokinetics study

All animal studies were performed at the College of Food Science and Technology, Huazhong Agricultural University (HZAU). Kunming mice (male, SPF, 20 ± 2 g) purchased from the Animal Center for Disease Prevention and Control (Wuhan, China) were used for the pharmacokinetics (PK) study. The experimental protocol was approved by HZAU and followed the international guidelines for animal experiments and ethical principles for laboratory animal use and care. Mice were caged under controlled laboratory conditions (25 ± 1 °C, 50% relative humidity, 12 h light/12 h dark cycle) with *ad libitum* water and feed. Then animals were randomly divided into control and experimental groups after one week of acclimation. Upon the PK experiment, all mice were fasted overnight before administrating 100 mg/kg of Q₁₀ in the delivery form of nanoemulsion or oil dispersion through oral gavage. At selected time intervals (1, 2, 4, 6, 8, 10, 12, 24 and 30 hr), blood samples were acquired through cardiac puncture after the animals were sacrificed under the ether anesthesia. In the current experimental design, 10 mice were sacrificed for each time point in each group. Collected whole blood samples

were immediately centrifuged at 10,000 rpm for 15 min at 4 °C, and blood plasma were collected and stored at -80 °C until analysis.

For sample analysis, 500 μ L of thawed plasma from each sample was first collected into 5 mL centrifuge tubes. Since CoQ₁₀ presented in the blood may exist in both oxidized and reduced form, the samples were oxidized with FeCl₃ in hydrochloric acid to convert any possible Q₁₀H₂ to Q₁₀ before analysis. Then aliquot amount of the CoQ₈-in-*n*-hexane stock solution (internal standard, I.S.) was added into each tube and well mixed, which gave the final concentration of I.S. to be 10 μ g/mL. Then 3 mL *n*-hexane was added to each sample for extraction of Q₁₀, and the contents were vortex-mixed for 3 min, and centrifuged at 5,000 rpm for 10 min. The *n*-hexane phase was then transferred to a new tube and dried under nitrogen. Upon analysis, the content in dried tube was re-dissolved with 100 μ L absolute ethanol, and carefully transferred into the HPLC vials with glass inserts (200 μ L in volume with plastic bottom spring) for analysis. Once the plasma concentration of Q₁₀ vs. time curves were acquired, peak concentration (C_{\max}) and time to peak concentration (T_{\max}) were recorded directly from the curves. The total areas-under-curve (AUC) of the time-concentration plot were calculated using the linear trapezoidal rule.

6.2.4. Tissue distribution study

Wistar rats (8 week old, male, SPF, 180-200 g) were purchased from the Animal Center for Disease Prevention and Control (Wuhan, China) for Q₁₀ tissue distribution study. Similarly, after one week of acclimation under standardized laboratory conditions, rats were randomly divided into two groups for testing. The experimental group was fed with Q₁₀ nanoemulsion, and the control group with Q₁₀ oil dispersion, both at the single-

time feeding dosage of 100 mg/kg by oral gavage after fasting one night before experiments. At selected time interval after oral administration, rats were sacrificed by ether anesthesia. 5 rats were sacrificed for each time point for each group in the current experimental design. Then four major organ tissues (heart, kidney, liver, small intestine) were collected at time intervals of 12 and 24 h after oral ingestion. The obtained organ tissues were carefully washed with phosphate-buffered saline (PBS) for two times, and stored at -80 °C. For analysis, the thawed organ was weighed and homogenized with physiological saline at the weight to volume ratio of 1:9, which produced the tissue concentration of 0.1 g/mL. Then 500 μ L of the tissue homogenate from different organs were collected into 5 mL centrifuge tubes. Similarly, oxidation treatment was conducted to convert any Q₁₀H₂ to Q₁₀, and then aliquoted CoQ₈ was added into each sample to provide a 5 μ g/mL of I.S. for reference, as determined by pre-experiments. After adding I.S., 1 mL of absolute ethanol was added to each sample and allowed 1 min vortex for deproteinization. The following extraction steps were the same as the PK study. Briefly, Q₁₀ accumulated in different organ tissues were extracted with *n*-hexane, dried with nitrogen, and then reconstituted for HPLC analysis. Finally, Q₁₀'s concentrations in different organ tissues were obtained by back calculation.

6.2.5. HPLC determination and analysis of Q₁₀

The concentration of Q₁₀ in blood plasma and organ tissues were determined using a Waters e2695 HPLC-diode array detection (DAD) system (Waters, Milford, MA, USA), equipped with a diode array detector, a vacuum degasser, an auto-sampler and a binary pump. The separation of Q₁₀ and other derivatives were carried out using a Agilent reverse phase C₁₈ column (250 mm \times 4.6 mm, 5 μ m). The mobile phase was ethyl

alcohol / methanol (60:40, v/v) with isocratic elution at a flow rate of 1 mL/min for a total program of 30 min. A 50 μ L aliquot of each reconstituted sample was directly injected into HPLC and detected at the wavelength of 275 nm for analysis.

6.2.6. Statistical analysis

All results were expressed as mean \pm standard deviation. When appropriate, data were analyzed by SigmaPlot 12.0 software with a student t-test or one-way analysis of variance (ANOVA). Significant difference was defined at $p < 0.05$.

6.3. Results and discussion

6.3.1. Pharmacokinetics study of Q₁₀

To better understand the oral bioavailability of Q₁₀ in our developed beverage emulsion formulations, a PK study was designed and conducted using mice fed with either nanoemulsion or oil dispersion containing same dosage of Q₁₀ through gavage ingestion. As a final step in evaluating ingested compound's bioavailability, *in vivo* PK study covers all physiological factors during the digestion and absorption cascade, including bioaccessibility, transport coefficient, and possible metabolisms, which gives a comprehensive assessment of compound's availability to reach systemic circulation after being orally administered. In the current study, we conducted a single-dose feeding experiment at the Q₁₀ level of 100 mg/kg animal weight with our experimental group and the control group. Distinctive pharmacokinetic profiles between these two testing groups were observed and shown in **Fig. 30**, and the key pharmacokinetic parameters, i.e. C_{\max} , T_{\max} , and, are summarized in **Table 10**.

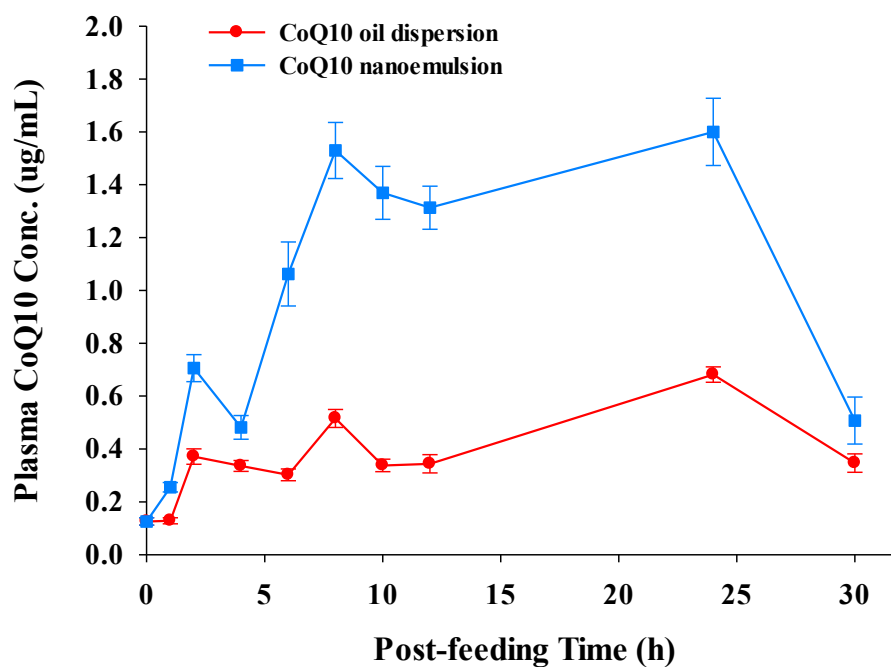


Figure 30. Pharmacokinetics (PK) curves of Q₁₀ in the testing formulations: nanoemulsion vs. oil dispersion.

Table 10. Pharmacokinetic parameters of Q₁₀ formulations after oral administration.

	C_{\max} ($\mu\text{g/mL}$)	T_{\max} (hr)	Area under the curve (AUC)
Q ₁₀ oil dispersion	0.6813	8, 24	13.7835
Q ₁₀ nanoemulsion	1.5998	8, 24	36.5647

Our results indicated much higher blood plasma Q₁₀ concentrations in nanoemulsion than oil dispersion during all recorded time course after oral administration. Which provided solid evidence for Q₁₀'s improved bioavailability in our developed nanoemulsion formulation compared with common oil based supplements. Overall, the Q₁₀ nanoemulsion group accumulated 36.56 µg/mL*hr of AUC, compared with 13.78 µg/mL*hr of AUC for the oil dispersion group, there was a 2.65 times increase in Q₁₀'s relative bioavailability. Considering the bioaccessibility of Q₁₀ determined by *in vitro* models to be about 5-6 times higher in nanoemulsion than the oil dispersion, we postulate that other factors associated with post-absorption of Q₁₀ may also largely affect its final bioavailability, such as permeability through the gut wall, first pass metabolism and lymphatic transport, etc. Nevertheless, the PK study confirmed the significantly improved bioavailability of Q₁₀ in our developed nanoemulsion formulation.

Besides the AUC and the corresponding bioavailability, it is notable that the concentration-time profiles of both testing groups were in “two-peak” patterns, with the first peak occurred at 8 hr and the second at 24 hr. This pattern is less often observed in PK studies, while we were still able to find some *in vivo* studies that can support our findings. Weis *et al* (79) examined the bioavailability of four different Q₁₀ formulations with ten healthy volunteers and found all concentration-time curves show a characteristic “two-peak pattern” with peaks at 6 and 24 hr after dosing. Likewise, Tomono *et al* (146) and Luecker *et al* (147) in earlier studies also reported similar observations. This unusual plasma level curve may probably due to the effects of enterohepatic recycling and redistribution from liver to circulation. As proposed by Tomono *et al*, the absorbed Q₁₀ was taken up by the liver and then transferred mainly to very low density lipoprotein

(VLDL) and redistributed from the liver to systemic circulation. However, it is still unknown why many other *in vivo* studies of Q₁₀ didn't observe similar pattern in the concentration-time curves. Apparently, different formulations, animal models, analytical methods and experimental designs may affect the obtained results. Therefore, more comprehensive researches are still needed to systematically investigate Q₁₀'s absorption kinetics in different animal models, and to look into detailed physiological factors that affect its oral bioavailability.

Moreover, our results also indicate that Q₁₀ was very slowly absorbed from the gastrointestinal tract to systemic circulation. Most drug and nutraceutical compounds usually peak during the first 2 hr after ingestion, while the first T_{\max} of Q₁₀ in current study is 8 hr, probably attributed to its hydrophobicity and very high molecular weight (863.34 g/mol). It seems that the nanoemulsion delivery system did not significantly improve Q₁₀'s absorption rate, as similar peak trends were observed in oil dispersion group. In another earlier study (148) where a straight tablet formulation of Q₁₀ was compared with a sustained release tablet formulation, both showed a T_{\max} of 6 hr and similar C_{\max} values, which indicated that the sustained release feature did not significantly delay the absorption rate of Q₁₀ either. These results suggested that the absorption rate of Q₁₀ may be less affected by its delivery form. While other factors, such as permeation rate through the gut wall and the subsequent metabolisms might be the rate-limiting steps.

6.3.2. Tissue uptake and distribution of Q₁₀

Besides investigating Q₁₀'s bioavailability after oral administration, we were also interested about the tissue distribution of Q₁₀ after being available in systemic circulation,

since very limited knowledge at present is known regarding the uptake and accumulation levels of Q_{10} in different organ tissues. One can often see the health benefits of taking Q_{10} supplements for reduced heart failure risks or enhanced energy levels, but rare convincing data actually exist in the current literature to support the claim with evidence of improved Q_{10} levels in targeted organ tissues after taking the supplements. The reason for shortage of such data is probably due to the complexity and ethics issue in conducting *in vivo* experiments. The objective of the current study was therefore to design and conduct an animal experiment that can provide direct information regarding the uptake and distribution of Q_{10} in major tissues after dosing with our developed nanoemulsion versus the oil dispersion control. As we know, CoQ_{10} ubiquitously exists in all human tissues since it is a vital component in cellular bioenergetics. As a general rule, tissues with high-energy requirements or metabolic activities need relatively high concentrations of CoQ_{10} (73). While, it is worth mentioning that in relatively short-lived species such as rats and mice, the predominant CoQ homolog is CoQ_9 , rather than CoQ_{10} in humans or other mammals. Therefore, in this experiment, we selected rats as the animal model, which can avoid any analytical bias contributed by endogenous Q_{10} . Also compared with mice, rats are relatively bigger thus easier for operation. Following the single-dose feeding of the two testing formulations, Q_{10} 's concentrations in four major organ tissues, including small intestine, liver, kidney, and heart, were determined at 12 hr and 24 hr, respectively. Results are compared and shown in **Fig. 31**.

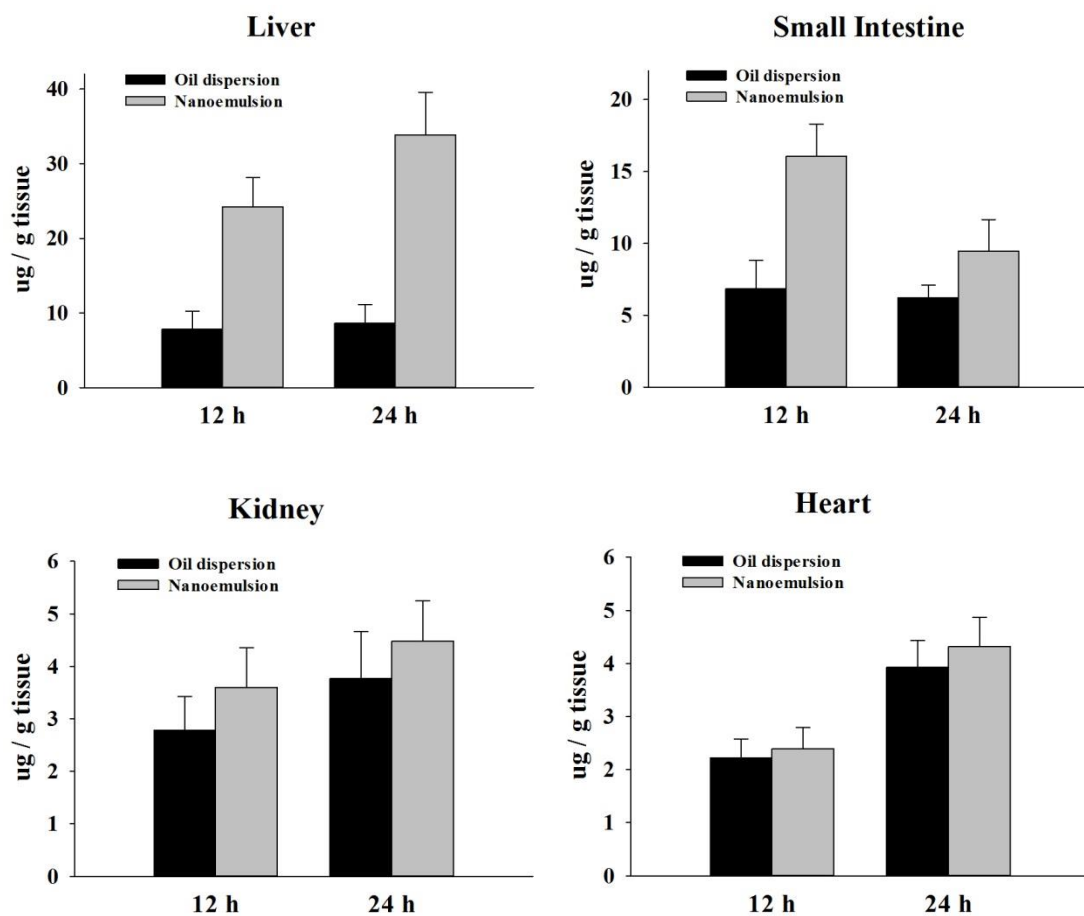


Figure 31. Q_{10} 's concentrations in major organ tissues after being fed with single dosage of nanoemulsion or oil dispersion for 12 hr and 24 hr.

Generally, compared with the oil dispersion, improved levels of Q₁₀ were observed in all tested organ tissues at 12 and 24 hr after ingestion with the nanoemulsion. These results proved our hypothesis that nanoemulsion can not only improve Q₁₀'s bioavailability in blood stream, but also increase the uptake levels of Q₁₀ in major organ tissues. By looking into the data of each organ tissue, more detailed information can be found and deduced. First of all, for small intestine, the major site where Q₁₀ got absorbed, data indicated a declining trend from 12 hr to 24 hr in both oil dispersion and nanoemulsion groups, meaning that Q₁₀ was being gradually absorbed then delivered from small intestine to systemic circulation. Significantly higher levels of Q₁₀ in small intestine tissues observed in nanoemulsion group compared with the control group also evidenced the improved absorption of Q₁₀, which further confirmed the results of the previous PK study.

In liver tissues, more significant differences were found between the two testing groups. At 12 hr, compared with 7.8 µg/g tissues in oil dispersion group, Q₁₀ level of 24.2 µg/g tissues was observed for the nanoemulsion group. Then at 24 hr, a nearly 4 times higher level of Q₁₀ was detected in nanoemulsion group (33.9 µg/g tissues) than the oil dispersion group (8.6 µg/g tissues). Interestingly, Q₁₀ concentration differences between the two testing groups observed in liver tissues were close to the previously observed bioaccessibility differences in GI tract, meaning that most of the bioaccessible Q₁₀ was possibly absorbed via the hepatic portal vein route after permeating through the gut wall barriers. Considering the Neobee 1053 oil used in the formulation is a medium chain triglyceride, our assumption is likely to be true. It was reported that the absorption of lipid and lipid digestion products are largely dependent on their chain lengths (*149*). For

long chain lipids (≥ 12 C), after entering into enterocytes, normally they will be packed into the chylomicron, a major transport lipoprotein, and then be delivered mainly via lymph ducts into systemic circulation. However, for short and middle chain lipids (≤ 10 C), they are more tend to be associated with fatty acids binding proteins and absorbed directly into the hepatic portal vein, then travel to the liver for processing before continuing to the systemic circulation. Accordingly, the absorption of nutraceutical compounds in the lipid matrix may also be affected by the absorption routes of the carrying lipids. Therefore, it is likely that a large proportion of Q₁₀ was absorbed via the hepatic portal vein route together with the digestion products of MCT in this study. As a result, the first-pass metabolism undergoes in liver will be the key limiting factor for Q₁₀ to further become bioavailable. Moreover, the trends of Q₁₀ levels in liver and small intestine tissues may be associated with the two-peak pattern observed in PK study, that the absorbed Q₁₀ possibly experienced enterohepatic recycling and redistributed from liver to circulation, which contributed to the second peak at 24 hr in the concentration-time curves.

Then, for kidney and heart tissues, similar trends were observed in the two testing groups, with the nanoemulsion group showed relatively higher levels of Q₁₀ compared with the oil dispersion group at both 12 hr and 24 hr, though not significantly different. And the increasing trends from 12 to 24 hr also indicated that the absorbed Q₁₀ were gradually delivered and accumulated by the kidney and heart tissues due to its slowly absorption kinetics. We believe that this trend can be more significant if repeated dosing was given or longer time was observed after dosing. Nevertheless, it is still exciting to see the improved levels of Q₁₀ in these functional organ tissues after single-dosing up to

24 hr. Previously, there is no clear evidence of the dietary Q₁₀ that secreted into circulation in association with lipoproteins in the liver is taken up by other tissues under normal conditions, since the intestinal absorption of dietary Q₁₀ is very limited (124). In one study with rats, orally-administered Q₁₀ was found to appear in circulation, liver and spleen, but not in heart or kidney (150). Compared with that study, we used higher dosage and more solubilized form of Q₁₀. Therefore, our results confirmed that dosage, formulation and duration of Q₁₀ administration are all important factors regulating its uptake by kidney, heart and other tissues.

6.4. Conclusions

Using mice as *in vivo* model, Q₁₀'s oral bioavailability and pharmacokinetic parameters were determined within two testing groups. A 2.65 times increase in AUC was found in the group fed with our developed nanoemulsions (experimental group) compared with the group fed with oil dispersions (control group), indicating significantly improved oral bioavailability was achieved by using nanoemulsion as the delivery system for Q₁₀. Moreover, a “two-peak” pattern was observed in the concentration-time curves for both groups, with the detected Q₁₀ levels peaked at 8 hr and 24 hr respectively after ingestion. The first peak indicated the slow absorption and permeation kinetics of Q₁₀ from the GI-tract to systemic circulation, while the second peak was probably due to the effect of enterohepatic recycling and Q₁₀ redistribution from liver to circulation. Therefore, we postulated that the majority of Q₁₀ might be absorbed through the hepatic portal vein route in the current experiment, from which the absorbed Q₁₀ firstly traveled to the liver for processing before continuing to the systemic circulation. As a consequence, the first-pass metabolisms occurred in the liver further limited Q₁₀ from

being bioavailable. Overall, our results confirmed the improved oral bioavailability of Q_{10} in our developed nanoemulsion formulation.

Subsequently, by using rats as the *in vivo* model, Q_{10} 's distribution levels in four major organ tissues, i.e. small intestine, liver, kidney and heart were determined and compared among two testing groups at 12 hr and 24 hr after single-dose feeding. Compared with the control, improved levels of Q_{10} were observed in all tested organ tissues after ingestion with the nanoemulsion. The results further proved our hypothesis that nanoemulsion can not only improve Q_{10} 's bioavailability in blood stream, but also increase the uptake levels of Q_{10} in major organ tissues.

CHAPTER 7: SUMMARY AND FUTURE WORK

7.1. Summary of the dissertation

A functional beverage nanoemulsion containing citral and CoQ₁₀ was successfully developed. The effects of antioxidant concentration and emulsifier type on the stability of citral in the nanoemulsion systems were carefully investigated and elucidated. Reduced form of CoQ₁₀ (i.e. ubiquinol or Q₁₀H₂), as a lipophilic antioxidant, can effectively inhibit citral from degradation in the emulsion systems when its concentration was optimized. Some natural derived small molecular emulsifiers, such as saponin and lyso-lecithin, showed improved emulsion stability as well as citral stability. It is promising for these natural emulsifiers to replace traditional synthetic surfactants in beverage emulsion systems for “clean label” solutions. CoQ₁₀’s bioavailability was significantly improved in our developed nanoemulsion formulation compared with the normal oil-based supplement, evidenced by *in vitro* bioaccessibility determination with two simulated digestion models (pH-stat and TIM-1), followed by an *in vivo* pharmacokinetic study on mice. Further investigation on Q₁₀’s distribution in major organ tissues (small intestine, liver, kidney, and heart) after dosing confirmed Q₁₀’s improved tissue uptake levels when fed with nanoemulsion. Therefore, enhanced health benefits of Q₁₀ can be expected when consuming with our developed functional beverage emulsion compared with the common oil-based Q₁₀ supplements. In summary, data generated in this research will be valuable references for the food industry to formulate and develop novel functional beverages fortified with sensitive flavors and lipophilic nutraceuticals.

7.2. Future work and directions

Due to the limitation of experimental design, time and resources, some meaningful experiments and ideas related with this dissertation were not able to be performed and tested. However, they are worth mentioning and thus can be proposed as future work and directions.

For the work of citral stability in emulsion systems, besides the conventional emulsion and nano-/micro-emulsions stabilized by small molecular surfactants or biopolymers, the use of solid particles to stabilize emulsions has recently attracted increasing interest due to their distinctive characteristics. This type of emulsion is referred to as Pickering emulsion, named after S.U. Pickering, who firstly described this phenomenon in the early 20th. Although the concept is by no means new, recent researches identified the potential use of some food-grade particles instead of traditional inorganic or synthetic particles in stabilizing Pickering emulsions, which extended the potential use of Pickering emulsions in the food related systems (151-155). It is reported that Pickering emulsion can display superior long-term stability and is usually more stable against coalescence and Ostwald ripening (156, 157). Theoretically, improved physical stability of emulsion will result in better protection of sensitive compounds in the emulsion system. Therefore, it will be interesting to test the Pickering emulsion as a potential delivery system for citral and see if better stability of citral can be retained. However, considering its relatively high oil content, big droplet size, and high viscosity, the usage of Pickering emulsion in beverage applications might be challenging. Moreover it might be a concern for the Pickering emulsion to lose its stability when diluted into beverage bases. Nevertheless, it is worth trying the idea since currently there is no

literature regarding the using of Pickering emulsion as delivery systems for flavor and beverage applications.

Then for the work of CoQ₁₀ bioavailability, we already proved that our developed nanoemulsion formulation can significantly improve CoQ₁₀'s bioavailability compared with oil-based supplements. While another interesting question remains that if taking the reduced form of CoQ₁₀ (Q₁₀H₂) will have better bioavailability and health benefits compared with the oxidized Q₁₀. We touched upon this question by simply testing the *in vitro* bioaccessibility differences of Q₁₀H₂ versus Q₁₀ in both oil dispersion and nanoemulsion formulations. Our results indicated that improved bioaccessibility of Q₁₀H₂ can be observed especially in the oil dispersion group, while less difference was found in the nanoemulsion group. Future work is still needed to further investigate the *in vivo* pharmacokinetics and tissue distribution of Q₁₀H₂ in comparison with Q₁₀ to provide better answer for this question. Moreover, in the animal study, we identified that the hepatic portal vein might be the major absorption route for Q₁₀ when fed with our formulations containing MCT, based on the results of pharmacokinetics and tissue distributions. As we know, the first-pass effect is a key limiting factor for Q₁₀ to become bioavailable, therefore designing delivery systems for Q₁₀ to possibly bypass the first-pass metabolism by alternating its absorption route might be a very attractive future research direction. It was reported that long chain lipid vehicles will largely stimulate the formation of chylomicron, and thus promote the transport of highly lipophilic compounds to go through intestinal lymphatic system rather than the hepatic portal vein route, thus avoiding the first-pass effect (149, 158-160). On the other hand, the down side of long chain lipids might be associated with their relatively slow digestion and absorption rates

compared with short/middle chain lipids. Therefore, it will be highly interesting in the future to conduct *in vivo* studies to directly compare Q₁₀'s bioavailability and tissue distribution in lipid vehicles composed of different chain lengths.

APPENDICES

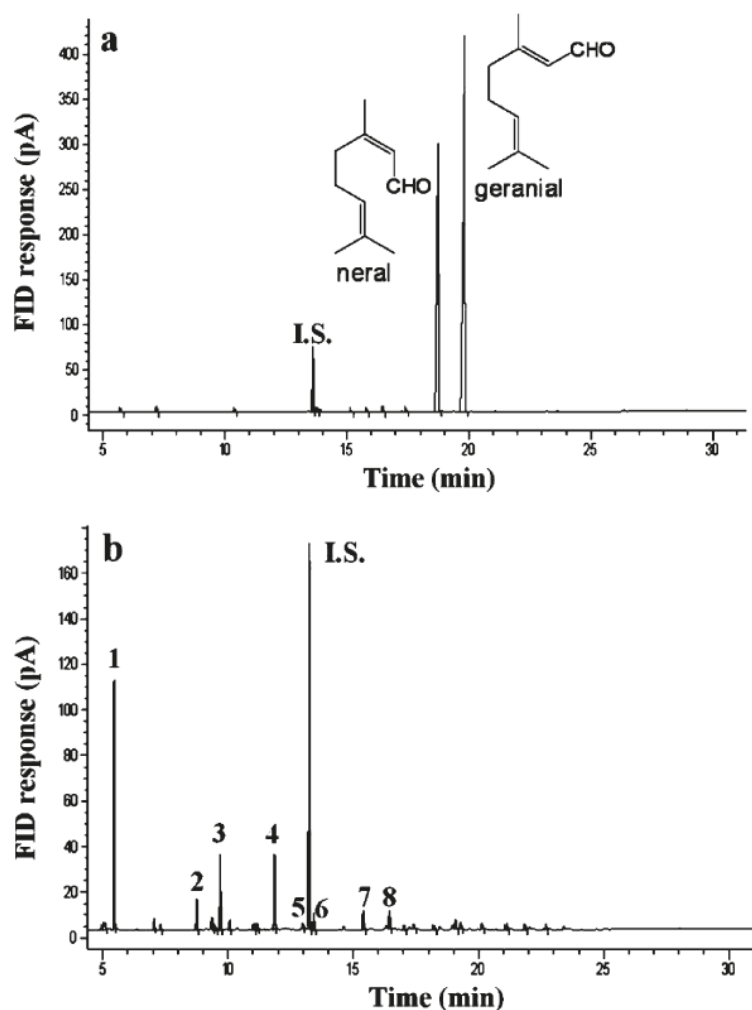
A. Optimization and validation of the SPME-GC method for citral measurement

To monitor and quantify the degradation trends of citral (neral & geranial) and generation of various off-flavors during the storage, a Head Space - Solid Phase Microextraction - Gas Chromatography (HS-SPME-GC) method was developed to extract volatile compounds from the citral-loaded emulsion systems and trace their concentration levels during the storage.

This method was optimized and validated by previous co-worker Dr. Huaixiang Tian. In brief, multiple variables, including types of SPME fiber, absorption temperature/time, salt concentration, were carefully evaluated through a Box-Behnken design. Based on the results, a 65 μm polydimethylsiloxane/divinylbenzene (PDMS/DVB) fiber was chosen due to its best reproducibility and comprehensive adsorption profiles for all target compounds. The optimized absorption temperature and time for extraction were determined to be at 50 °C for 40 min. And finally, salt concentration was optimized to be at 6 M to improve the overall peak profiles for low concentration compounds with different volatilities. Overall, good linearity, high recovery, good reproducibility and low limit of detection for all key off-odor compounds indicated that the developed SPME method was suitable for the analysis of citral degradation products in headspace volatile of emulsions. Detailed information can be referred to the publication by Tian *et al* (161).

A representative gas chromatogram of citral and its degradation products was shown below. Narrative descriptions of the off-flavor identification methods, retention index and concentration calculation were also given.

❖ **Figure S1.** Representative gas chromatogram of citral and its degradation off-flavors generated under 50 °C storage at day 0 (a) and day 30 (b). Numbered compounds correspond to those degradation products listed in the following Table.



- ❖ Degradation products generated and identified from citral-loaded emulsions stored at 50 °C after 30 days.

Compound No. ^a	Degradation Compounds	Retention Index (RI)	Identification Method ^b
1	2-heptanone	881	A
2	1-octen-3-ol	991	A
3	δ-2-carene	1033	A
4	<i>p</i> -cresol	1060	B
5	α, <i>p</i> -dimethylstyrene	1093	B
6	butanoic acid	1174	A
7	<i>p</i> -mentha-1,5-dien-8-ol	1185	B
8	<i>p</i> -methylacetophenone	1190	B

^a Numbers correspond to those in the above Figure.

^b Compounds were identified on the basis of the following criteria: A, mass spectrum agrees with that of Wiley mass spectra database and considered to be “tentatively identified”; B, mass spectrum and retention index agree with those of authentic compounds.

❖ **Retention Index calculation:**

$$RI = 100 * n + 100 \times \frac{t - t_n}{t_{n+1} - t_n}$$

t: r.t. of the compound corresponding to whose RI value that is being calculated;

t_n: r.t. of the I.S.; i.e. undecane (C₁₁)

t_{n+1}: r.t. of the I.S.; i.e. dodecane (C₁₂)

n: C numbers of the I.S.

❖ **Compound concentration (mol/L) calculation:**

$$\frac{\text{Conc. of I. S. (C}_{11}\text{)}}{\text{Area of I. S. (C}_{11}\text{)}} = \frac{\text{Conc. of X}}{\text{Area of X}}$$

B. Reagents and secretion fluids preparation for the TIM-1 model

Reagents & Solutions	Recipe	Amount/Flow rate
Pancreatin Solution	Pancreatin powder: 17.5 g (\pm 0.5 g) DI-water: 250 g (\pm 5g) - Mix for 10 min, centrifuge for 20 min at 9,000 rpm at 4 °C, use the supernatant	267.5 g 0.25 mL/min
Bile Solution	- Use 50 °C water bath to melt the frozen bile, filter through a 250 μ m cloth filter	500 g
Gastric Electrolyte Solution (GES)	NaCl: 6.2 g/L KCl: 2.2 g/L CaCl ₂ : 0.3 g/L	500 g
Gastric Enzymes	GES: 150 g (\pm 3 g) 1M CH ₃ COONa buffer (pH 5): 1.5 mL Lipase: 37.5 mg Pepsin: 30.0 mg	151.5 g
Small Intestinal Electrolyte Solution (SIES)	NaCl: 5 g/L KCl: 0.6 g/L CaCl ₂ : 0.3 g/L	2000 g 3.2 mL/min
Duodenum Electrolyte Solution (DES)	Same as SIES	450 g 0.5 mL/min
Jejunum Secretion	SIES: 1250 g (\pm 10 g) DI-water: 100 g (\pm 5 g) Bile: 150 g (\pm 1 g)	1500 g 3.2 mL/min
Ileum Secretion	Same as SIES	1500 g 3.9 mL/min
Gastric Start Residue	Same as Gastric Enzyme	5 g
Duodenum Start Residue	SIES: 15 g (\pm 0.3 g) Pancreatin solution: 15 g (\pm 0.3 g) Bile: 30 g (\pm 0.5 g) Trypsin solution (2 mg/cup): 1 cup - Incubate for 5 min at 37 °C	60 g
Jejunum Start Residue	SIES: 40 g (\pm 0.5 g) Pancreatin solution: 40 g (\pm 0.5 g) Bile: 80 g (\pm 1 g)	160 g
Ileum Start Residue	Same as SIES	160 g

REFERENCES

1. McClements, D. J., *Food Emulsions: Principles, Practices, and Techniques, Second Edition*. Taylor & Francis: 2004.
2. Benichou, A.; Aserin, A.; Garti, N., Double emulsions stabilized with hybrids of natural polymers for entrapment and slow release of active matters. *Advances in Colloid and Interface Science* **2004**, 108–109, 29-41.
3. Garti, N.; Bisperink, C., Double emulsions: Progress and applications. *Current Opinion in Colloid & Interface Science* **1998**, 3, 657-667.
4. McClements, D. J.; Decker, E. A.; Weiss, J., Emulsion-Based Delivery Systems for Lipophilic Bioactive Components. *Journal of Food Science* **2007**, 72, R109-R124.
5. Samad, A.; Sultana, Y.; Aqil, M., Liposomal Drug Delivery Systems: An Update Review. *Current Drug Delivery* **2007**, 4, 297-305.
6. Vemuri, S.; Rhodes, C. T., Preparation and characterization of liposomes as therapeutic delivery systems: a review. *Pharmaceutica Acta Helvetiae* **1995**, 70, 95-111.
7. Bombardelli, E., Phytosome: new cosmetic delivery system. *Boll Chim Farm* **1991**, 130, 431-438.
8. Dinsmore, A. D.; Hsu, M. F.; Nikolaidis, M. G.; Marquez, M.; Bausch, A. R.; Weitz, D. A., Colloidosomes: Selectively Permeable Capsules Composed of Colloidal Particles. *Science* **2002**, 298, 1006-1009.
9. Rao, J.; McClements, D. J., Food-grade microemulsions, nanoemulsions and emulsions: Fabrication from sucrose monopalmitate & lemon oil. *Food Hydrocolloids* **2011**, 25, 1413-1423.
10. McClements, D. J., Critical Review of Techniques and Methodologies for Characterization of Emulsion Stability. *Critical Reviews in Food Science and Nutrition* **2007**, 47, 611-649.
11. Huang, Q.; Yu, H.; Ru, Q., Bioavailability and Delivery of Nutraceuticals Using Nanotechnology. *Journal of Food Science* **2010**, 75, R50-R57.
12. McClements, D. J., Nanoemulsions versus microemulsions: terminology, differences, and similarities. *Soft Matter* **2012**, 8, 1719-1729.
13. Komaiko, J. S.; McClements, D. J., Formation of Food-Grade Nanoemulsions Using Low-Energy Preparation Methods: A Review of Available Methods. *Comprehensive Reviews in Food Science and Food Safety* **2016**, 15, 331-352.
14. McClements, D. J.; Rao, J., Food-Grade Nanoemulsions: Formulation, Fabrication, Properties, Performance, Biological Fate, and Potential Toxicity. *Critical Reviews in Food Science and Nutrition* **2011**, 51, 285-330.
15. Schubert, H.; Ax, K.; Behrend, O., Product engineering of dispersed systems. *Trends in Food Science & Technology* **2003**, 14, 9-16.
16. Schubert, H.; Engel, R., Product and Formulation Engineering of Emulsions. *Chemical Engineering Research and Design* **2004**, 82, 1137-1143.
17. Jafari, S. M.; Assadpoor, E.; He, Y.; Bhandari, B., Re-coalescence of emulsion droplets during high-energy emulsification. *Food Hydrocolloids* **2008**, 22, 1191-1202.
18. Sharma, V. K. Preparation of micron-size pharmaceutical particles by microfluidization. US Patent 6555139, 2003.
19. Washington, C.; Davis, S. S., The production of parenteral feeding emulsions by Microfluidizer. *International Journal of Pharmaceutics* **1988**, 44, 169-176.

20. Henry, J. V. L.; Fryer, P. J.; Frith, W. J.; Norton, I. T., The influence of phospholipids and food proteins on the size and stability of model sub-micron emulsions. *Food Hydrocolloids* **2010**, *24*, 66-71.
21. Klein, M.; Aserin, A.; Svitov, I.; Garti, N., Enhanced stabilization of cloudy emulsions with gum Arabic and whey protein isolate. *Colloids and Surfaces B: Biointerfaces* **2010**, *77*, 75-81.
22. Qian, C.; McClements, D. J., Formation of nanoemulsions stabilized by model food-grade emulsifiers using high-pressure homogenization: Factors affecting particle size. *Food Hydrocolloids* **2011**, *25*, 1000-1008.
23. Bai, L.; McClements, D. J., Development of microfluidization methods for efficient production of concentrated nanoemulsions: Comparison of single- and dual-channel microfluidizers. *Journal of Colloid and Interface Science* **2016**, *466*, 206-212.
24. Kentish, S.; Wooster, T. J.; Ashokkumar, M.; Balachandran, S.; Mawson, R.; Simons, L., The use of ultrasonics for nanoemulsion preparation. *Innovative Food Science & Emerging Technologies* **2008**, *9*, 170-175.
25. Leong, T. S. H.; Wooster, T. J.; Kentish, S. E.; Ashokkumar, M., Minimising oil droplet size using ultrasonic emulsification. *Ultrasonics Sonochemistry* **2009**, *16*, 721-727.
26. Jafari, S. M.; He, Y.; Bhandari, B., Nano-Emulsion Production by Sonication and Microfluidization—A Comparison. *International Journal of Food Properties* **2006**, *9*, 475-485.
27. Anton, N.; Vandamme, T. F., The universality of low-energy nano-emulsification. *International Journal of Pharmaceutics* **2009**, *377*, 142-147.
28. Given Jr, P. S., Encapsulation of Flavors in Emulsions for Beverages. *Current Opinion in Colloid & Interface Science* **2009**, *14*, 43-47.
29. Buffo, R. A.; Reineccius, G. A., Shelf-life and mechanisms of destabilization in dilute beverage emulsions. *Flavour and Fragrance Journal* **2001**, *16*, 7-12.
30. Friberg, S.; Larsson, K.; Sjoblom, J., *Food Emulsions*. Taylor & Francis: 2003.
31. Piorkowski, D. T.; McClements, D. J., Beverage emulsions: Recent developments in formulation, production, and applications. *Food Hydrocolloids* **2014**, *42*, Part 1, 5-41.
32. Shachman, M., *The Soft Drinks Companion: A Technical Handbook for the Beverage Industry*. Taylor & Francis: 2004.
33. Olsen, N. J.; Heitmann, B. L., Intake of calorically sweetened beverages and obesity. *Obesity Reviews* **2009**, *10*, 68-75.
34. Gibson, S., Sugar-sweetened soft drinks and obesity: a systematic review of the evidence from observational studies and interventions. *Nutrition Research Reviews* **2008**, *21*, 134-147.
35. Slavin, J., Beverages and body weight: challenges in the evidence-based review process of the Carbohydrate Subcommittee from the 2010 Dietary Guidelines Advisory Committee. *Nutrition Reviews* **2012**, *70*, S111-S120.
36. Zhang, F.; Klebansky, B.; Fine, R. M.; Liu, H.; Xu, H.; Servant, G.; Zoller, M.; Tachdjian, C.; Li, X., Molecular mechanism of the sweet taste enhancers. *Proceedings of the National Academy of Sciences* **2010**, *107*, 4752-4757.
37. Servant, G.; Tachdjian, C.; Tang, X.-Q.; Werner, S.; Zhang, F.; Li, X.; Kamdar, P.; Petrovic, G.; Ditschun, T.; Java, A.; Brust, P.; Brune, N.; DuBois, G. E.; Zoller, M.; Karanewsky, D. S., Positive allosteric modulators of the human sweet taste receptor

enhance sweet taste. *Proceedings of the National Academy of Sciences* **2010**, *107*, 4746-4751.

38. DuBois, G. E.; Prakash, I., Non-Caloric Sweeteners, Sweetness Modulators, and Sweetener Enhancers. *Annual Review of Food Science and Technology* **2012**, *3*, 353-380.

39. Corbo, M. R.; Bevilacqua, A.; Petruzzi, L.; Casanova, F. P.; Sinigaglia, M., Functional Beverages: The Emerging Side of Functional Foods. *Comprehensive Reviews in Food Science and Food Safety* **2014**, *13*, 1192-1206.

40. *Functional Drinks Industry Profile: United States*; MarketLine, a Datamonitor business: 2014; pp 1-37.

41. Yang, Y.; McClements, D. J., Encapsulation of vitamin E in edible emulsions fabricated using a natural surfactant. *Food Hydrocolloids* **2013**, *30*, 712-720.

42. Qian, C.; Decker, E. A.; Xiao, H.; McClements, D. J., Nanoemulsion delivery systems: Influence of carrier oil on β -carotene bioaccessibility. *Food Chemistry* **2012**, *135*, 1440-1447.

43. Liang, R.; Shoemaker, C. F.; Yang, X.; Zhong, F.; Huang, Q., Stability and Bioaccessibility of β -Carotene in Nanoemulsions Stabilized by Modified Starches. *Journal of Agricultural and Food Chemistry* **2013**, *61*, 1249-1257.

44. Yu, H.; Huang, Q., Improving the Oral Bioavailability of Curcumin Using Novel Organogel-Based Nanoemulsions. *Journal of Agricultural and Food Chemistry* **2012**, *60*, 5373-5379.

45. Walker, R.; Decker, E. A.; McClements, D. J., Development of food-grade nanoemulsions and emulsions for delivery of omega-3 fatty acids: opportunities and obstacles in the food industry. *Food & Function* **2015**, *6*, 41-54.

46. Maswal, M.; Dar, A. A., Formulation challenges in encapsulation and delivery of citral for improved food quality. *Food Hydrocolloids* **2014**, *37*, 182-195.

47. Clark Jr, B. C.; Powell, C. C.; Radford, T., The acid catalyzed cyclization of citral. *Tetrahedron* **1977**, *33*, 2187-2191.

48. Kimura, K.; Iwata, I.; Nishimura, H., Relationship between Acid-catalyzed Cyclization of Citral and Deterioration of Lemon Flavor. *Agricultural and Biological Chemistry* **1982**, *46*, 1387-1389.

49. Kimura, K.; Nishimura, H.; Iwata, I.; Mizutani, J., Deterioration mechanism of lemon flavor. 2. Formation mechanism of off-odor substances arising from citral. *Journal of Agricultural and Food Chemistry* **1983**, *31*, 801-804.

50. Peacock, V. E.; Kuneman, D. W., Inhibition of the formation of .alpha.-p-dimethylstyrene and p-cymen-8-ol in a carbonated citral-containing beverage system. *Journal of Agricultural and Food Chemistry* **1985**, *33*, 330-335.

51. Schieberle, P.; Grosch, W., Identification of potent flavor compounds formed in an aqueous lemon oil/citric acid emulsion. *Journal of Agricultural and Food Chemistry* **1988**, *36*, 797-800.

52. Ueno, T.; Masuda, H.; Ho, C.-T., Formation Mechanism of p-Methylacetophenone from Citral via a tert-Alkoxy Radical Intermediate. *Journal of Agricultural and Food Chemistry* **2004**, *52*, 5677-5684.

53. Yang, X.; Tian, H.; Ho, C.-T.; Huang, Q., Inhibition of Citral Degradation by Oil-in-Water Nanoemulsions Combined with Antioxidants. *Journal of Agricultural and Food Chemistry* **2011**, *59*, 6113-6119.

54. Bertolini, A. C.; Siani, A. C.; Grosso, C. R. F., Stability of Monoterpenes Encapsulated in Gum Arabic by Spray-Drying. *Journal of Agricultural and Food Chemistry* **2001**, *49*, 780-785.
55. Liang, C.-P.; Wang, M.; Simon, J. E.; Ho, C.-T., Antioxidant activity of plant extracts on the inhibition of citral off-odor formation. *Molecular Nutrition & Food Research* **2004**, *48*, 308-317.
56. Ueno, T.; Kiyohara, S.; Ho, C.-T.; Masuda, H., Potent Inhibitory Effects of Black Tea Theaflavins on Off-Odor Formation from Citral. *Journal of Agricultural and Food Chemistry* **2006**, *54*, 3055-3061.
57. Djordjevic, D.; Cercaci, L.; Alamed, J.; McClements, D. J.; Decker, E. A., Chemical and Physical Stability of Citral and Limonene in Sodium Dodecyl Sulfate-Chitosan and Gum Arabic-Stabilized Oil-in-Water Emulsions. *Journal of Agricultural and Food Chemistry* **2007**, *55*, 3585-3591.
58. Djordjevic, D.; Cercaci, L.; Alamed, J.; McClements, D. J.; Decker, E. A., Stability of citral in protein- and gum arabic-stabilized oil-in-water emulsions. *Food Chemistry* **2008**, *106*, 698-705.
59. Choi, S. J.; Decker, E. A.; Henson, L.; Popplewell, L. M.; McClements, D. J., Stability of Citral in Oil-in-Water Emulsions Prepared with Medium-Chain Triacylglycerols and Triacetin. *Journal of Agricultural and Food Chemistry* **2009**, *57*, 11349-11353.
60. Mei, L.; Choi, S. J.; Alamed, J.; Henson, L.; Popplewell, M.; McClements, D. J.; Decker, E. A., Citral Stability in Oil-in-Water Emulsions with Solid or Liquid Octadecane. *Journal of Agricultural and Food Chemistry* **2009**, *58*, 533-536.
61. Choi, S. J.; Decker, E. A.; Henson, L.; Popplewell, L. M.; McClements, D. J., Influence of Droplet Charge on the Chemical Stability of Citral in Oil-in-Water Emulsions. *Journal of Food Science* **2010**, *75*, C536-C540.
62. Choi, S. J.; Decker, E. A.; Henson, L.; Popplewell, L. M.; McClements, D. J., Inhibition of citral degradation in model beverage emulsions using micelles and reverse micelles. *Food Chemistry* **2010**, *122*, 111-116.
63. Strassburger, K.; Startup, W.; Levey, V.; Mattingly, T.; Briggs, J.; Harrison, J.; Wilson, T., Enhanced Stability of Citral in Juice Beverages by Applying Cyclodextrin Micro Emulsion Technology. In *Flavors in Noncarbonated Beverages*, American Chemical Society: 2010; Vol. 1036, pp 143-158.
64. Rungsardthong Ruktanonchai, U.; Srinuanchai, W.; Saesoo, S.; Sramala, I.; Puttipipatkachorn, S.; Soottitantawat, A., Encapsulation of Citral Isomers in Extracted Lemongrass Oil with Cyclodextrins: Molecular Modeling and Physicochemical Characterizations. *Bioscience, Biotechnology, and Biochemistry* **2011**, *75*, 2340-2345.
65. Sosa, N.; Zamora, M. C.; Chirife, J.; Schebor, C., Spray-drying encapsulation of citral in sucrose or trehalose matrices: physicochemical and sensory characteristics. *International Journal of Food Science & Technology* **2011**, *46*, 2096-2102.
66. Yang, X.; Tian, H.; Ho, C.-T.; Huang, Q., Stability of Citral in Emulsions Coated with Cationic Biopolymer Layers. *Journal of Agricultural and Food Chemistry* **2011**, *60*, 402-409.
67. Zhao, Q.; Ho, C.-T.; Huang, Q., Effect of Ubiquinol-10 on Citral Stability and Off-Flavor Formation in Oil-in-Water (O/W) Nanoemulsions. *Journal of Agricultural and Food Chemistry* **2013**, *61*, 7462-7469.

68. Maswal, M.; Dar, A. A., Inhibition of citral degradation in an acidic aqueous environment by polyoxyethylene alkylether surfactants. *Food Chemistry* **2013**, *138*, 2356-2364.
69. Park, S. J.; Hong, C. R.; Choi, S. J., Citral degradation in micellar structures formed with polyoxyethylene-type surfactants. *Food Chemistry* **2015**, *170*, 443-447.
70. Yang, Y.; Cui, S. W.; Gong, J.; Guo, Q.; Wang, Q.; Hua, Y., A soy protein-polysaccharides Maillard reaction product enhanced the physical stability of oil-in-water emulsions containing citral. *Food Hydrocolloids* **2015**, *48*, 155-164.
71. Xiang, J.; Liu, F.; Fan, R.; Gao, Y., Physicochemical stability of citral emulsions stabilized by milk proteins (lactoferrin, α -lactalbumin, β -lactoglobulin) and beet pectin. *Colloids and Surfaces A: Physicochemical and Engineering Aspects* **2015**, *487*, 104-112.
72. Heng, L.; van Koningsveld, G. A.; Gruppen, H.; van Boekel, M. A. J. S.; Vincken, J. P.; Roozen, J. P.; Voragen, A. G. J., Protein-flavour interactions in relation to development of novel protein foods. *Trends in Food Science & Technology* **2004**, *15*, 217-224.
73. Ernster, L.; Dallner, G., Biochemical, physiological and medical aspects of ubiquinone function. *Biochimica et Biophysica Acta (BBA) - Molecular Basis of Disease* **1995**, *1271*, 195-204.
74. Overvad, K.; Diamant, B.; Holm, L.; Holmer, G.; Mortensen, S. A.; Stender, S., Coenzyme Q10 in health and disease. *Eur J Clin Nutr* **1999**, *53*, 764-770.
75. Langsjoen, P. H.; Langsjoen, A. M., Overview of the use of CoQ10 in cardiovascular disease. *BioFactors* **1999**, *9*, 273-284.
76. Flint Beal, M., Coenzyme Q 10 as a Possible Treatment for Neurodegenerative Diseases. *Free Radical Research* **2002**, *36*, 455-460.
77. Frei, B.; Kim, M. C.; Ames, B. N., Ubiquinol-10 is an effective lipid-soluble antioxidant at physiological concentrations. *Proceedings of the National Academy of Sciences* **1990**, *87*, 4879-4883.
78. Mellors, A.; Tappel, A. L., Quinones and quinols as inhibitors of lipid peroxidation. *Lipids* **1966**, *1*, 282-284.
79. Weis, M.; Mortensen, S. A.; Rassing, M. R.; Møller-Sonnergaard, J.; Poulsen, G.; Rasmussen, S. N., Bioavailability of four oral Coenzyme Q10 formulations in healthy volunteers. *Molecular Aspects of Medicine* **1994**, *15*, Supplement 1, s273-s280.
80. Miles, M. V.; Horn, P.; Miles, L.; Tang, P.; Steele, P.; DeGrauw, T., Bioequivalence of coenzyme Q10 from over-the-counter supplements. *Nutrition Research* **2002**, *22*, 919-929.
81. Beg, S.; Javed, S.; Jkholi, K., Bioavailability Enhancement of Coenzyme Q10: An Extensive Review of Patents. *Recent Patents on Drug Delivery & Formulation* **2010**, *4*, 245-257.
82. Kommuru, T. R.; Gurley, B.; Khan, M. A.; Reddy, I. K., Self-emulsifying drug delivery systems (SEDDS) of coenzyme Q10: formulation development and bioavailability assessment. *International Journal of Pharmaceutics* **2001**, *212*, 233-246.
83. Zaghloul, A.-a.; Gurley, B.; Khan, M.; Bhagavan, H.; Chopra, R.; Reddy, I., Bioavailability Assessment of Oral Coenzyme Q10 Formulations in Dogs. *Drug Development and Industrial Pharmacy* **2002**, *28*, 1195-1200.
84. Schulz, C.; Obermüller-Jevic, U. C.; Hasselwander, O.; Bernhardt, J.; Biesalski, H. K., Comparison of the relative bioavailability of different coenzyme Q10 formulations

with a novel solubilizate (Solu™ Q10). *International Journal of Food Sciences and Nutrition* **2006**, *57*, 546-555.

85. Terao, K.; Nakata, D.; Fukumi, H.; Schmid, G.; Arima, H.; Hirayama, F.; Uekama, K., Enhancement of oral bioavailability of coenzyme Q10 by complexation with γ -cyclodextrin in healthy adults. *Nutrition Research* **2006**, *26*, 503-508.

86. Hosoe, K.; Kitano, M.; Kishida, H.; Kubo, H.; Fujii, K.; Kitahara, M., Study on safety and bioavailability of ubiquinol (Kaneka QH™) after single and 4-week multiple oral administration to healthy volunteers. *Regulatory Toxicology and Pharmacology* **2007**, *47*, 19-28.

87. Hatanaka, J.; Kimura, Y.; Lai-Fu, Z.; Onoue, S.; Yamada, S., Physicochemical and pharmacokinetic characterization of water-soluble Coenzyme Q10 formulations. *International Journal of Pharmaceutics* **2008**, *363*, 112-117.

88. Liu, Z.-X.; Artmann, C., Relative bioavailability comparison of different coenzyme Q10 formulations with a novel delivery system. *Alternative Therapies* **2009**, *15*, 42-46.

89. Ok, H.-M.; Kim, S.-M.; Park, J.-W.; Kim, K.-S.; Nam, H.-K.; Kim, J.; Kwon, O., Development of nanoparticulate formulation of coenzyme Q10 and comparison of plasma coenzyme Q10 response in a single supplementation with regular coenzyme Q10 using rats. *J Korean Soc Appl Biol Chem* **2012**, *55*, 619-623.

90. Cho, H. T.; Salvia-Trujillo, L.; Kim, J.; Park, Y.; Xiao, H.; McClements, D. J., Droplet size and composition of nutraceutical nanoemulsions influences bioavailability of long chain fatty acids and Coenzyme Q10. *Food Chemistry* **2014**, *156*, 117-122.

91. Zhou, H.; Liu, G.; Zhang, J.; Sun, N.; Duan, M.; Yan, Z.; Xia, Q., Novel Lipid-Free Nanoformulation for Improving Oral Bioavailability of Coenzyme Q10. *BioMed Research International* **2014**, *2014*, 9.

92. Chan, H. O.; Stewart, B. H., Physicochemical and drug-delivery considerations for oral drug bioavailability. *Drug Discovery Today* **1996**, *1*, 461-473.

93. Shargel, L.; Wu-Pong, S.; Yu, A. B., *Applied biopharmaceutics & pharmacokinetics*. McGraw-Hill: 2007.

94. Srinivasan, V. S., Bioavailability of Nutrients: A Practical Approach to In Vitro Demonstration of the Availability of Nutrients in Multivitamin-Mineral Combination Products. *The Journal of Nutrition* **2001**, *131*, 1349S-1350S.

95. Johnson, L. R.; Gerwin, T. A., *Gastrointestinal physiology*. Mosby Elsevier Philadelphia: 2007.

96. Fernández-García, E.; Carvajal-Lérida, I.; Pérez-Gálvez, A., In vitro bioaccessibility assessment as a prediction tool of nutritional efficiency. *Nutrition Research* **2009**, *29*, 751-760.

97. Benito, P.; Miller, D., Iron absorption and bioavailability: An updated review. *Nutrition Research* **1998**, *18*, 581-603.

98. McClements, D. J.; Li, Y., Review of in vitro digestion models for rapid screening of emulsion-based systems. *Food & Function* **2010**, *1*, 32-59.

99. Dahan, A.; Hoffman, A., Rationalizing the selection of oral lipid based drug delivery systems by an in vitro dynamic lipolysis model for improved oral bioavailability of poorly water soluble drugs. *Journal of Controlled Release* **2008**, *129*, 1-10.

100. Li, Y.; Hu, M.; McClements, D. J., Factors affecting lipase digestibility of emulsified lipids using an in vitro digestion model: Proposal for a standardised pH-stat method. *Food Chemistry* **2011**, *126*, 498-505.
101. Hur, S. J.; Decker, E. A.; McClements, D. J., Influence of initial emulsifier type on microstructural changes occurring in emulsified lipids during in vitro digestion. *Food Chemistry* **2009**, *114*, 253-262.
102. Klinkesorn, U.; Julian McClements, D., Impact of Lipase, Bile Salts, and Polysaccharides on Properties and Digestibility of Tuna Oil Multilayer Emulsions Stabilized by Lecithin–Chitosan. *Food Biophysics* **2010**, *5*, 73-81.
103. Ting, Y.; Zhao, Q.; Xia, C.; Huang, Q., Using in Vitro and in Vivo Models To Evaluate the Oral Bioavailability of Nutraceuticals. *Journal of Agricultural and Food Chemistry* **2015**, *63*, 1332-1338.
104. Anson, N. M.; Selinheimo, E.; Havenaar, R.; Aura, A.-M.; Mattila, I.; Lehtinen, P.; Bast, A.; Poutanen, K.; Haenen, G. R. M. M., Bioprocessing of Wheat Bran Improves in vitro Bioaccessibility and Colonic Metabolism of Phenolic Compounds. *Journal of Agricultural and Food Chemistry* **2009**, *57*, 6148-6155.
105. Minekus, M.; Jelier, M.; Xiao, J.-z.; Kondo, S.; Iwatsuki, K.; Kokubo, S.; Bos, M.; Dunnewind, B.; Havenaar, R., Effect of Partially Hydrolyzed Guar Gum (PHGG) on the Bioaccessibility of Fat and Cholesterol. *Bioscience, Biotechnology, and Biochemistry* **2005**, *69*, 932-938.
106. Arkbåge, K.; Verwei, M.; Havenaar, R.; Witthöft, C., Bioaccessibility of Folic Acid and (6S)-5-Methyltetrahydrofolate Decreases after the Addition of Folate-Binding Protein to Yogurt as Studied in a Dynamic In Vitro Gastrointestinal Model. *The Journal of Nutrition* **2003**, *133*, 3678-3683.
107. Bel-Rhliid, R.; Crespy, V.; Pagé-Zoerkler, N.; Nagy, K.; Raab, T.; Hansen, C.-E., Hydrolysis of Rosmarinic Acid from Rosemary Extract with Esterases and *Lactobacillus johnsonii* in Vitro and in a Gastrointestinal Model. *Journal of Agricultural and Food Chemistry* **2009**, *57*, 7700-7705.
108. Lila, M. A.; Ribnicky, D. M.; Rojo, L. E.; Rojas-Silva, P.; Oren, A.; Havenaar, R.; Janle, E. M.; Raskin, I.; Yousef, G. G.; Grace, M. H., Complementary Approaches To Gauge the Bioavailability and Distribution of Ingested Berry Polyphenolics. *Journal of Agricultural and Food Chemistry* **2011**, *60*, 5763-5771.
109. Brouwers, J.; Anneveld, B.; Goudappel, G.-J.; Duchateau, G.; Annaert, P.; Augustijns, P.; Zeijdner, E., Food-dependent disintegration of immediate release fosamprenavir tablets: In vitro evaluation using magnetic resonance imaging and a dynamic gastrointestinal system. *European Journal of Pharmaceutics and Biopharmaceutics* **2011**, *77*, 313-319.
110. Souliman, S.; Beyssac, E.; Cardot, J.-M.; Denis, S.; Alric, M., Investigation of the Biopharmaceutical Behavior of Theophylline Hydrophilic Matrix Tablets Using USP Methods and an Artificial Digestive System. *Drug Development and Industrial Pharmacy* **2007**, *33*, 475-483.
111. Krul, C.; Humblot, C.; Philippe, C.; Vermeulen, M.; van Nuenen, M.; Havenaar, R.; Rabot, S., Metabolism of sinigrin (2-propenyl glucosinolate) by the human colonic microflora in a dynamic in vitro large-intestinal model. *Carcinogenesis* **2002**, *23*, 1009-1016.

112. Maathuis, A.; Hoffman, A.; Evans, A.; Sanders, L.; Venema, K., The Effect of the Undigested Fraction of Maize Products on the Activity and Composition of the Microbiota Determined in a Dynamic in Vitro Model of the Human Proximal Large Intestine. *Journal of the American College of Nutrition* **2009**, *28*, 657-666.
113. Kovatcheva-Datchary, P.; Egert, M.; Maathuis, A.; Rajilić-Stojanović, M.; De Graaf, A. A.; Smidt, H.; De Vos, W. M.; Venema, K., Linking phylogenetic identities of bacteria to starch fermentation in an in vitro model of the large intestine by RNA-based stable isotope probing. *Environmental Microbiology* **2009**, *11*, 914-926.
114. Maathuis, A. J. H.; van den Heuvel, E. G.; Schoterman, M. H. C.; Venema, K., Galacto-Oligosaccharides Have Prebiotic Activity in a Dynamic In Vitro Colon Model Using a ¹³C-Labeling Technique. *The Journal of Nutrition* **2012**, *142*, 1205-1212.
115. Acosta, E., Bioavailability of nanoparticles in nutrient and nutraceutical delivery. *Current Opinion in Colloid & Interface Science* **2009**, *14*, 3-15.
116. Lin, J. H.; Chiba, M.; Baillie, T. A., Is the Role of the Small Intestine in First-Pass Metabolism Overemphasized? *Pharmacological Reviews* **1999**, *51*, 135-158.
117. Hubatsch, I.; Ragnarsson, E. G. E.; Artursson, P., Determination of drug permeability and prediction of drug absorption in Caco-2 monolayers. *Nat. Protocols* **2007**, *2*, 2111-2119.
118. Chabane, M. N.; Ahmad, A. A.; Peluso, J.; Muller, C. D.; Ubeaud-Séquier, G., Quercetin and naringenin transport across human intestinal Caco-2 cells. *Journal of Pharmacy and Pharmacology* **2009**, *61*, 1473-1483.
119. Zhang, L.; Zheng, Y.; Chow, M. S. S.; Zuo, Z., Investigation of intestinal absorption and disposition of green tea catechins by Caco-2 monolayer model. *International Journal of Pharmaceutics* **2004**, *287*, 1-12.
120. Bailey, C. A.; Bryla, P.; Malick, A. W., The use of the intestinal epithelial cell culture model, Caco-2, in pharmaceutical development. *Advanced Drug Delivery Reviews* **1996**, *22*, 85-103.
121. Guengerich, F. P., Cytochrome P450 and Chemical Toxicology. *Chemical Research in Toxicology* **2008**, *21*, 70-83.
122. Ding, X.; Kaminsky, L. S., Human Extrahepatic Cytochromes P450: Function in Xenobiotic Metabolism and Tissue-Selective Chemical Toxicity in the Respiratory and Gastrointestinal Tracts. *Annual Review of Pharmacology and Toxicology* **2003**, *43*, 149-173.
123. Fujita, T.; Tanayama, S.; Shirakawa, Y.; Suzuoki, Z., Metabolic Fate of Ubiquinone-7: I. Absorption, Excretion and Tissue Distribution in Rats. *Journal of Biochemistry* **1971**, *69*, 53-61.
124. Bhagavan, H. N.; Chopra, R. K., Coenzyme Q10: Absorption, tissue uptake, metabolism and pharmacokinetics. *Free Radical Research* **2006**, *40*, 445-453.
125. Fujita, T.; Tanayama, S.; Suzuoki, Z., Metabolic Fate of Ubiquinone-7: II. Isolation and Identification of Metabolites in the Urine, Liver, Bile and Feces. *Journal of Biochemistry* **1971**, *69*, 63-71.
126. Nakamura, T.; Ohno, T.; Hamamura, K.; Sato, T., Metabolism of coenzyme Q10: Biliary and urinary excretion study in guinea pigs. *BioFactors* **1999**, *9*, 111-119.
127. Bentinger, M.; Dallner, G.; Chojnacki, T.; Swiezewska, E., Distribution and breakdown of labeled coenzyme Q10 in rat. *Free Radical Biology and Medicine* **2003**, *34*, 563-575.

128. Ferrua, M. J.; Singh, R. P., Modeling the Fluid Dynamics in a Human Stomach to Gain Insight of Food Digestion. *Journal of Food Science* **2010**, *75*, R151-R162.
129. Ferrua, M. J.; Kong, F.; Singh, R. P., Computational modeling of gastric digestion and the role of food material properties. *Trends in Food Science & Technology* **2011**, *22*, 480-491.
130. Tharakan, A.; Norton, I. T.; Fryer, P. J.; Bakalis, S., Mass Transfer and Nutrient Absorption in a Simulated Model of Small Intestine. *Journal of Food Science* **2010**, *75*, E339-E346.
131. Kagan, V. E.; Nohl, H.; Quinn, P. J., Coenzyme Q: Its role in scavenging and generation of radicals in membranes. In *Handbook of Antioxidants*, Dekker: New York: 1996; pp 157-202.
132. Rich, P. R.; Bendall, D. S., The kinetics and thermodynamics of the reduction of cytochrome c by substituted p-benzoquinols in solution. *Biochimica et Biophysica Acta (BBA) - Bioenergetics* **1980**, *592*, 506-518.
133. Swallow, A. J., Physical Chemistry of Semiquinones. In *Function of Quinones in Energy Conserving Systems*, Bernard, T., Ed. Academic Press: 1982; pp 59-72.
134. Edge, R.; McGarvey, D. J.; Truscott, T. G., The carotenoids as anti-oxidants — a review. *Journal of Photochemistry and Photobiology B: Biology* **1997**, *41*, 189-200.
135. Bowen, P. E., Carotenoids: Physical, Chemical, and Biological Functions and Properties. In Landrum, J. T., Ed. CRC Press: 2010; pp 437-464.
136. Böhm, F.; Edge, R.; Truscott, G., Interactions of dietary carotenoids with activated (singlet) oxygen and free radicals: Potential effects for human health. *Molecular Nutrition & Food Research* **2012**, *56*, 205-216.
137. Ozturk, B.; McClements, D. J., Progress in natural emulsifiers for utilization in food emulsions. *Current Opinion in Food Science* **2016**, *7*, 1-6.
138. Uluata, S.; McClements, D. J.; Decker, E. A., Physical Stability, Autoxidation, and Photosensitized Oxidation of ω -3 Oils in Nanoemulsions Prepared with Natural and Synthetic Surfactants. *Journal of Agricultural and Food Chemistry* **2015**, *63*, 9333-9340.
139. Yoshiki, Y.; Kahara, T.; Okubo, K.; Sakabe, T.; Yamasaki, T., Superoxide- and 1,1-Diphenyl-2-picrylhydrazyl Radical-scavenging Activities of Soyasaponin β g Related to Gallic Acid. *Bioscience, Biotechnology, and Biochemistry* **2001**, *65*, 2162-2165.
140. Takahashi, T.; Okamoto, T.; Mori, K.; Sayo, H.; Kishi, T., Distribution of ubiquinone and ubiquinol homologues in rat tissues and subcellular fractions. *Lipids* **1993**, *28*, 803-809.
141. Yamamoto, Y.; Yamashita, S., Biomedical and Clinical Aspects of Coenzyme Q Plasma ratio of ubiquinol and ubiquinone as a marker of oxidative stress. *Molecular Aspects of Medicine* **1997**, *18*, 79-84.
142. Xia, S.; Xu, S.; Zhang, X.; Zhong, F.; Wang, Z., Nanoliposomes Mediate Coenzyme Q10 Transport and Accumulation across Human Intestinal Caco-2 Cell Monolayer. *Journal of Agricultural and Food Chemistry* **2009**, *57*, 7989-7996.
143. Yu, H.; Shi, K.; Liu, D.; Huang, Q., Development of a food-grade organogel with high bioaccessibility and loading of curcuminoids. *Food Chemistry* **2012**, *131*, 48-54.
144. Sek, L.; Porter, C. J. H.; Kaukonen, A. M.; Charman, W. N., Evaluation of the in-vitro digestion profiles of long and medium chain glycerides and the phase behaviour of their lipolytic products. *Journal of Pharmacy and Pharmacology* **2002**, *54*, 29-41.

145. Failla, M. L.; Chitchumroonchokchai, C.; Aoki, F., Increased Bioavailability of Ubiquinol Compared to That of Ubiquinone Is Due to More Efficient Micellarization during Digestion and Greater GSH-Dependent Uptake and Basolateral Secretion by Caco-2 Cells. *Journal of Agricultural and Food Chemistry* **2014**, *62*, 7174-7182.
146. Tomono, Y.; Hasegawa, J.; Seki, T.; Motegi, K.; Morishita, N., Pharmacokinetic study of deuterium-labelled coenzyme Q10 in man. *Int J Clin Pharmacol Ther Toxicol* **1986**, *24*, 536-541.
147. Luecker, P. W.; Wetzelsberger, N.; Hennings, G.; Rehn, D., Pharmacokinetics of coenzyme ubidecarenone in healthy volunteers. *Biomed. Clin. Aspects Coenzyme Q* **1984**, *4*, 143-51.
148. Lu, W.-L.; Zhang, Q.; Lee, H.-S.; Zhou, T.-Y.; Sun, H.-D.; Zhang, D.-W.; Zheng, L.; Lee, M.; Wong, S.-M., Total Coenzyme Q10 Concentrations in Asian Men Following Multiple Oral 50-mg Doses Administered as Coenzyme Q10 Sustained Release Tablets or Regular Tablets. *Biological and Pharmaceutical Bulletin* **2003**, *26*, 52-55.
149. Lichtenstein, A. H.; Jones, P. J., Lipids: absorption and transport. In *Present Knowledge in Nutrition*, 2001.
150. Zhang, Y.; Aberg, F.; Appelkvist, E.-L.; Dallner, G.; Ernster, L., Uptake of dietary coenzyme Q supplement is limited in rats. *The Journal of Nutrition* **1995**, *125*, 446-453.
151. Gao, Z.-M.; Yang, X.-Q.; Wu, N.-N.; Wang, L.-J.; Wang, J.-M.; Guo, J.; Yin, S.-W., Protein-Based Pickering Emulsion and Oil Gel Prepared by Complexes of Zein Colloidal Particles and Stearate. *Journal of Agricultural and Food Chemistry* **2014**, *62*, 2672-2678.
152. Destribats, M.; Rouvet, M.; Gehin-Delval, C.; Schmitt, C.; Binks, B. P., Emulsions stabilised by whey protein microgel particles: towards food-grade Pickering emulsions. *Soft Matter* **2014**, *10*, 6941-6954.
153. Luo, Z.; Murray, B. S.; Yusoff, A.; Morgan, M. R. A.; Povey, M. J. W.; Day, A. J., Particle-Stabilizing Effects of Flavonoids at the Oil-Water Interface. *Journal of Agricultural and Food Chemistry* **2011**, *59*, 2636-2645.
154. Liu, F.; Tang, C.-H., Phytosterol Colloidal Particles as Pickering Stabilizers for Emulsions. *Journal of Agricultural and Food Chemistry* **2014**, *62*, 5133-5141.
155. Yusoff, A.; Murray, B. S., Modified starch granules as particle-stabilizers of oil-in-water emulsions. *Food Hydrocolloids* **2011**, *25*, 42-55.
156. Aveyard, R.; Binks, B. P.; Clint, J. H., Emulsions stabilised solely by colloidal particles. *Advances in Colloid and Interface Science* **2003**, *100-102*, 503-546.
157. Chevalier, Y.; Bolzinger, M.-A., Emulsions stabilized with solid nanoparticles: Pickering emulsions. *Colloids and Surfaces A: Physicochemical and Engineering Aspects* **2013**, *439*, 23-34.
158. O'Driscoll, C. M., Lipid-based formulations for intestinal lymphatic delivery. *European Journal of Pharmaceutical Sciences* **2002**, *15*, 405-415.
159. Porter, C. J. H.; Trevaskis, N. L.; Charman, W. N., Lipids and lipid-based formulations: optimizing the oral delivery of lipophilic drugs. *Nature Reviews Drug Discovery* **2007**, *6*, 231-248.
160. Trevaskis, N. L.; Charman, W. N.; Porter, C. J. H., Lipid-based delivery systems and intestinal lymphatic drug transport: A mechanistic update. *Advanced Drug Delivery Reviews* **2008**, *60*, 702-716.

161. Tian, H.; Yang, X.; Ho, C.-T.; Huang, Q.; Song, S., Development of a solid phase microextraction protocol for the GC–MS determination of volatile off-flavour compounds from citral degradation in oil-in-water emulsions. *Food Chemistry* **2013**, *141*, 131-138.